1-1-1984

Optimization of hydraulic pulse-length-modulated circuits.

Ata S. Koseogla

OPTIMIZATION OF HYDRAULIC PULSE-LENGTH-MODULATED CIRCUITS

by

Ata S. Köseoğlu

A Thesis

Presented to the Graduate Committee

of Lehigh University

in Candidacy for the Degree of

Master of Science

in

Mechanical Engineering

Lehigh University

1984

STATEMENT OF APPROVAL

This thesis is accepted and approved in partial fulfillment of the requirements for the degree of Master of Science.

5/10/84
date

Forbes T. Brown
Professor in charge

Robert P. Wei
Acting Chairman
Department of Mechanical Engineering and Mechanics

ACKNOWLEDGEMENTS

I would like to express special appreciation for the assistance and guidance provided by Prof. Forbes T. Brown. His expertise and continued support over the entire project were invaluable for the author's professional and personal development.

I must also express my sincere thanks to the Parker Hannifin Company and Mr. Philip Rauen for providing me with the opportunity to work on this project.

Finally, I would like to say that I am indebted to my father, İlhan Köseoğlu, for the motivation which he provided me and his continuing encouragement which made this work possible.

TABLE OF CONTENTS

LIST OF FIGURES

ABSTRACT

Microprocessor-controlled hydraulic switching valves offer the potential of replacing analog servovalves with advantages in cost, reliability and energy efficiency. A hydraulic pulse-length-modulated (PLM) switching valve may be connected to its load by a fluid channel exhibiting significant inertance and/or resistance. It is shown that if the channel which couples the valve to the load is a tube with a largely inertive impedance, the energy dissipation can be greatly reduced, while reasonable bandwidth is maintained and smooth performance is achieved. An analytical model is developed which permits minimization of energy dissipation under appropriate constraints defining a broad abstract class of switching valves, including both sliding and seating types. Both laminar and turbulent flows are considered in the tube.

Universal design charts are developed, for both seating and sliding valves, relating the optimal key parameters of the valve and the tube and the optimal cycle time to the fluid parameters, switching time and load power. Comparisons within and between families of geometrically similar valve designs are expedited, and results are given which aid the global minimization of energy dissipation with respect to a duty cycle.

1. INTRODUCTION

Switching circuits form the basis of low-frequency fluid power control such as in most industrial and earth-moving applications, while analog control has been customary for high-frequency fluid power control such as in most aircraft, robot and machine tool applications. Switching circuits, however, also can be applied to high-frequency fluid power control partly by using the microprocessor.

Two general modes of operation are particularly attractive: periodic and aperiodic. Periodic operation implies pulse-length modulation (PLM), which must be carried out at a relatively high frequency to provide adequate bandwidth and to prevent excessive energy dissipation. The idea of pulse-length modulation originated years ago at the Applied Physics Laboratory of John Hopkins University [1]. It essentially is a method of controlling the time-rate-change of flow to an output member in a manner such that a desired position (or velocity) of the driven load is obtained. It could be either a two-state or a three-state control; the simpler two-state (bang-bang) is exclusively treated herein. Aperiodic operation of a two-state control implies much less frequent switching, and is exemplified by time-optimal bang-bang control [2]. Both two-state modes might

appropriately be applied to a given system for different portions of the load cycle, but this thesis concentrates on the periodic mode. (Aperiodic excitation also could be used to advantage with three or four-state control.)

A significant difference is assumed from other PLM valves regarding the location at which the conversion from discrete to analog signals takes place. This D/A conversion, or effective filtering of the switching signal to give a largely smooth output, can occur either in the second stage of the valve, in the fluid impedance coupling between the valve and the load, or in the load itself [3]. Conversion in the second stage of the valve was assumed by Murtaugh [1] and Tsai and Ukrainetz [4] and recently Mansfeld [5] considers D/A conversion in the fluid impedance coupling to the load. Brown [3], however, introduces the third system (using a fluid coupling impedance) that can tolerate a much larger load compliance with less energy dissipation and have the advantage of greatly smoother behavior of the output. This thesis also assumes conversion in the fluid impedance.

Both seating and sliding types of two-state three-way valves are considered. Each has special advantages.

The results, however, are generic and no experimental results are given. The objective of the present research

is to specify the desired system characteristics for the optimal design before too much developmental effort is undertaken.

2. BASIC CONFIGURATION

The valve configuration considered is shown in Figure 1. This schematic is not intended to represent a practical configuration, and the pilot actuating mechanism is not shown, but rather it portrays the generic portality. The load is connected alternately to supply pressure and to tank, through the intervening fluid inertance (labelled "tube") and load fluid compliance (due to the cavity volume). As it can be seen from Figure 2, the seating valve actually is the limiting case of the sliding valve with b=0. Therefore some of the definitions used in the analysis are based on the ones for the seating valves, which are simpler to analyze. The dimensionless parameter b is one of the key parameters of the system to be optimized. The maximum opening for the seating valve is a function of the maximum stroke, x, and the length of the additional opening for the sliding valve is defined as bx. The upper effective orifice area is proportional to a_s and the lower effective orifice area is proportional to a_t. The sum of the upper and lower effective orifice areas of the valves is assumed to be a constant in seating valves (especially those with strokes that are small compared with other dimensions, which may give the best response). This sum is denoted as a_0;

$$a_0 = a_0(x). \tag{1}$$

Therefore the maximum orifice areas for a_s and a_t are,

for sliding valves,

$$a_{smax} = a_{tmax} = a_0(1+b) \tag{2a}$$

and for seating valves,

$$a_{smax} = a_{tmax} = a_0 . \tag{2b}$$

Note that, throughout the whole text, the equations to be used with sliding or seating valves only will be designated by the letters a and b, respectively (as in 2a and 2b above). Equations with no letters apply to both types of valve.

In lieu of detailed design and dynamic analysis of the switching, two limiting cases can be assumed, both of which have the switching time T_{st}. The running time is denoted as t, as can be seen on Figure 3. These cases are

1. Constant velocity, n=1.
2. Constant acceleration, n=2.

Turning on:

$$a_s(t) = \begin{cases} 0 & 0 \le t \le t_1 \\ a_o(1+2b)\left[\left(\frac{t}{T_{st}}\right)^n - \frac{b}{1+2b}\right] & t_1 \le t \le T_{st} \end{cases} \tag{3a}$$

$$a_t(t) = \begin{cases} a_o(1+2b)\left[\frac{1+b}{1+2b} - \left(\frac{t}{T_{st}}\right)^n\right] & 0 \le t \le t_2 \\ 0 & t_2 \le t \le T_{st} \end{cases}$$

Turning off:

$$a_s(t) = \begin{cases} a_o(1+2b)\left[\frac{1+b}{1+2b} - \left(\frac{t}{T_{st}}\right)^n\right] & 0 \le t \le t_2 \\ 0 & t_2 \le t \le T_{st} \end{cases}$$

$$a_t(t) = \begin{cases} 0 & 0 \le t \le t_1 \\ a_o(1+2b)\left[\left(\frac{t}{T_{st}}\right)^n - \frac{b}{1+2b}\right] & t_1 \le t \le T_{st} \end{cases} \qquad (4a)$$

where

$$t_1 = \left(\frac{b}{1+2b}\right)^{\frac{1}{2}} * T_{st} \qquad t_2 = \left(\frac{1+b}{1+2b}\right)^{\frac{1}{2}} * T_{st} \; . \qquad (5a)$$

The meanings of the time limits t_1 and t_2 might be better understood by referring to Figure 3. It is also seen in Figure 3 that at $t=(t_1+t_2)/2$, a_s and a_t are equal.

Notice that above equations simplify to the following for the seating valves

Turning on:

$$a_s(t) = a_o\left(\frac{t}{T_{st}}\right)^n \qquad 0 \le t \le T_{st}$$

$$a_t(t) = a_o\left[1 - \left(\frac{t}{T_{st}}\right)^n\right] \qquad 0 \le t \le T_{st} \qquad (3b)$$

Turning off:

$$a_s(t) = a_o\left[1 - \left(\frac{t}{T_{st}}\right)^n\right] \qquad 0 \le t \le T_{st}$$

$$a_t(t) = a_o\left(\frac{t}{T_{st}}\right)^n \qquad 0 \le t \le T_{st} \qquad (4b)$$

with

$$t_1=0,\ t_2=T_{st}\ . \tag{5b}$$

Brown [3] has shown (for seating valves) that the extreme cases n=1 and n=2 produce nearly the same consequences (assuming the same value of T_{st}). Since the latter appears to be considerably more realistic, it has been used exclusively by the author.

The series fluid impedance element (normally a single uniform tube) has frequency-dependent resistance, R, and , inertance, I, but is assumed to be short enough so its compliance (compressibility effect or wave propagation effect) can be neglected. This assumption is reasonable in that wave delay effects would complicate the behavior so as to compromise the effectiveness of the control, and thus should be avoided. A constraint on the length of the element, ℓ , is used to insure small effects. In particular, the ratio of the wavelength of a wave of period T to ℓ, defined as N,

$$N\equiv v_p T/\ell \tag{6}$$

(where v_p is the phase velocity of waves, equal to β/ρ) is kept at or above some large value

$$N=N_{in}\ . \tag{7}$$

In practice, N_m=20 or more is presumably satisfactory [3].

A fluid compliance, C, is located directly between the series impedance element and the input moving member of the load. This may be associated with an effective minimum cavity volume of the output ram or motor, or may be increased purposefully to further decrease the filter frequency, ω_n.

3. EFFECT OF NON-ZERO SWITCHING TIME

The cycle time is defined as T, and the fraction of the cycle for which the valve is nominally on will be called α. The periodic mode introduces the fundamental question of what constitutes an optimum switching cycle period, T. The answer is simple, interpreted from the viewpoints of either bandwidth or dissipation, if instantaneous switching ($T_{st}=0$) is assumed. The smaller the period T the better; the cycling dissipation goes to zero as T goes to zero, and the system bandwidth increases monotonically.

When the non-instantaneous character of the actual switching is considered, however, the story changes. From the bandwidth viewpoint control would be lost if T was reduced to the order of the switching time, T_{st}. A reasonable limit might be taken as

$$T/T_{st} \geq 10 \ . \qquad (8)$$

Further, from the energy dissipation viewpoint, there is a shunt leakage path through the valve during switching, causing momentarily large dissipation; again one might prefer to have a large value of T/T_{st}.

Another key parameter to be optimized is the valve size, as represented by a_0. The shunt leakage can be reduced by making the valve smaller, but then the series resistance (principal porting loss) of the valve

increases. Thus, introducing non-zero switching time and non-zero valve losses implies the existence of a minimum energy dissipation for some combination of cycle time and valve size.

In the case of the sliding valves the parameter b is added. Increasing b causes the overall switching time to increase but the time that both ports are open to decrease. Therefore for a particular situation an optimum value of b exists.

In the following analysis there are two flows which can be considered to be independent: the flow Q_s from the supply port and the flow Q_t through the tube. The return flow to the tank is then $Q_s - Q_t$.

The flow through the impedance element, Q_t, will not change much during the switching transient, since $T_{st} << T$ and the inertia I plays a dominant role. On the other hand Q_s undergoes a large transient surge. As can be seen from Figure 4, whenever $|Q_t|$ is smaller than $|Q_s|$, Q_t is negative when the valve is being turned on (downward motion) and positive when the valve is being turned off (upward motion). The variations between switching events can be represented in terms of α, Q_ℓ (average of Q_t) and Q_j, the last being the half amplitude.

For analysis purposes, the flow Q_t is approximated to

be constant at one of its two extreme values throughout each switch. The equations of motion can be taken as

$$I_s \frac{dQ_s}{dt} + \frac{Q_s^2}{a_s^2} \operatorname{sgn} Q_s = P-p \tag{9}$$

$$I_t \frac{d}{dt}(Q_s-Q_t) + \frac{(Q_s-Q_t)^2}{a_t^2} \operatorname{sgn}(Q_s-Q_t) = p \tag{10}$$

according to the usual Bernoulli orifice equation. Note that, according to Bernoulli's equation,

$$\begin{aligned} a_s &= a_s^* c_d \sqrt{2/\rho} \\ a_t &= a_t^* c_d \sqrt{2/\rho} \end{aligned} \tag{11}$$

and

$$\begin{aligned} a_s^* &= a_s(x) \\ a_t^* &= a_t(x) \end{aligned} \tag{12}$$

where a_s^* and a_t^* are the actual areas , c_d is the flow coefficient and ρ is the fluid density.

I_s and I_t in the above equation refer to inertias of the flows from the supply and to the tank, respectively. These inertias likely are negligible unless one purposely makes them large. Even though large values can reduce the energy dissipation, they have been neglected during the analysis. This is because Brown [6] shows (for seating valves) that the use of the inertances I_s and I_t to reduce

the flow surge and energy dissipation is not as desirable as it may appear. Use of a large I_t leads to cavitation just to the left of the lower valve port (and to the right of the inertance element, not shown explicitly in Figure 4) when the valve is turned on, and to the right of the valve (pressure p) with it is turned off. This problem can be eliminated by letting I_t=0 and placing the burden on I_s. However, large I_s produces very large pressures in the upper valve port just before that port is shut off, so that the forces on the moving part and the erosion of the valving surfaces could be a major problem. Further, if the magnitude of I_s becomes comparable to the tube inertance, I, the basic response of the system changes since the effective inertia is larger when the valve is on than when it is off. Finally, the reduction in energy dissipation resulting from a substantial I_s+I_t is limited to cases with small c_v (large valve area, as defined below) and is not dramatic. It will also be seen, later, that introducing o causes c_v to be even larger for sliding valves.

After the elimination of the inertances the equations of motion become simply

$$\frac{Q_s^2}{a_s^2} \operatorname{sgn} Q_s = P - p \tag{13}$$

$$\frac{(Q_s - Q_t)^2}{a_t^2} \operatorname{sgn} (Q_s - Q_t) = p \ . \tag{14}$$

The above equations can then be summed to eliminate p, and solved for Q_s using equations (3) and (4). The results are given in Figure 5. The energy dissipation during a single switch, ε_s, then can be computed from the relation

$$\frac{d\varepsilon_s}{dt} = \frac{|Q_s|^3}{a_s^2} + \frac{|Q_s - Q_t|^3}{a_t^2} \quad . \tag{15}$$

A numerical integration was done in three stages (when the valve is being turned on) to calculate

(i) ε_{s1} between $0 \leq t \leq t_1$

$$\text{using} \qquad \frac{d\varepsilon_{s1}}{dt} = \frac{|Q_t|^3}{a_t^2} \tag{16}$$

(ii) ε_{s2} between $t_1 \leq t \leq t_2$

$$\text{using} \qquad \frac{d\varepsilon_{s2}}{dt} = \frac{|Q_s|^3}{a_s^2} + \frac{|Q_s - Q_t|^3}{a_t^2} \tag{17}$$

(iii) ε_{s3} between $t_2 \leq t \leq T_{st}$

$$\text{using} \qquad \frac{d\varepsilon_{s3}}{dt} = \frac{|Q_s|^3}{a_s^2} \tag{18}$$

and the results are most conveniently expressed in nondimensional terms as

$$E_s = E_{s1} + E_{s2} + E_{s3} \tag{19}$$

and

$$E_{s1} + E_{s3} = g(b) \tag{20a}$$

$$E_{s2} = E(c_v, b) \tag{21a}$$

where

$$E_s \equiv \frac{a_o^2 \varepsilon_s}{T_{st} |Q_t|^3} \tag{22}$$

$$c_v \equiv \frac{Q_t}{a_o \sqrt{P}} \tag{23}$$

$$g(b) = \frac{1}{(1+2b)^2} \left[\int_o^{\gamma_1} \frac{d\gamma}{\left(\gamma^2 - \frac{1+b}{1+2b}\right)^2} + \int_{\gamma_2}^{1} \frac{d\gamma}{\left(\gamma^2 - \frac{b}{1+2b}\right)^2} \right] \tag{24a}$$

$$\text{with} \quad \gamma_i \equiv t_i / T_{st} \qquad (i=1,2) \ .$$

As it will be seen later, for the case of seating valves

$$g(b) = 0 \tag{24b}$$

giving

$$E_s = E_{s2} = E(c_v) \ . \tag{21b}$$

A small value of c_v (large valve area) gives a large surge flow and a large energy dissipation. As explained before, if c_v is small, the flow and the dissipation might be reduced by introducing substantial inertances. The energy dissipated when the valve turns on is the same as when the valve turns off, assuming no cavitation.

The remainder of this section considers the special case of zero load flow ($Q_\ell=0$), so that both switches have virtually the same $|Q_t|=Q_d$ (Q_ℓ is allowed to be non-zero in the following section). The normalized energy dissipation in the two switches per cycle under these conditions becomes

$$\frac{\varepsilon_s}{PQ_dT_{st}} = 2c_v^2[g(b) + E(c_v,b)] \qquad (25a)$$

or for seating valves

$$\frac{\varepsilon_s}{PQ_dT_{st}} = 2c_v^2E(c_v) \quad . \qquad (25b)$$

This nondimensional energy dissipation is given in Figure 6 for some cases of interest. It can be seen that the larger the value of b, the smaller the energy dissipation when there is no constraint on the control and/or the performance.

In a broad range of interest, the energy dissipation during these switches has been calculated and the results [Appendix A] show that

$$E(c_v,b)=f(b)*E(c_v) \tag{26a}$$

and

$$E(c_v,0)=E(c_v) \tag{26b}$$

as

$$f(0)=1 \text{ for seating valves.}$$

Then, over the range of interest, these three functions can be well approximated by

$$2c_v^2E(c_v) = a_1/c_v + a_2c_v + a_3c_v^3 \tag{27}$$

$$f(b) = \sum_{i=0}^{10} f_i b^i \tag{28}$$

$$g(b) = \sum_{i=0}^{10} g_i b^i \ . \tag{29}$$

The coefficients and the approximation ranges are given in Appendix A.

The energy dissipated in the valve when it is not switching is calculated assuming that the flow varies linearly as shown in Figure 4. Even though the following

derivation has been made for $\alpha = 1/2$, the result applies within 97 percent for $0.3 \leq \alpha \leq 0.7$.

$$\frac{\varepsilon_{ns}}{PQ_d T_{st}} = \frac{c_v^2}{(1+b)^2}\left[\frac{1}{4} - 2\left(\frac{T_{st}}{T}\right) - 6\left(\frac{T_{st}}{T}\right)^2 + 8\left(\frac{T_{st}}{T}\right)^3 - 4\left(\frac{T_{st}}{T}\right)^4\right] \quad (30a)$$

Therefore the total average power dissipated in the valve is

$$\frac{\varepsilon_v}{T} = \frac{\varepsilon_s}{T} + \frac{\varepsilon_{ns}}{T} \quad (31)$$

or

$$\frac{\varepsilon_v}{T} = \{[2c_v^2 g(b) + (a_1/c_v + a_2 c_v + a_3 c_v^3) f(b)]\left(\frac{T_{st}}{T}\right) + \frac{c_v^2}{(1+b)^2}\left[\frac{1}{4} - 2\left(\frac{T_{st}}{T}\right) - 6\left(\frac{T_{st}}{T}\right)^2 + 8\left(\frac{T_{st}}{T}\right)^3 - 4\left(\frac{T_{st}}{T}\right)^4\right]\}PQ_d \quad . \quad (32a)$$

In the case of the seating valves, this equation reduces to:

$$\frac{\varepsilon_v}{T} = \{(a_1/c_v + a_2 c_v + a_3 c_v^3)\left(\frac{T_{st}}{T}\right) + c_v^2\left[\frac{1}{4} - 2\left(\frac{T_{st}}{T}\right) - 6\left(\frac{T_{st}}{T}\right)^2 + 8\left(\frac{T_{st}}{T}\right)^3 - 4\left(\frac{T_{st}}{T}\right)^4\right]\}PQ_d \quad (32b)$$

If we choose Q_d independently (to provide an adequate maximum velocity of the load) the optimum value of a_0, represented as an optimum value of c_v, minimizes this power for assumed discrete values of b. The resulting values of c_v are plotted in Figure 7, with the labels of "c_q=0", as a function of T/T_{st}. Clearly the shorter the switching time T_{st}, the smaller the optimum value of c_v and the larger the orifice area of the valve. Note that in all cases the optimum c_v must be to the left of the respective minima in Figure 6. However, introducing b (for sliding valves), we see that for the same switching time, the optimum value of c_v becomes larger giving a smaller orifice area when compared with the one for seating valves. This difference is especially noticeable for the small values of T/T_{st}. The fact that the switching time itself increases (weakly) with valve parameters (c_v and b) complicates the situation, but also serves more sharply define the optimum size.

4. EFFECT OF LOAD MOTION

In equations (25), (27) and (32), the mean load flow Q_ℓ was taken to be zero and two independent dimensionless groups (c_v and b) resulted. Non-zero Q_ℓ now will be introduced via another dimensionless group defined as the ratio of Q_ℓ to the half-amplitude Q_d:

$$c_q \equiv \frac{Q_\ell}{Q_d} = \frac{\tau}{T} \quad . \tag{33}$$

For small values of $\omega_n T$, it has been shown [2] that an approximate simple asymptote can be found. Assuming the inertance dominates over the resistance (small damping ratios or very small $\omega_n T$) and the perturbations of the downstream cavity pressures are small, the flow variations comprise virtually linear segments as shown in Figure 4. The maximum excursions of the flow, then, can be readily found to be

$$Q_d = (1-\alpha)\alpha TP/2I \quad . \tag{34}$$

From equation (34), the right-most form corresponds approximately to

$$\tau \cong \frac{2I|Q_\ell|}{\alpha(1-\alpha)P} \quad . \tag{35}$$

The definition of the first dimensionless group, c_v, is now generalized to

$$c_v \equiv \frac{Q_d}{a_o\sqrt{P}} \quad . \tag{36}$$

This can be viewed as a dimensionless measure of the pressure drop across the valve. The optimization process also gives a value for c_v and b (for sliding valves), and thus an optimum orifice area and the size of the additional openings of the valve.

The switching time, T_{st}, also is normalized with respect to τ;

$$c_s \equiv \frac{T_{st}}{\tau} \tag{37}$$

which gives

$$\frac{T}{T_{st}} = \frac{1}{c_s c_q} \quad . \tag{38}$$

Note that

$$T_{st} \equiv T_s(1+2b)^{1/2} \tag{39a}$$

which reduces to

$$T_{st} = T_s \tag{39b}$$

for seating valves.

A small value for c_s implies considerable design flexibility and potentially high energy efficiency; if c_s

gets too large a switching circuit might not be practical at all.

The flows Q_t during the two switches for each cycle now are different:

$$Q_{t1}=Q_\ell+Q_d$$
$$Q_{t2}=Q_\ell-Q_d \quad . \tag{40}$$

Equation (25a) becomes

$$\frac{\varepsilon_s}{PQ_dT_{st}} = [c_{v1}{}^2(\frac{Q_{t1}}{Q_d}) + c_{v2}{}^2|\frac{Q_{t2}}{Q_d}|]g(b) + c_{v1}{}^2E(c_{v1},b)\ \frac{Q_{t1}}{Q_d} + c_{v2}{}^2E(c_{v2},b)\ \frac{Q_{t2}}{Q_d} \tag{41a}$$

or for seating valves

$$\frac{\varepsilon_s}{PQ_dT_s} = c_{v1}{}^2E(c_{v1})\ \frac{Q_{t1}}{Q_d} + c_{v2}{}^2E(c_{v2},b)\ \frac{Q_{t2}}{Q_d} \tag{41b}$$

and the power loss in the orifice for the intervals in which the valve is not switching becomes

$$\frac{\varepsilon_{ns}}{T} = \begin{cases} \dfrac{|Q_\ell|}{a_o{}^2(1+b)^2}\ [(Q_\ell{}^2+Q_d{}^2)-2(Q_\ell{}^2+3Q_d{}^2)(\frac{T_{st}}{T})] & c_q\leq 1 \\ \dfrac{1}{a_o{}^2(1+b)^2}\ [\dfrac{(Q_{t1}{}^4+Q_{t2}{}^4)}{8Q_d} - (|Q_{t1}|^3+|Q_{t2}|^3)(\frac{T_{st}}{T})] & c_q\geq 1 \end{cases} \tag{42a}$$

The above equations are approximations due to the

complexity of the actual formula, but its error is strictly negligible and they simplify to

$$\frac{\varepsilon_{ns}}{T} = \begin{cases} \frac{|Q_\ell|}{a_o^2}\left[(Q_\ell^2+Q_d^2)-2(Q_\ell^2+3Q_d^2)\left(\frac{T_s}{T}\right)\right] & c_q \leq 1 \\ \frac{1}{a_o^2}\left[\frac{(Qt_1^4+Qt_2^4)}{8Q_d}-(|Qt_1|^3+|Qt_2|^3)\left(\frac{T_s}{T}\right)\right] & c_q \geq 1 \end{cases} \tag{42b}$$

for seating valves. As a result, equation (32a) for the total dissipation in the valve is generalized to;

$$\frac{\varepsilon_v}{P|Q_\ell|T} = [(a_1/c_v+a_2r_1c_v+a_3r_2c_v^3)f(b)+2mc_v^2g(b)]c_s + \frac{r_3}{(1+b)^2}\frac{c_v^2}{c_q} \tag{43a}$$

or

$$\frac{\varepsilon_v}{P|Q_\ell|T} = (a_1/c_v+a_2r_1c_v+a_3r_2c_v^3)c_s+r_3\frac{c_v^2}{c_q} \tag{43b}$$

where

$$r_1=1+c_q^2 \tag{44}$$

$$r_2=r_1^2+4c_q^2 \tag{45}$$

$$m = \begin{cases} 1+3c_q^2 & c_q \leq 1 \\ c_q(3+c_q^2) & c_q \geq 1 \end{cases} \qquad (46)$$

$$r_3 = \begin{cases} r_2/4 - 2mc_s c_q & c_q \leq 1 \\ r_1 c_q - 2mc_s c_q & c_q \geq 1 \end{cases} . \qquad (47)$$

This expression is minimized with respect to c_v, as before; results for c_q=0,1,2 and b=0,0.5,1 are given in Figure 7. It is apparent that, for the same switching time, introducing load flow (therefore c_q) causes a larger orifice area (smaller c_v) for an optimum solution. All these results have been taken with a constant acceleration case which appears (from considerations beyond the scope of this research) to be closer to what would occur in practice. Even though we get the optimizing values for c_v for predefined values for b and c_q, we wish, simultaneously, to find the values of c_q and b for minimum dissipation. Since the viscous dissipation in the tube is also affected by c_q, this dissipation must be added to equation (43) before the minimization is undertaken. These tube losses both in laminar and turbulant flows are discussed in the following sections.

5. TUBE LOSSES, LAMINAR FLOW

The total dissipation in the system can be represented as the sum of the valve dissipation which was found in the previous sections (equation 43) plus the dissipation in the tube.

The tube losses comprise a steady-flow loss plus a surge loss.

(i) the steady-flow loss:

The steady flow loss in laminar flow becomes

$$\frac{\varepsilon_{st}}{T} = RQ_\ell^2 = c_t P|Q_\ell| \qquad (48)$$

therefore a new dimensionless group is defined as

$$c_t \equiv \frac{R|Q_\ell|}{P} \quad . \qquad (49)$$

The dimensionless group c_t can be considered as measure of the importance of viscous dissipation; were it the only loss the steady state efficiency would be $1-c_t$.

Of all shapes, a round tube gives the minimum ratio of resistance to inertance squared. For a tube of diameter d and length ℓ with a laminar flow with assymptotically slow perturbations, it is found [2] that

$$R = \frac{128\mu\ell}{\pi d^4} \tag{50}$$

$$I = \frac{16}{3}\frac{\rho\ell}{\pi d^2} \cdot \tag{51}$$

This gives

$$c_t = \frac{9\pi I^2\mu|Q_\ell|}{2\rho^2\ell P} \cdot \tag{52}$$

(ii) the surge loss:

If the resistance and inertance of the tube were constant, the surge loss, assuming the linear flow variations as before, is shown to be [6]

$$\frac{\epsilon_{su}}{T} \equiv r_d \cong \frac{c_t}{3c_q^2} P|Q_\ell| \cdot \tag{53}$$

The result above would be in serious error, however, because the frequencies are virtually always high enough to cause the instanteneous resistance to flow of the tube to exceed considerably its quasi-steady-flow value.

The equations given for the resistance and the inertance of the tube should, then, be corrected for the unsteady flow. The effective actual resistance and inertance, called R_d and I_d here, depend strongly on the history of the flow. Their ratios r_R and r_I to the static values R and I, respectively, are plotted in Figure 8 as a

function of the dimensionless frequency

$$\Omega = \frac{\omega \rho d^2}{4\mu} \tag{54}$$

where ω is an actual frequency of oscillation. For $\Omega > 20$ the following are very close approximations,

$$R_d/R \equiv r_R = [3+2\Omega(1+15/8\Omega)]/8 \tag{55}$$

$$I_d/I \equiv r_I = 3[1+2/\Omega-15/2(2\Omega)^{3/2}]/4 . \tag{56}$$

These results are given in [3] and they are based on work by Brown [7] and Nichols [8].

These approximations have been corrected for the surge loss by Brown [6] using a Fourier approach in which the pressure drop is taken as a square wave, but, as a practical matter for optimal design such small corrections are of little significance. Therefore the results of the previous sections are used except for the substitutions of $R_d=r_R R$ for R and $I_d=r_I I$ for I in the relevant equations.

It is convenient to implement this model by introducing dynamic versions of the dimensionless groups c_v, c_q, c_s and c_t where b is independent of the frequency. These key parameters become

$$c_{vd} = \frac{c_v}{r_I} \tag{57}$$

$$c_{qd} = c_q r_I \tag{58}$$

$$c_{sd} = \frac{c_s}{r_I} \tag{59}$$

$$c_{td} = c_t r_R \tag{60}$$

and the total tube loss, ε_t, becomes

$$\frac{\varepsilon_t}{T} = \frac{\varepsilon_{st}}{T} + \frac{\varepsilon_{su}}{T} \cong [c_t + \frac{c_{td}}{3c_{qd}^2}]P|Q_\ell| \ . \tag{61}$$

Notice that the steady-flow dissipation uses the steady-flow group, c_t.

6. TUBE LOSSES, TURBULENT FLOW

The valve losses given in previous sections do not change, assuming turbulent flow in the tube, but both steady-state and surge losses in the tube change dramatically. These losses are given below.

(1) the steady-flow loss:

The steady-flow loss in turbulent flow becomes

$$\frac{\varepsilon_{st}}{T} \equiv gP|Q_\ell| \tag{62}$$

giving a new dimensionless group which replaces c_t in the laminar case. This dimensionless group, g, is defined as

$$g \equiv 8f\rho Q_\ell{}^2 \ell/\pi^2 d^5 P = c_1 f(c_{qd})^{3/2} \tag{63}$$

where

$$c_1 \equiv \frac{3\sqrt{\pi}}{32\sqrt{2}} \left[\frac{\alpha(1-\alpha)}{r_I}\right]^{3/2} \frac{1}{g_\mu{}^2} \tag{64}$$

in which the friction factor, f, was evaluated using the conventional formula

$$\frac{1}{\sqrt{f}} = 2 \log_{10}(Re\sqrt{f}) - 0.8 \tag{65}$$

(ii) the surge loss:

The surge loss is taken to be

$$\frac{\varepsilon_{su}}{T} = r_d \cong rgP|Q_\ell|/3c_q^2 \qquad (66)$$

which is the same form as equation (37) except for the factor r [3]. This factor is in turn factored to

$$r = \frac{\tilde{f}}{f} r_\Omega = \frac{2f}{1+0.8686\sqrt{f}} r_\Omega \qquad (67)$$

in which f is the apparent friction factor for low-frequency (quasi-steady) perturbations and r_Ω is a factor to correct for the effects of non-zero frequency (as the ratios r_R and r_I do in laminar flow).

It is known that above a sufficiently high frequency the surge loss is the same in turbulent flow as in laminar flow [9,10], so that $rg=r_t$ or $r_\Omega=r_t f/\tilde{f}g$. Below a sufficiently low frequency, by definition $r_\Omega=1$. Brown [3] has recently proposed a function to bridge this gap:

$$r_\Omega = \sqrt{1+r_\infty^2}\,[1-0.3\,\exp(-0.2|ar_\infty-1/ar_\infty|)] \qquad (68)$$

$$r_\infty = r_t f/\tilde{f}g \qquad (69)$$

$$a = [Re^{0.23}/4] \qquad (70)$$

(This may seem more elaborate than the limited data and theoretical models justify, but seems necessary at least to describe that data. Minor variations in this model would have insignificant consequences below, fortunately.) The square root term gives almost appropriate continuous blending between the known assymptotes, and the exponential function describes a correction due to the observed fact that a phase lag in the perturbations of eddy viscosity effectively converts what would be a resistance phenomenon into a reactance phenomenon [3].

The results above complete the analytical model necessary for the optimization. Optimization with certain constraints is applied to this model to minimize the energy dissipation using the appropriate equations for the system under consideration (namely, laminar or turbulent flow in the tube with seating or sliding valve in use).

7. SYSTEM OPTIMIZATION

The total dissipation in the system (valve + tube), assuming laminar flow, becomes

(sliding valves)

$$p_d=[(a_1/c_{vd}+a_2r_1c_{vd}+a_3r_2c_{vd}^3)f(b)+2mc_{vd}^2g(b)]c_{sd}$$

$$+\frac{r_3}{(1+b)^2}\frac{c_{vd}^2}{c_{qd}}+c_{td}(1/r_R+1/3\,c_{qd}^2) \qquad (71a)$$

(seating valves)

$$p_d=(a_1/c_{vd}+a_2r_1c_{vd}+a_3r_2c_{vd}^3)c_{sd}+r_3\frac{c_{vd}^2}{c_{qd}}+c_{td}(1/r_R+1/3c_{qd}^2) \qquad (71b)$$

and assuming turbulent flow becomes

(sliding valves)

$$p_d=[(a_1/c_{vd}+a_2r_1c_{vd}+a_3r_2c_{vd}^3)f(b)+2mc_{vd}^2g(b)]c_{sd}$$

$$+\frac{r_3}{(1+b)^2}\frac{c_{vd}^2}{c_{qd}}+c_1f\,c_{qd}^{3/2}+rg/3c_q^2 \qquad (72a)$$

(seating valves)

$$p_d=(a_1/c_{vd}+a_2r_1c_{vd}+a_3r_2c_{vd}^3)c_{sd}+r_3\frac{c_{vd}^2}{c_{qd}}+c_1fc_{qd}^{3/2}+rg/3c_q^2 \qquad (72b)$$

The minimization problem assumes certain parameters are known while others are to be chosen to give minimum dissipation. In particular we assume that

$$k_a \equiv \sqrt{\mu P T_s N_m / 32\pi\rho^2 |Q_\ell| v_p} \tag{73}$$

is known, and that T, a_0, b(for sliding valves only), ℓ and d are to be found. The choice was first used by Brown [6] and appears to be reasonable. Note that because the definition of κ_a uses T_s, for the analysis purposes, rather than the actual switching time (although $T_{st}=T_s$ for seating valves), an iteration will be necessary in the case of sliding valves. However, T_s would likely be a function of a_0 (proportional to the one-quarter power) anyway, so an iteration is indicated in any case. Convergence of the iterations is rapid, fortunately.

Note further that, since the results are plotted as functions of the single parameter κ_a, one also can locate its optimal value. The substitution of

$$\sqrt{\frac{c_{qd}c_{sd}}{c_{td}}} = k_a \Omega \frac{(1+2b)^{1/4}}{\sqrt{r_R}} \tag{74}$$

and

$$c_{qd} = \frac{c_t r_I \Omega}{6\pi\alpha(1-\alpha)} \tag{75}$$

equations (45) , (46) and (47) recast as functions of c_{qd} and Ω , and equations (55) and (56) give the total dissipation p_d as a function of c_{vd}, c_{qd}, b (for sliding valves), Ω and α. The dependence on α , as can be seen in equation (75), is in terms of the factor $\alpha(\alpha-1)$ which is a parabola with a stationary point at $\alpha=0.5$ in the center of the region of interest. The factor changes by only four percent if $\alpha=0.4$ or 0.6 etc., and the effect on major results of interest is even less. Thus all remaining numerical results and plots assume $\alpha=0.5$.

After the value of α is chosen, only four variables remain: c_{qd}, c_{vd}, b and Ω. A four-parameter (numerical Newton-Raphson) optimization is carried out. The resulting optimal system is expressed in terms of Γ/T_{st}, b and two newly-defined dimensionless groups (which are more convenient than previous c_{qd} and c_{vd}). These groups are a valve size group

$$g_v \equiv \frac{a_o\sqrt{P}}{Q_\ell} = \frac{1}{c_{qd}c_{vd}} \tag{76}$$

and a tube-diameter group

$$g_d \equiv \frac{d^2}{\nu T_{st}} = \frac{r_I}{3\pi^2\alpha(1-\alpha)k_a^2 c_{qd}} \tag{77}$$

Two associated optimal properties of interest, Ω and

the dimensionless dissipation p_d, also can be given as functions of κ_a. A third, the Reynolds number for the time-mean flow Q_ℓ, cannot, but definition of the normalized viscosity μ (more in Section 8)

$$g_\mu \equiv \mu\sqrt{v_p/\rho N_m^3 PQ_\ell} \tag{78}$$

which depends on a subset of the parameters giving κ_a, gives

$$Re = (\sqrt{2\pi^3\, g_d}\;\; g_\mu k_a)^{-1} \quad . \tag{79}$$

As can be seen from Figures 9 and 10, whether the flow is laminar (Re<2000) or turbulent depends almost exclusively on g_μ. It is seen that $\sqrt{g_d}\kappa_a$ is almost a constant for a specified g_μ. For the optimal solutions, turbulent flow occurs virtually whenever $g_\mu < 1.3*10^{-4}$, and laminar flow results otherwise. Practical limits for ρ, v_p, μ and N_m therefore imply, through equation (78), that laminar flow is indicated only for fairly low power (small PQ_ℓ) applications.

The total dissipation functions p_d above were minimized for particular values of g_μ and κ_a to give optimal values of Γ/Γ_{st}, g_v, g_d, b and Ω. A Newton-Raphson iteration procedure was used, which required considerable

effort particularly in turbulent flow because of the complexity of the needed first and second partial derivatives of p_j. Convergence, however, was rapid from a broad range of starting guesses. The iteration of Ω was handled seperately and interactively to avoid excessive analytical complication.

The optimization process has been applied to both seating and sliding valves for both laminar and turbulent flow. Four different values of g_μ ($1.3*10^{-4}$, 10^{-4}, 10^{-5}, 10^{-6}) have been used (which can also be interpreted as four different levels of turbulence). Even though the region of principal interest, from bandwidth considerations, is expected to be $10 \leq T/T_{st} \leq 40$, the energy dissipation has also been minimized (when a minimum exists) with no constraint imposed on the bandwidth. Larger values of T/T_{st}, however, would mean longer cycle times and less bandwidth since T_{st} is probably nearly fixed by the valve design (more in Section 8) and the constraints for $T/T_{st} < 10$ have already been discussed before. The "no-constraint" minimization for seating valves has given the results plotted in Figures (11) through (14). The corresponding optimization attempts for the sliding valves showed that the minimizing values of b are mostly out of the range of practical interest ($0. \leq b \leq 2.$); therefore the results are not plotted.

For all the minimum dissipation solution plots (with or without constraints), the following range for K_a has been chosen:

$$4*10^{-4} \leq k_a \leq 0.04 .$$

The results are not shown for $K_a > 0.04$ since the losses are excessively large. They are also not shown for $K_a < 4*10^{-4}$ since simple extrapolation applies there. Consequently, the curves represent virtually all cases of potential interest.

In Figures (11) through (14) which give the "no-constraint" minimization results for seating valves , the dissipated power can be seen to be less for laminar flow than turbulent flow if K_a is fixed. This may be misleading, however. If the viscosity μ is decreased while the other parameters in K_a are held constant, both K_a and g_μ decrease. When g_μ reaches about $1.3*10^{-4}$ the flow becomes turbulent, and the operating point jumps from laminar to turbulent flow with $g_\mu=1.3*10^{-4}$. The jump in the dissipation is modest, however, and continued decrease in μ reduces the losses below the laminar minimum. Thus deep penetration into the turbulent regime gives less loss than high Reynolds number laminar flow.

One could extend the useful range of laminar flow by

using two or more parallel tubes, or better by using a rectangular cross-section with adequate aspect ratio. Such a costly possibility would have a very restricted domain of advantage over the outright use of turbulent flow in a single tube, however [3]. Excessive transition between laminar and turbulent regimes, which might result from changing load flow Q_ℓ, ought to be avoided. Nevertheless such a transition should cause a rather small effect on the control dynamics, presumably less than is apparent for the dissipation, since the dynamics depend more on I (which changes little) than R (which affects the dissipation).

Reducing K_a also results in larger values of T/T_{st} for both laminar and turbulent flows. For the reasons discussed above, however, these plots are useful in a rather narrow range of K_a values. The bandwidth gets very small for $K_a < 0.003$, especially when laminar flow is being used. For very high Reynolds number turbulent flow ($g_\mu = 10^{-6}$), however, the optimal bandwidth values (therefore T/T_{st}) are quite applicable (going into the region with $f/T_{st} < 10$ is not recommended, however). The frequency of oscillations, ω, and the valve size, a_0, also are quite sensitive to the Reynolds number. For high Reynolds number turbulent flows (small g_μ) the valve becomes smaller for laminar flow, while the diameter of the tube seems to stay nearly the same for both flows in

the region of principal interest. It should be noticed, however, that when the transition from laminar to turbulent flow (or between different levels of turbulence) occurs due to the decrease in μ, this region of interest, too, changes (because K_a is also changing).

As seen above, the "no-constraint" minimization gives, for most of the region of interest, excessively large values of T/T_{st} (too small a bandwidth). For sliding valves, this minimization becomes even less relevant because of the impractical values of b. This suggests, then, that the designer should specify T/T_{st} (or at least a range) before the minimization of dissipation is carried out, trading dissipation for bandwidth or viable modulation. Further results are obtained, then, through an optimization with a constraint on T/T_{st}. In the region that seems to be practical, the author has carried the optimization with T/T_{st}=10,20,30,40. The results for the seating valves are plotted in Figures (15) through (34). For sliding valves, the results, which are possible to obtain in this case, are plotted in Figures (35) through (54). All the results obtained for constrained T/T_{st}, for both laminar and turbulent flows and with $g_\mu = 1.3*10^{-4}, 10^{-4}, 10^{-5}, 10^{-6}$, are given in 40 plots.

After specifying the type of the valve, the type of the flow (g_μ) and K_a, which represents the fluid to be

used (μ,ρ) and some of the system characteristics (T_s, P, Q_ℓ, N_m, v_p^*), the designer easily can get the optimizing values for the remaining parameters by using one of these plots. After the choices mentioned above, the number of relevant plots reduces to four. Either he uses one of these plots directly, or he uses a simple interpolation according to his choice of bandwidth. If he is using seating valves, he also has the option of using the Figures (11) through (14) as long as the results give an acceptable value of T/T_{st}.

The first 20 plots, which are for seating valves show that the optimal valve size stays nearly the same for any g_μ and K_a, once the bandwidth is chosen. (This is especially true for smaller K_a, as the curves approach to the same asymptote for laminar and turbulent flows.) However, the smaller the bandwidth (larger T/T_{st}), the larger these asymptotes.

The dissipated power curves, for a specified T/T_{st} and smaller values of K_a, again have the same asymptotes for both laminar and turbulent flows. The cases with large values of K_a give such large losses as not to be of interest. When the bandwidth is decreased (larger T/T_{st}) the asymptotic values for p_d get smaller.

One might be tempted to generalize from these results

for small values of k_a, that if one specifies a small bandwidth and fixes all the remaining parameters of the system, increasing the size of the valve (larger g_v) always decreases energy dissipation. This is wrong, however. When a smaller bandwidth is specified, a longer cycle time T is obtained and the actual energy dissipation becomes larger since

$$\varepsilon \equiv p_d * P |Q_\ell| T \tag{80}$$

according to the definition.

The optimal tube diameter, on the other hand, is not affected much by the bandwidth specification and the type of the flow in use.

The quest for futher minimizations in the energy dissipation makes the idea of using sliding valves very attractive. The next step, then, is to apply the same optimization on the sliding valves. The constraints on the bandwidth and the very same range for k_a are maintained (even though the definition of k_a includes T_s, the principal range of interest would change very little, however).

A quick glance on the remaining 20 plots, show, first of all, that the optimal parameters of the valve (except

b) and the tube are quite similar to those obtained by using seating valves. Another interesting and important result is that, for large values of K_a, whatever the value of the bandwidth, the optimum values of b are so small the valve is virtually a seating valve. Making b large enough to warrant the name "sliding valve" would increase the losses which are already large. For these cases the designer might well use the results given in Figures (11) through (34).

When the g_v curves are examined carefully, it can be seen that g_v stays nearly the same throughout the whole range of K_a for both types of flows. The additional valve parameter b, however, is quite sensitive to changes in K_a. The smaller K_a, the larger b. Increasing T/T_{st} gives even larger values for the optimal b (for smaller K_a); these curves do not depend on the type of the flow. Decreasing the bandwidth also causes g_v (or a_0) to increase as it is the case for seating valves.

In the region where sliding valves are attractive ($K_a < 0.02$) and T/T_{st} is relatively small, the optimal a_0 gets larger than its value for seating valves even though using the sliding valve increases the effective orifice area. This is not the general trend, however. When the sizes of the two types of optimal valves are compared, it is seen that this increase gets smaller with a larger

T/T_{st} (which gives a larger b).

The curves for minimum p_d have the same shape for both seating and sliding valves revealing less energy dissipation for smaller k_a. For a larger k_a, there is simply no way to get futher minimization than already obtained with seating valves. The curves again approach the same asymptote independent of the type of the flow. It is clear that p_d becomes less by specifying a larger constraint for T/T_{st} via using a larger b. We do not want to have too small a bandwidth or too large a b, however; this trade-off is discussed further in Section 8. The curves for the dimensionless frequency Ω and the optimal tube diameter d remain more or less the same when they are compared to the respective ones for seating valves, although the changes in Ω are not insignificant.

The value of the compliance C is the final issue to be resolved. The D/A conversion occurs because of the natural frequency

$$\omega_n = \frac{1}{\sqrt{IC}} \tag{81}$$

where I is the inertia of the narrow channel and C is

$$C = \frac{V}{\beta} \tag{82}$$

where V is the volume of the load chamber and β is the effective bulk modulus.

If $\omega_n T$ is small ($\omega_n T \leq 2$), the pressure in the cavity does not vary much in a single cycle, compared with P, so it can be said that D/A conversion occurs in the fluid impedance [3]. The behavior then is relatively simple and predictable, which is crucial from a control point of view, and the losses are small, especially when the resistance and consequently ζ are small. Thus we are left with only the requirement

$$C \geq \frac{T^2}{4I} \quad . \tag{83}$$

Examined more closely, the maximum change in the load pressure decreases as C is made larger. If this change is too large (violates the inequality) the assumptions for the analysis become invalid and the actual behavior becomes excessively complicated. If on the other hand the change is very small, the system bandwidth suffers directly. The best compromise might be about $C=T^2/I$ (this corresponds to $\omega_n T=1$ and the corresponding flow is given in Figure 2b of [3]), although other considerations also can enter. These considerations include the minimum load volume the designer is stuck with, and the load stiffness which is inversely proportional to C.

8. APPLICATION TO GEOMETRICALLY SIMILAR VALVES

A characterization of geometrically similar valves permits the virtue of different designs to be compared, independent of the individual size or material, and permits a particular valve to be scaled optimally for a particular application [11]. For this purpose, some characteristic length (perhaps a key diameter) of members of such a family and the material density are defined as ℓ_0 and ρ_s, respectively. The new dimensionless groups are defined by Brown [11], as follows:

A dimensionless group which relates the valve opening parameter a_0 to ℓ_0 is defined as

$$g_a \equiv a_0\sqrt{\rho}/\ell_0^2 \quad . \tag{84}$$

Another dimensionless group is sought to characterize the switching time, T_{st}. The mass of the moving part is proportional to $\rho_s \ell_0^3$, the force producing motion is proportional to $P\ell_0^2$, and the total displacement is proportional to ℓ_0. Assuming constant acceleration, then, the dimensionless group is taken as

$$g_s \equiv T_{st}\sqrt{P}/\ell_0\sqrt{\rho_s} \quad . \tag{85}$$

The virtue of these dimensionless groups is that they remain constant as ℓ_0 changes. They cannot be used directly to compare different designs, but the ratio

$$g_s/\sqrt{g_a} = T_{st}\sqrt{P}/\sqrt{a_o \rho_s \sqrt{\rho}} \quad (86)$$

can because it is independent of the (arbitrarily defined) length ℓ_0. The smaller this ratio, the faster the valve for a given effective size.

It is convenient to make further nondimensionalizations with respect to parameters that are most likely predetermined in a particular application. These parameters are taken to be the fluid properties ρ and β and the power (PQ_ℓ). The quantities being nondimensionalized are the length ℓ_0, the pressure P, the cycle time T, the viscosity μ and the density of the moving part ρ_s. They have been defined in [11] as follows:

$$g_\ell \equiv \ell_o \beta^{3/4}/\rho^{1/4}\sqrt{PQ_\ell} = \ell_o\sqrt{V_p{}^3\rho/PQ_\ell} \quad (87)$$

$$g_p \equiv P/\beta \quad (88)$$

$$g_t \equiv T\beta^{5/4}/\rho^{3/4}\sqrt{PQ_\ell} = T\sqrt{V_p{}^5\rho/PQ_\ell} \tag{89}$$

$$g_\mu \equiv \mu\beta^{1/4}/\rho^{3/4}\sqrt{N_m PQ_\ell} = \mu\sqrt{V_p/\rho N_m PQ_\ell} \tag{90}$$

$$g_\rho \equiv \rho_s/\rho \tag{91}$$

The predefined k_a then becomes

$$k_a = \sqrt{\frac{N_m{}^{3/2}\, g_s g_\mu}{32\pi(1+2b)^{1/2}}\,(g_\rho{}^{1/2}\, g_p{}^{3/2} g_\ell)} \tag{92}$$

The minimum dissipation at particular values of T/T_{st}, g_μ, and k_a implies a particular valve size

$$g_v = g_a g_p{}^{3/2} g_\ell{}^2 \ . \tag{93}$$

Thus, if both g_a and g_p are assumed given, only a unique value of g_ℓ will give the proper value of g_v, and the solution is unique. (The same is true if g_ℓ is assumed given; then a unique value of g_p results.) Note that once

P and ℓ_0 are known, T_{st} is found from the knowledge of g_s, and T from the knowledge of T/T_{st}. Note also that as the ratio T/T_{st} is varied from its lower limit of about 10 to its upper limit of the unspecified value, T gets longer (undesired) while the efficiency increases (desired). This is the trade-off between bandwidth and efficiency.

The dimensionless cycle time becomes

$$g_t = \left(\frac{g_s}{\sqrt{g_a}}\right)\left(\frac{T}{T_{st}}\sqrt{g_v}\right)\left(\frac{g_\rho^{1/4}}{g_p^{5/4}}\right) \qquad (94)$$

The first factor in parantnesis is an exclusive function of the design of the valve but is independent of its size, as pointed out in the text referring to equation (67). Over most of the region of interest, g_v is almost exclusively dependent on T/T_{st}, so the second factor in paranthesis is almost a function of T/T_{st}. The equation, then, clearly reveals how pressure (through g_p) affects the cycle time.

The dissipation number p_d is a function of T/T_{st}, g_μ and κ_a. For much of the region of interest, however, particularly for the smaller values of g_μ, the values of p_d are asymptotic to a simple function of T/T_{st}. In this case, therefore,

$$p_d = \psi\left[\frac{g_t g_p^{5/4}}{\sqrt{g_\rho}\ (g_s/\sqrt{g_a})} \right] \quad . \qquad (95)$$

These functions $\psi[\ ]$, for both seating and sliding valves, are plotted in Figure 55 and represent the minimum possible dissipation. A trade-off between minimum energy dissipation and cycle time is clearly revealed by these plots. The effect of the other parameters is indicated by the definition of the abcissa.

9. CONCLUSION

This research is intended to specify a system (valve plus tube) to satisfy reasonable requirements of dynamic response and energy dissipation. Different classes of switching valves have been used and the idea of the D/A conversion in the fluid impedance coupling between the valve and the load [3] has been adapted.

Dissipation (with smooth performance and acceptable bandwidth) is affected largely by the viscosity of the fluid in use. Therefore a very broad range of viscosity is treated, including both laminar and turbulent flow regimes, so the results can be applied to any high or low power system.

Handling the turbulent flow is not a simple endeavor, however, for the resistances become highly nonlinear and the role of inertance is substantially reduced. The analytical model for wave propagation in tubes with turbulent flow proposed by Brown, which was never done completely in the literature before, has been used.

Another dominant factor in the energy dissipation, in addition to the viscosity which has already been mentioned, is the switching time, and the small dissipation is made possible by small values of T_{st}. Therefore using an appropriately designed tube connecting

an appropriately sized and sufficiently fast switching valve to a load can deliver significantly higher power than use of the obvious alternatives.

The work has used both seating and sliding valves. The desire to greatly reduce or eliminate the short-circuit flow path between supply and tank inherent in the constant-area-sum valves (seating valves assumed herein) introduce the use of sliding valves. The results indicate an advantage , particularly when κ_a is small, for sliding valves; the real problem is economical design, however (small advantages might be outweigned, of course, by practical design considerations). When κ_a gets large enough the losses become excessive (even for the minimum acceptable value of T/T_{st}) whether a sliding or seating valve is used, although the latter is close to the optimum. The trade-off between the efficiency and economical design, however, is not the subject of the research. Therefore no prejudice against seating valves is intended.

All the results obtained in the research are expressed in terms of dimensionless groups of parameters. The universal design charts are used by choosing the predefined parameters κ_a, g_μ ([6,12] respectively) and T/T_{st}. To specify the optimal system, the designer determines the acceptable ranges for these parameters, and

then pinpoints the optimal design on the given charts from which the remaining parameters are deduced.

The next step in the development of optimization procedures presumably would be the extension of the studies to entire anticipated duty cycles, using equations (71) and (72) and related equations to predict the energy dissipation including the non-optimal conditions. Some characteristics of the changes in actual instantaneous flow have been obtained by multiplying the equation (71) by $Q_\ell/Q_{\ell r}$, where $Q_{\ell r}$ is a constant reference load flow for the optimal or design condition and Q_ℓ is the actual instantaneous flow. Note that the definition of the nondimensional dissipated power now changes to

$$p_d \equiv \frac{\varepsilon}{PQ_{\ell r}T} \tag{96}$$

The changes in p_d have been examined for low power systems (laminar flow), which is the easier case. Figures (56) and (58) for seating and sliding valves, respectively, show that the dissipation is less when the system is in its null state. Figures (57) and (59), on the other hand, reveal that for $0 \leq Q_\ell/Q_{\ell r} \leq 2$, the ratio of $\varepsilon/\varepsilon_n$ (or p_d/p_{dn}) remain almost the same for any K_a. The results with seating valves (Figures 56 and 57) have been obtained with no constraint on the bandwidth of the system. The ones with sliding valves (Figures 58 and 59), however,

have been obtained by imposing a constraint on bandwidth ($T/T_{st}=40$). As can be seen from Figure 59, in the range for $Q_\ell/Q_{\ell r}$ given above, an important deviation occurs for large κ_a values and this is because the constraint used is far from being optimal for those large values of κ_a. Figures (35) through (38) show that the optimal bandwidth for large values of κ_a is much larger ($T/T_{st}\cong 10$) even though losses are still unacceptable.

Figures 57 and 59 (to be used with the asymptotic null state values obtained from the previous ones) might simplify the process of finding the global minima of the dissipation regarding the entire duty cycle.

The analysis, however, might be extremely difficult for turbulent flow, since changing Q_ℓ would change both g_μ and the governing equations (as laminar flow would probably occur at null).

FIGURES 1-59

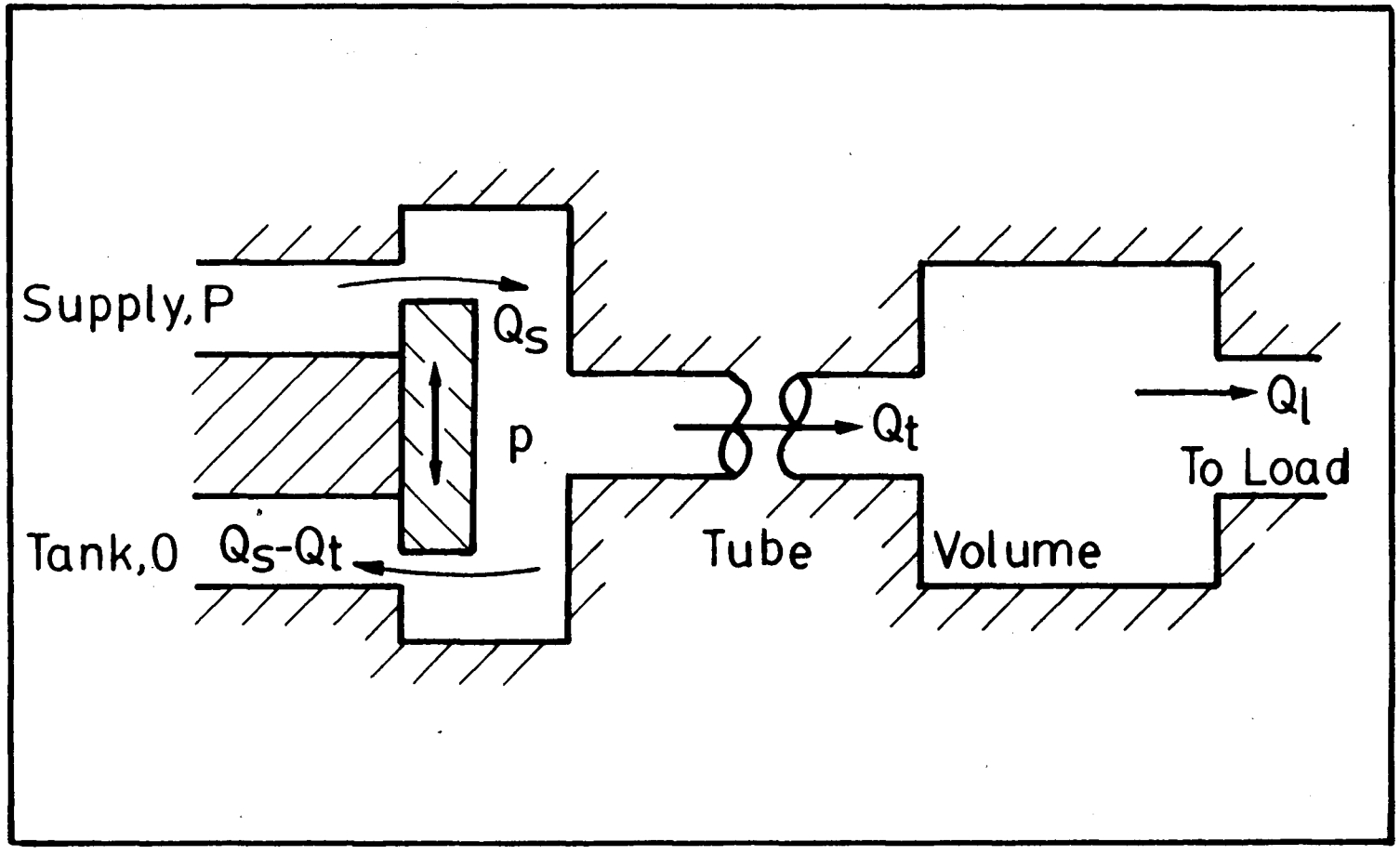

Figure 1. Hydraulic PLM Circuit

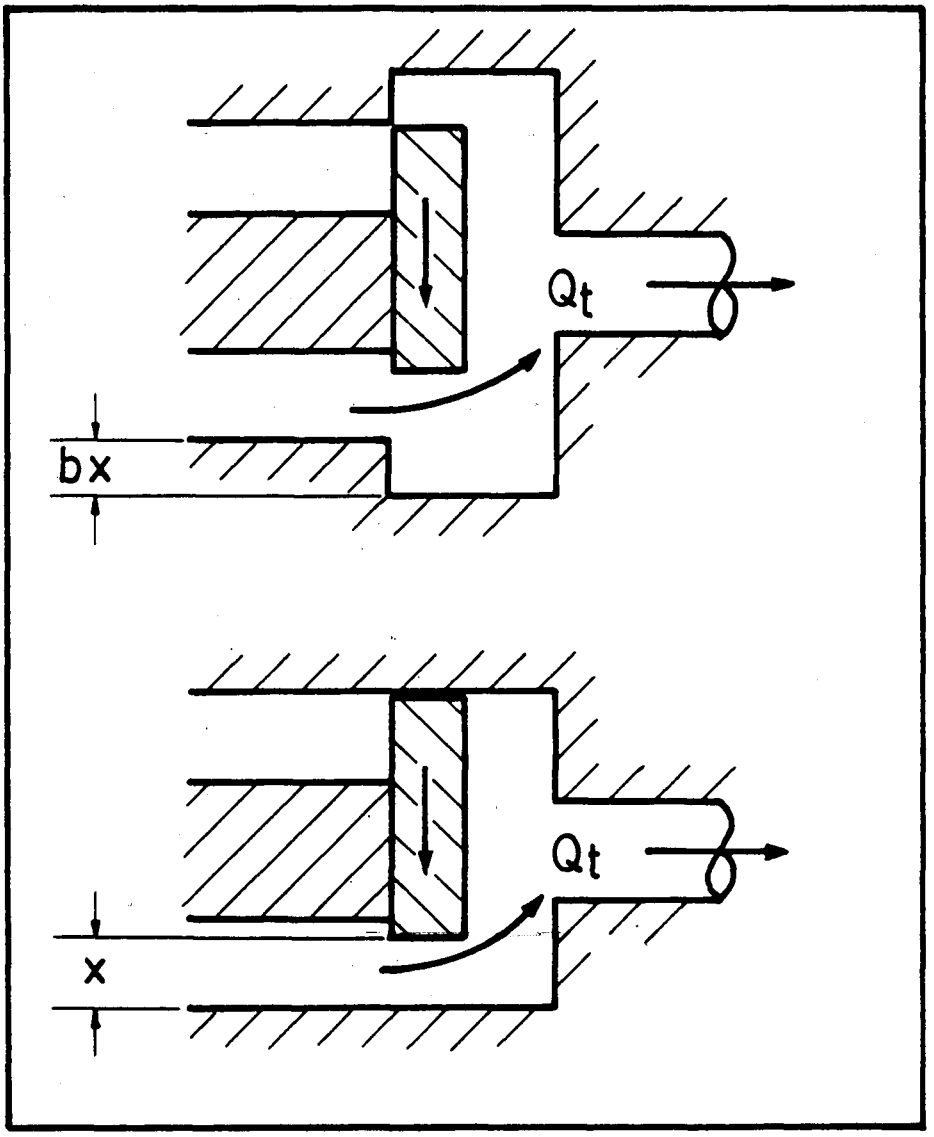

$a_o = f(x)$

maximum orifice areas :

seating valve : a_o

sliding valve : $a_o(1+b)$

Figure 2. Sliding Valve vs. Seating Valve

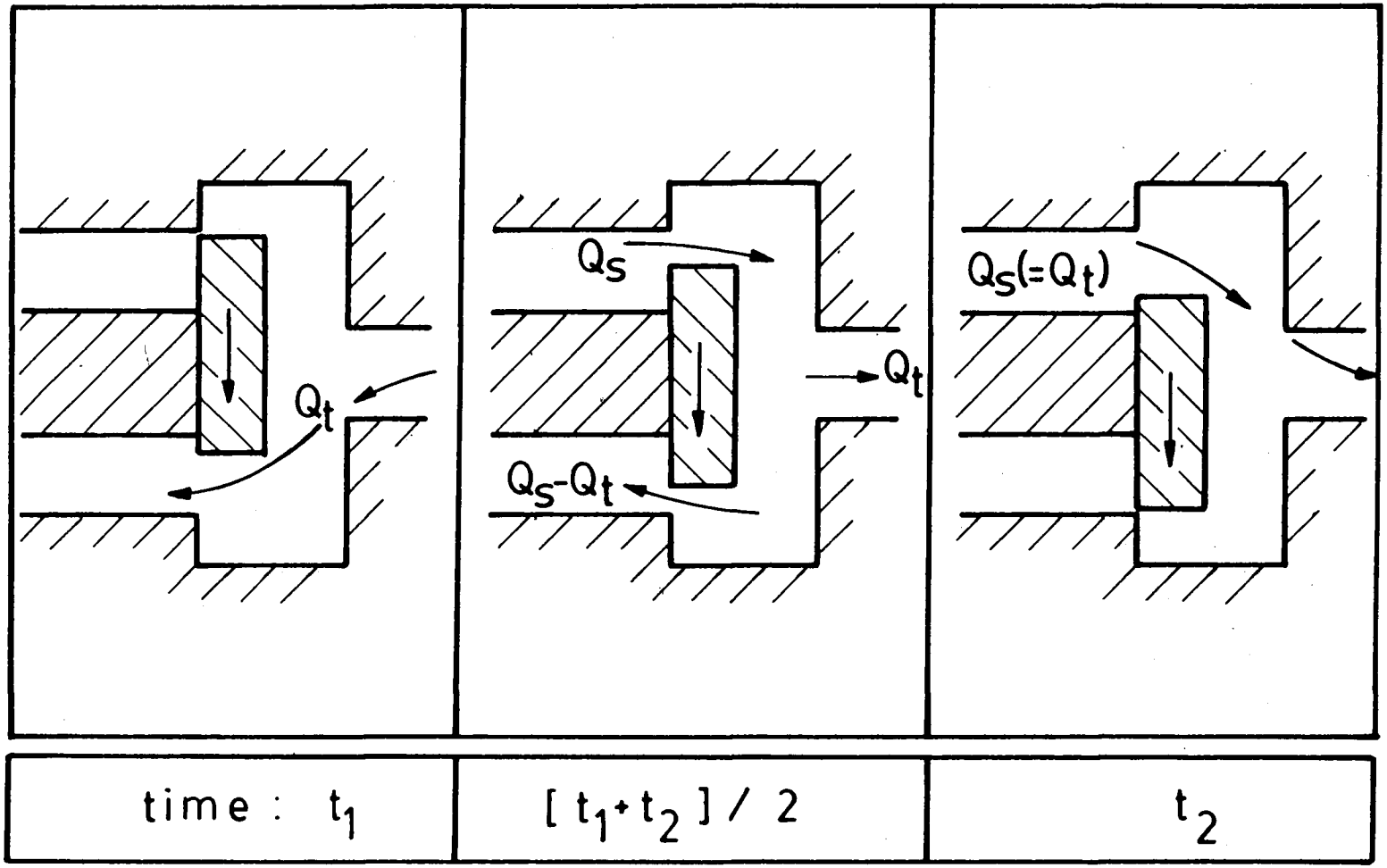

Figure 3. Sliding Valve During Switching

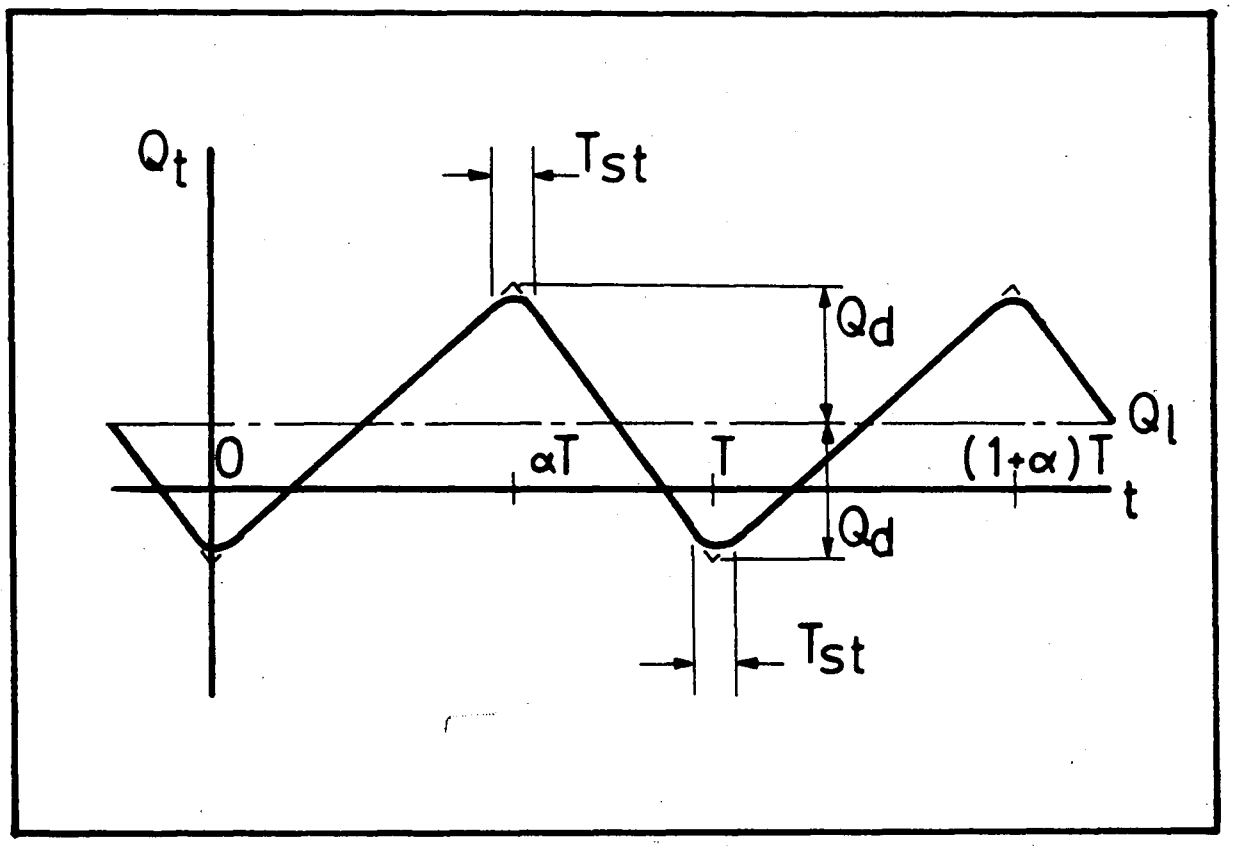

Q_t : volume flow through tube
Q_l : mean load flow
Q_d : amplitude flow perturbations
T_{st} : switching time
T : cycle time

Figure 4. Assumed Tube Flow, Fluid Impedance D/A Mode

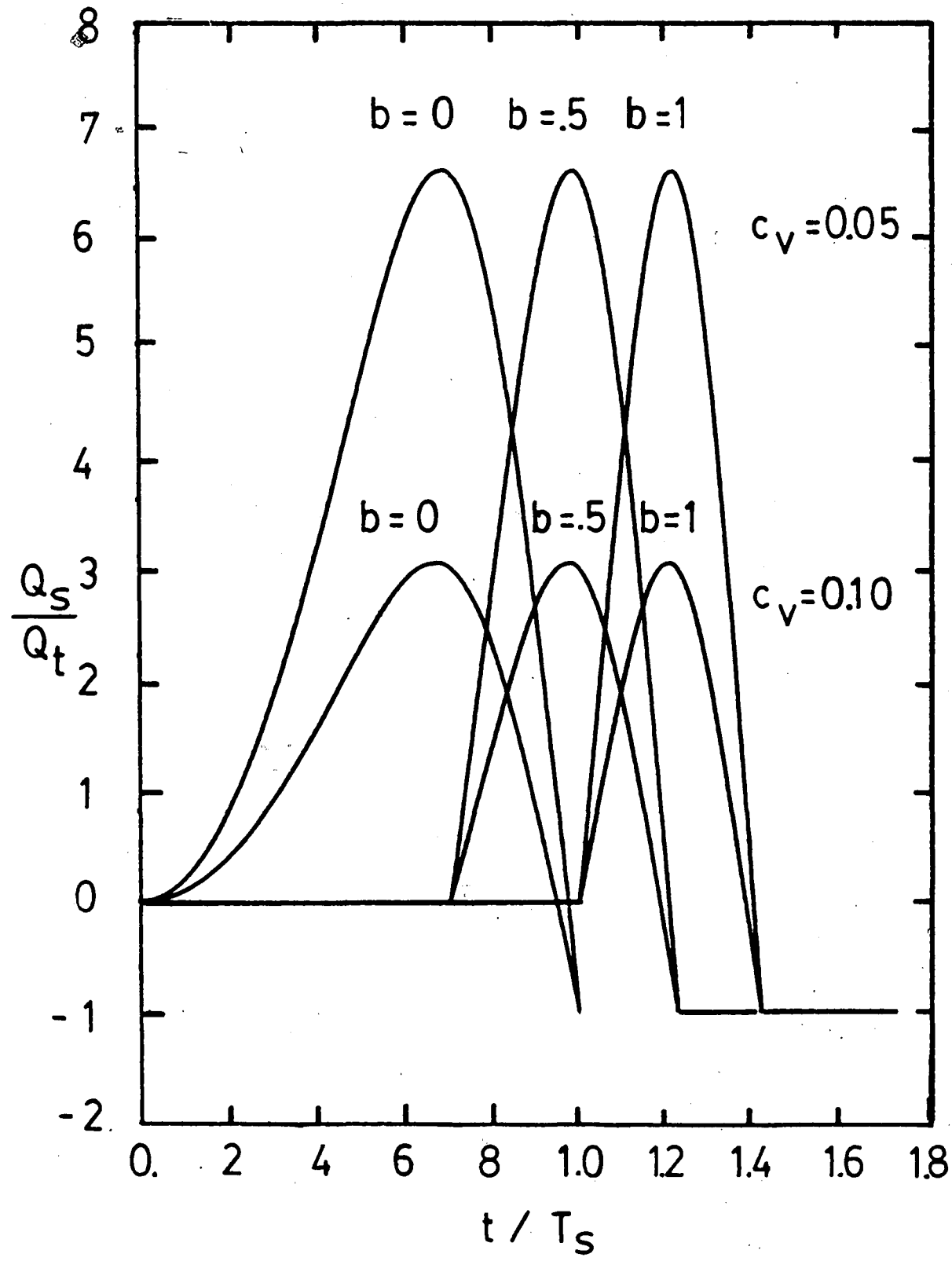

Figure 5. Typical Surge Flows Through Wave During Switching.

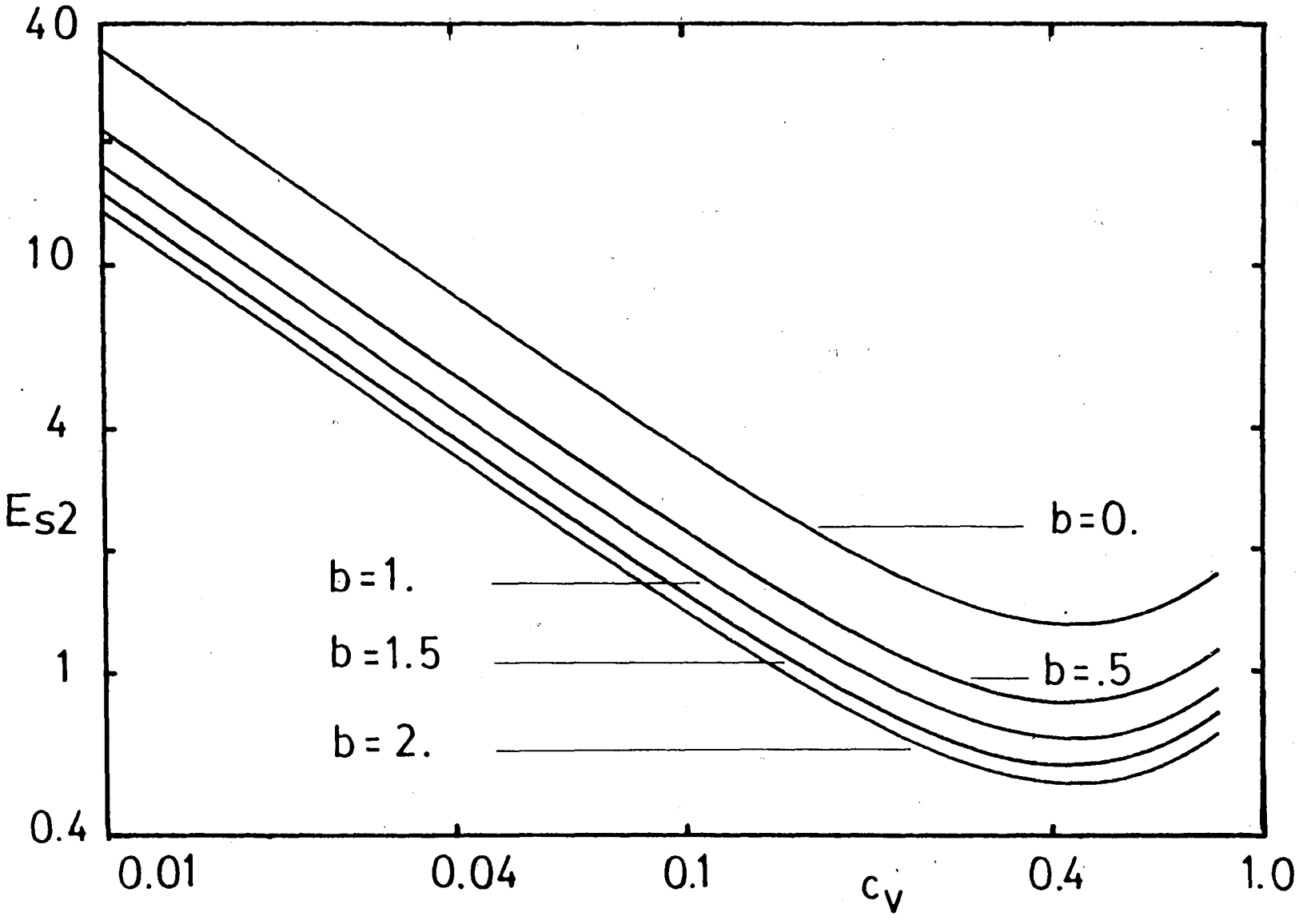

Figure 6. Energy Dissipation During Switching While Both Ports are Open (Zero Load Flow)

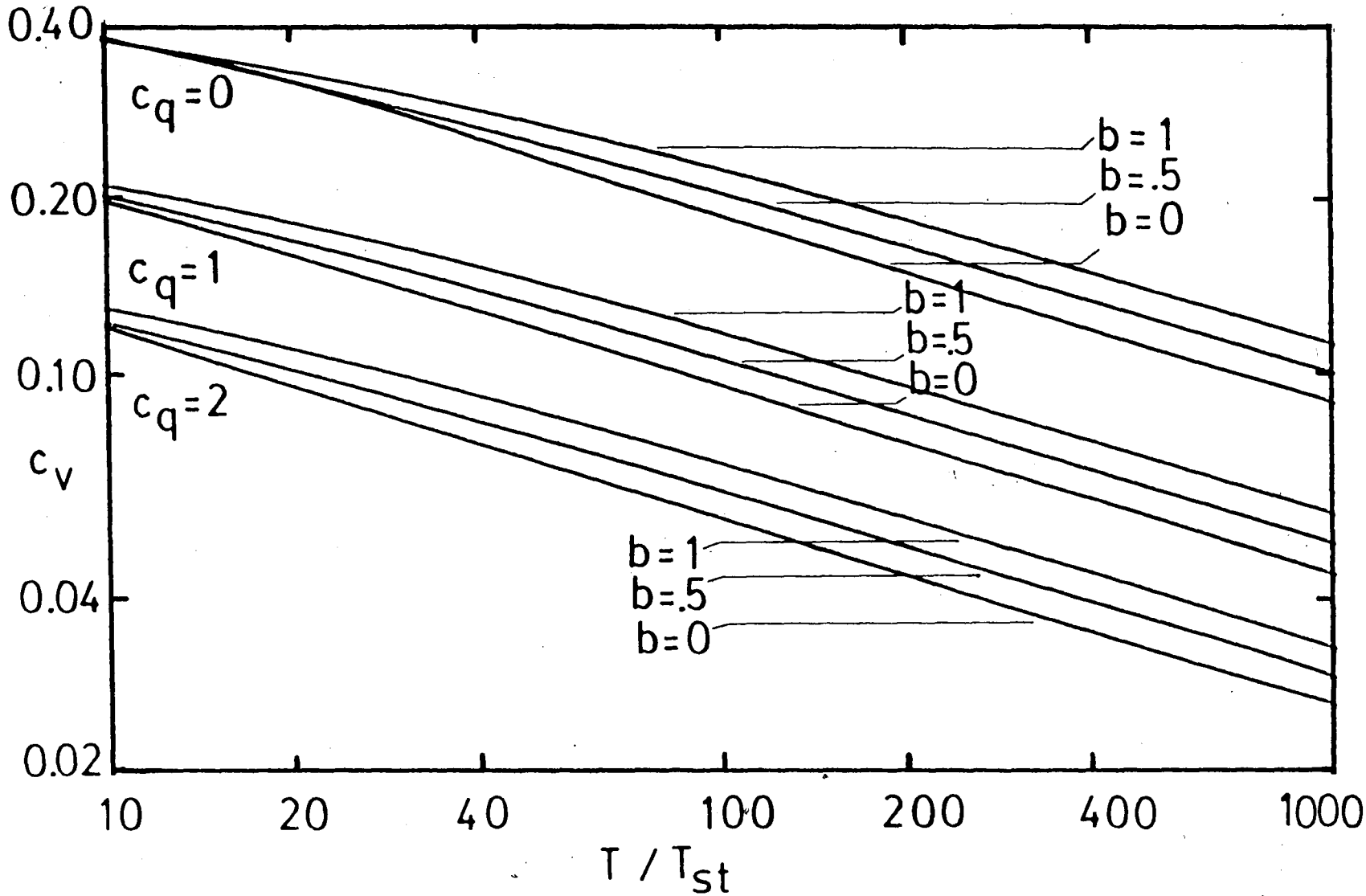

Figure 7. Valve Size for Minimum Cycle Dissipation

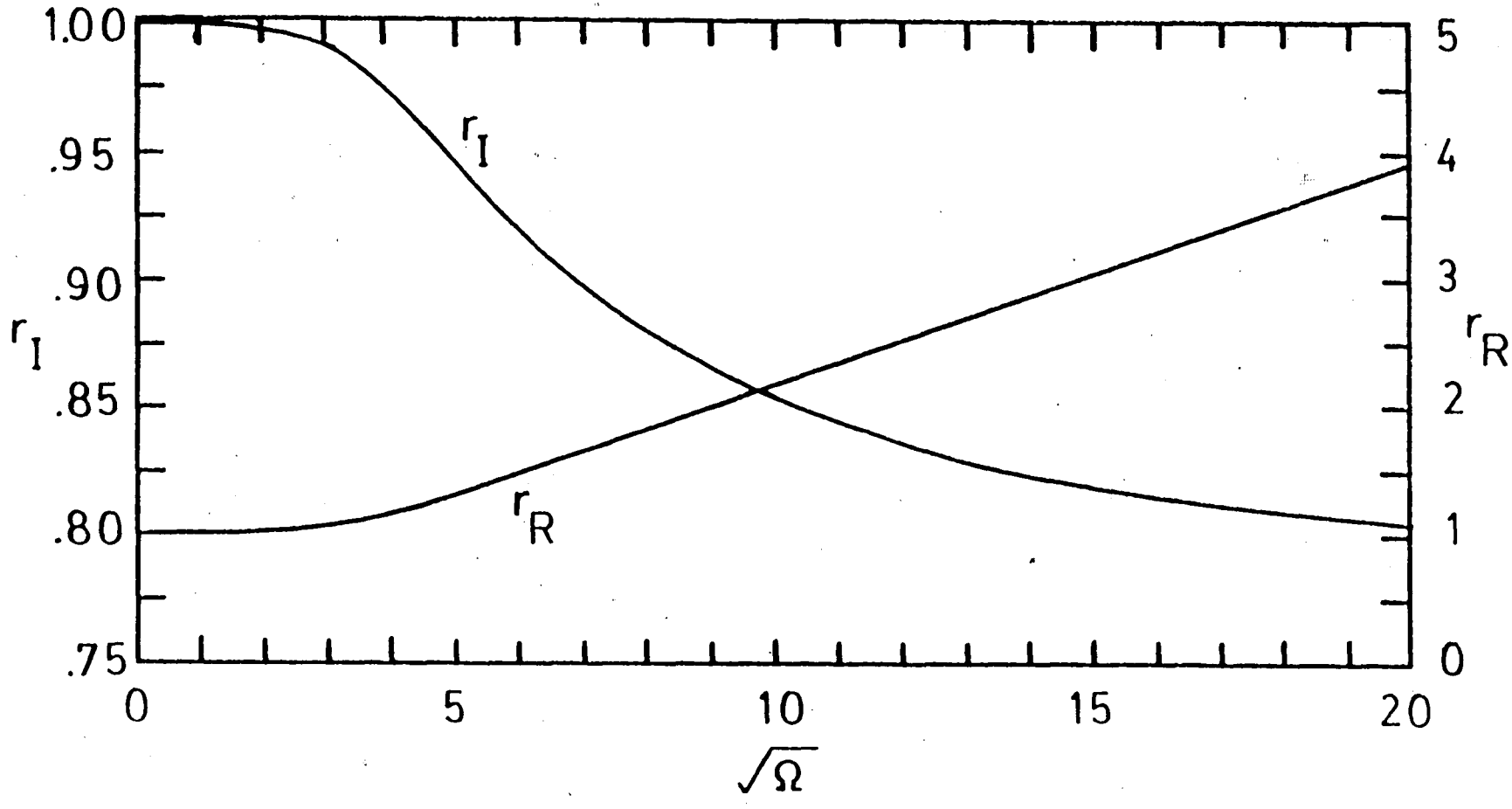

Figure 8. Resistance and Inertance for Sinusoidally Varying Flow in a Circular Tube

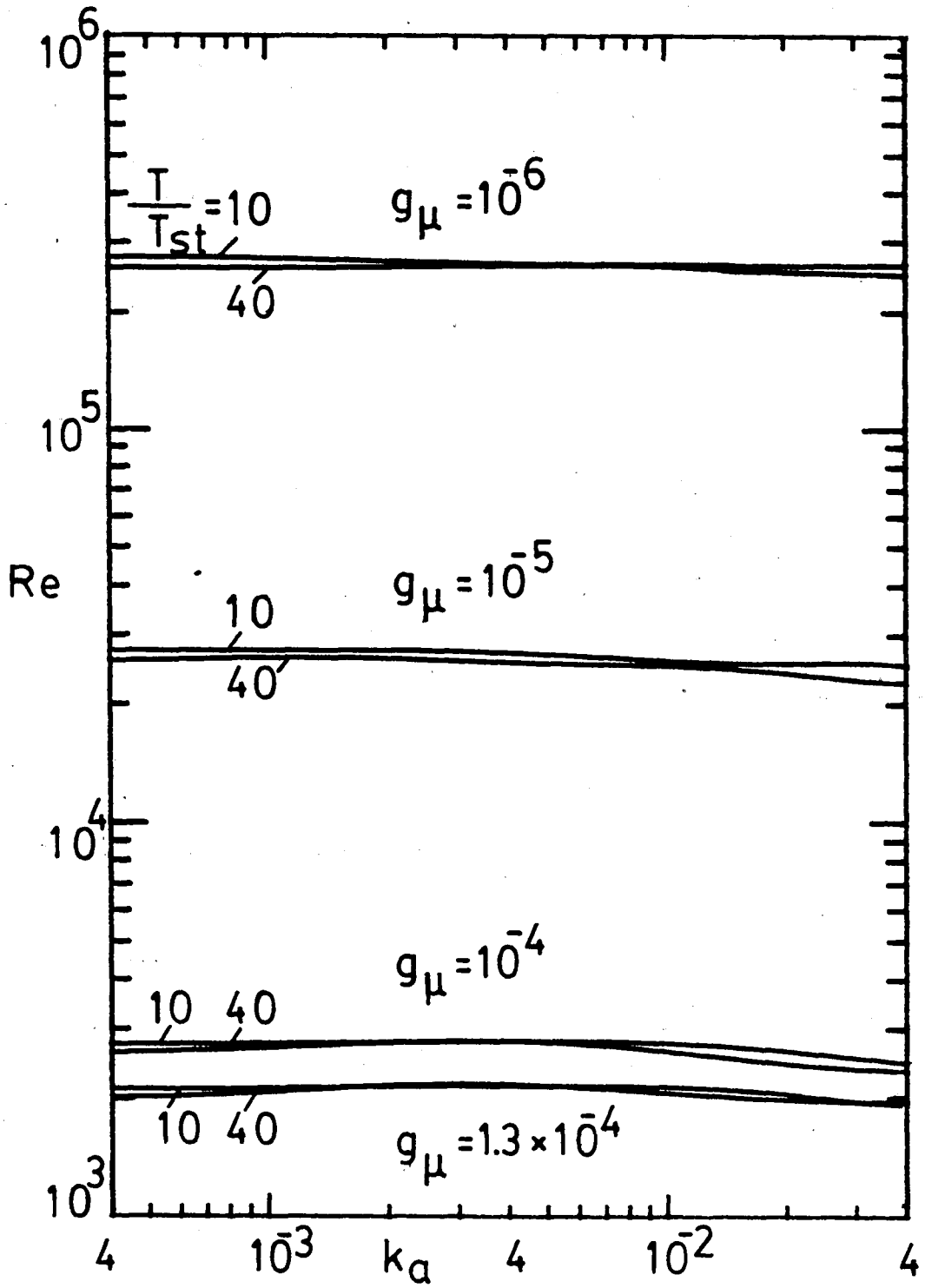

Figure 9. Reynolds Number Corresponding to Optimal Solutions, Seating Valve.

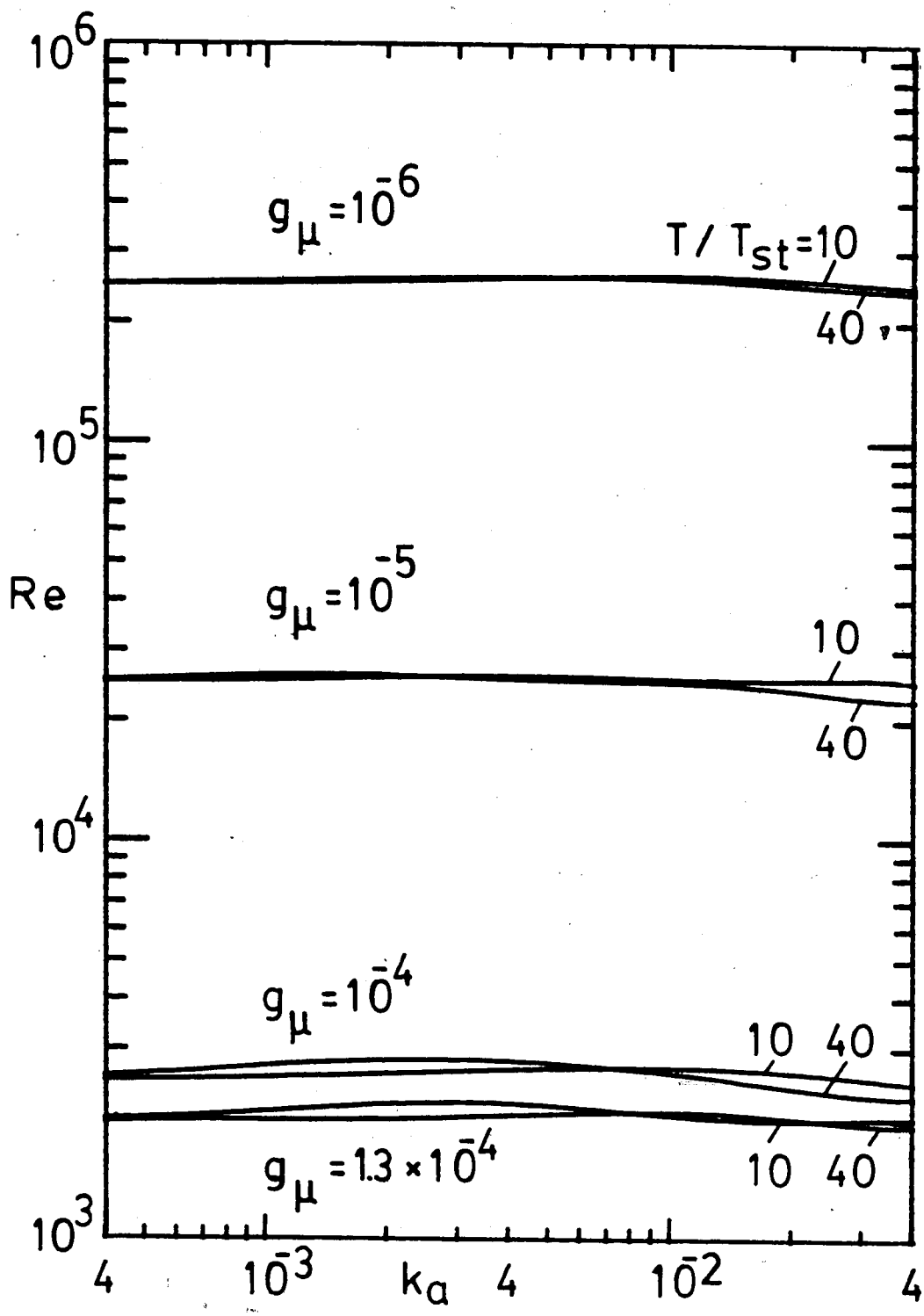

Figure 10. Reynolds Number Corresponding to Optimal Solutions, Sliding Valve.

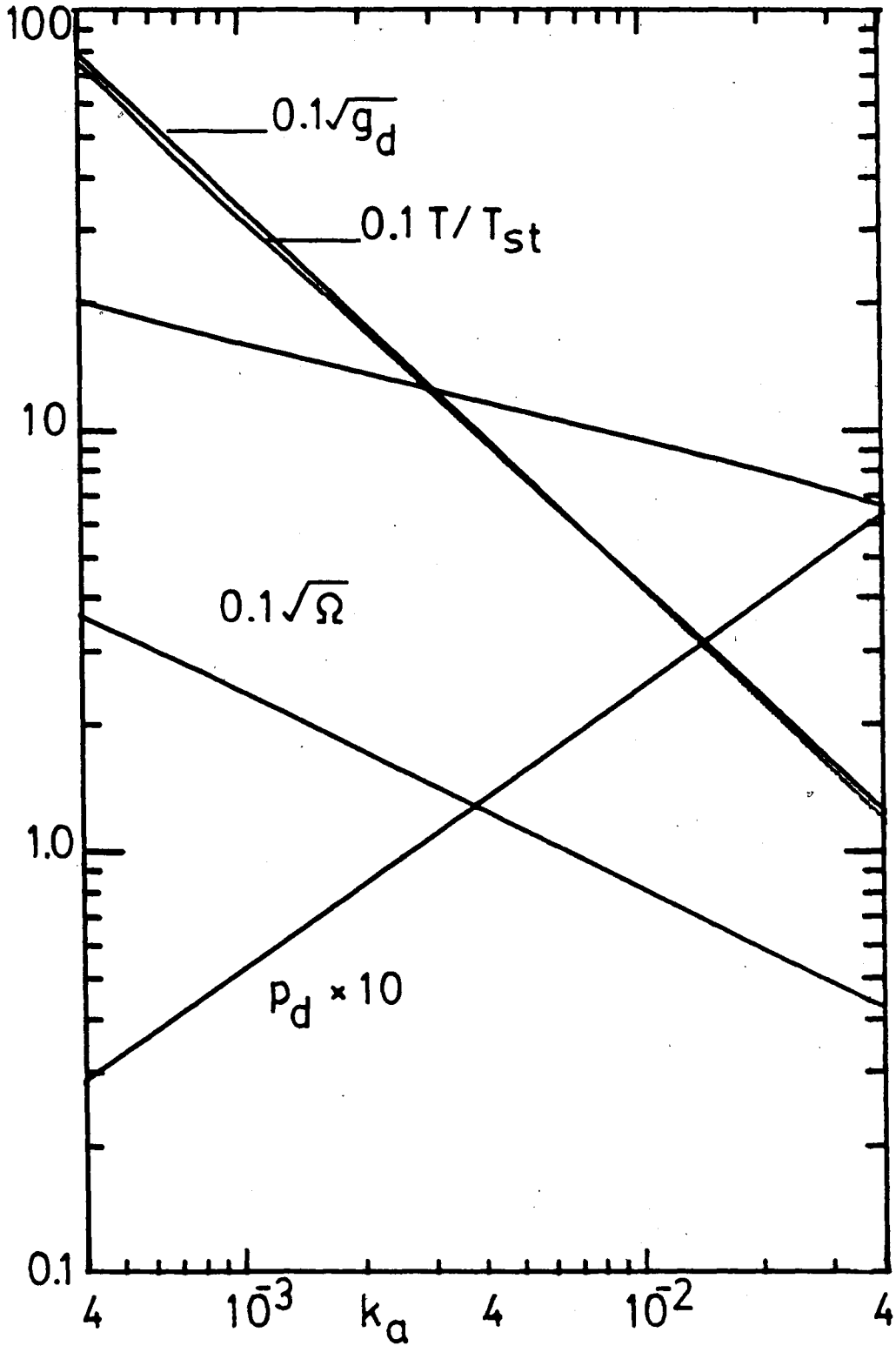

Figure 11. "No-constraint" Minimum Dissipation Solution Laminar Flow, Seating Valve.

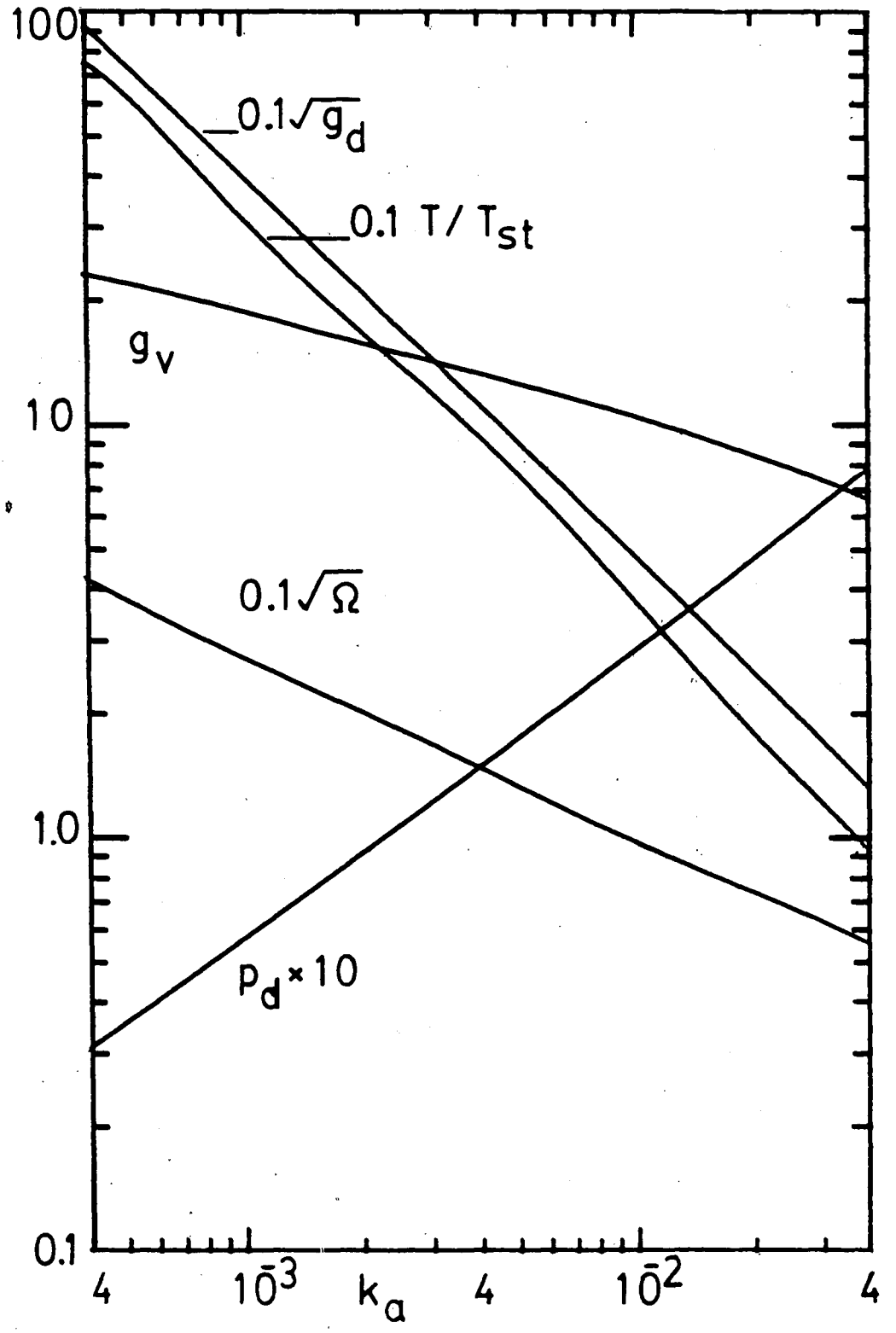

Figure 12. "No-Constraint" Minimum Dissipation Solution $g_v = 1.3*10^{-4}$, Seating Valve.

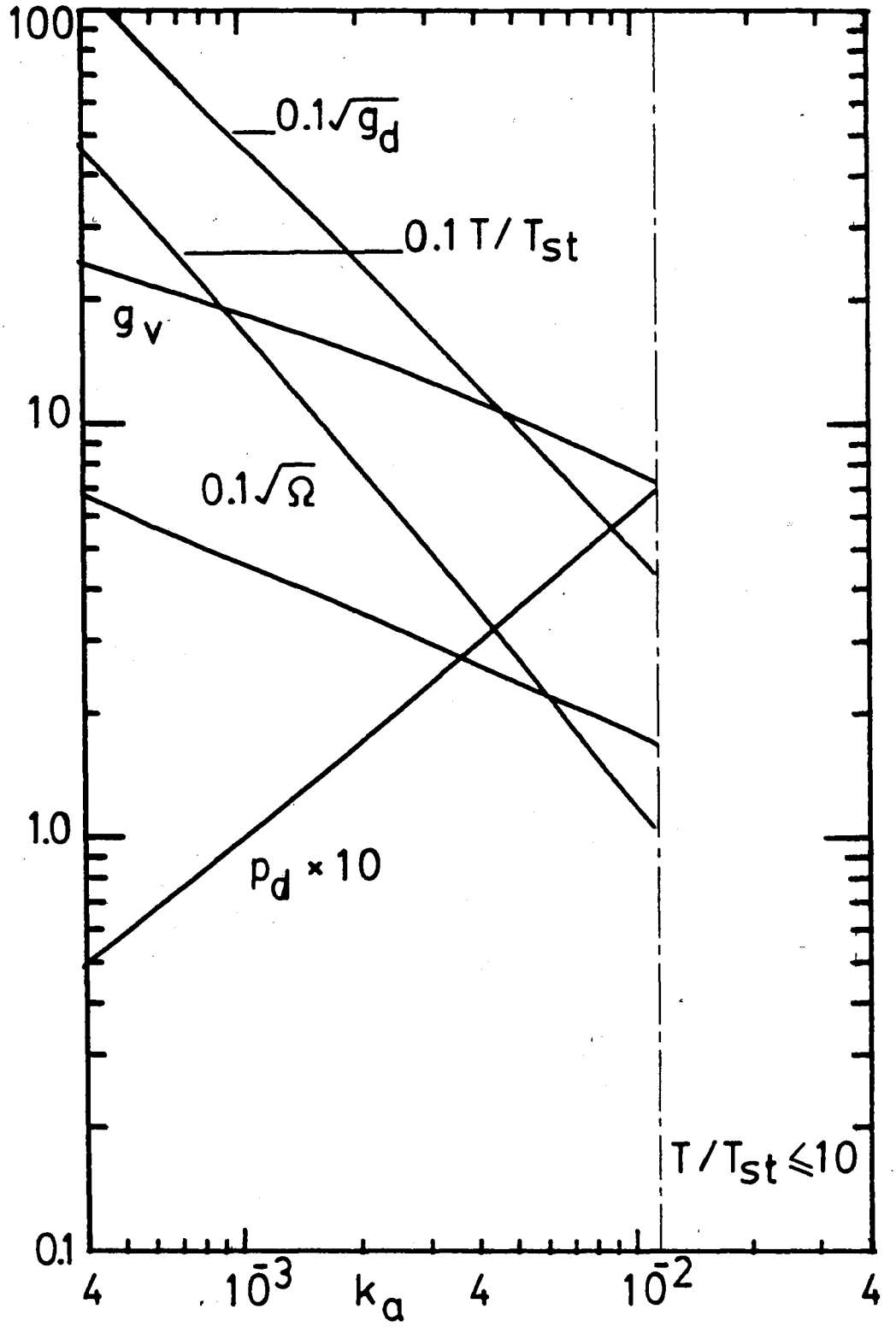

Figure 13. "No-Constraint" Minimum Dissipation Solution $g_\mu = 10^{-5}$, Seating Valve.

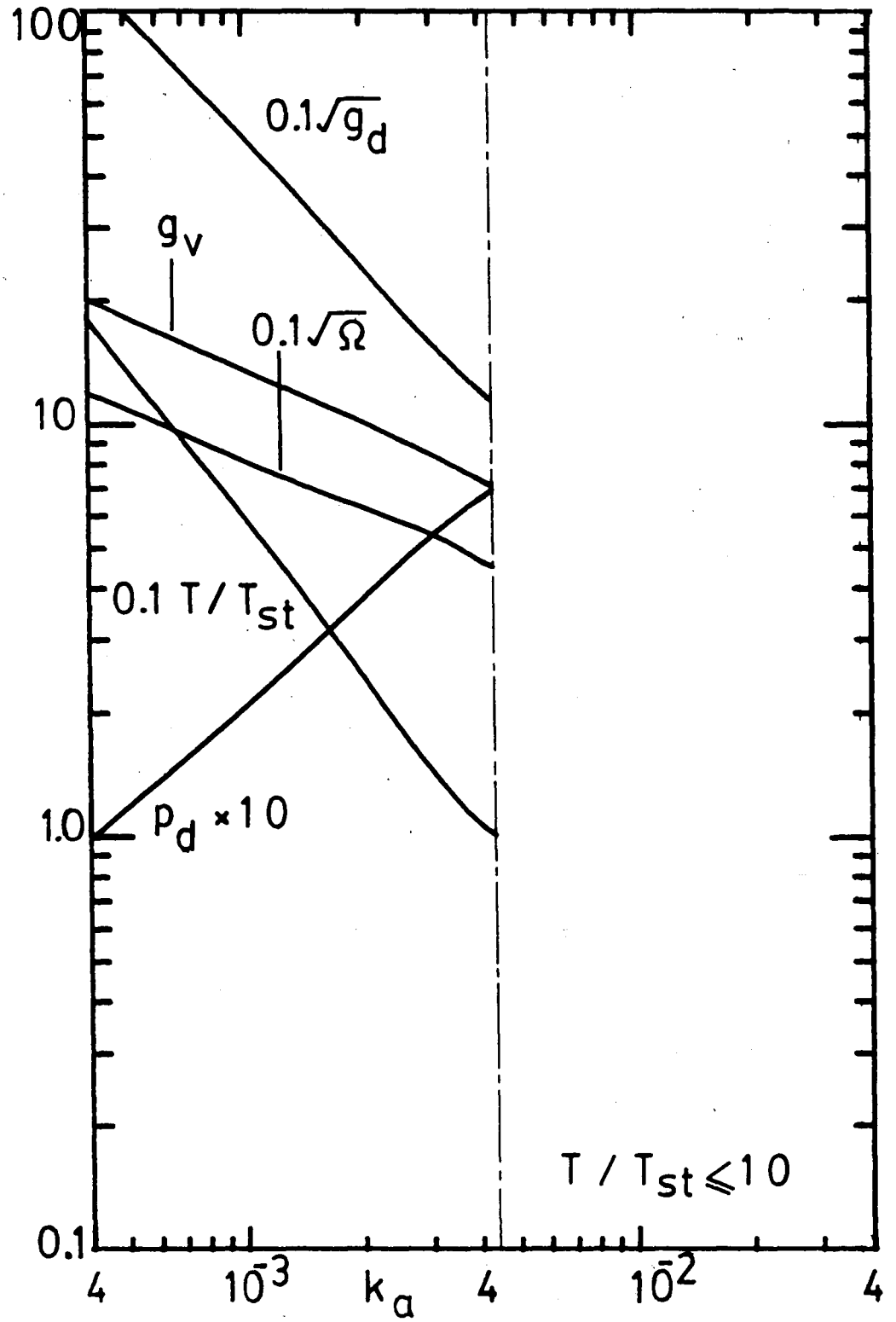

Figure 14. "No-Constraint" Minimum Dissipation Solution $g_\mu = 10^{-6}$, Seating Valve.

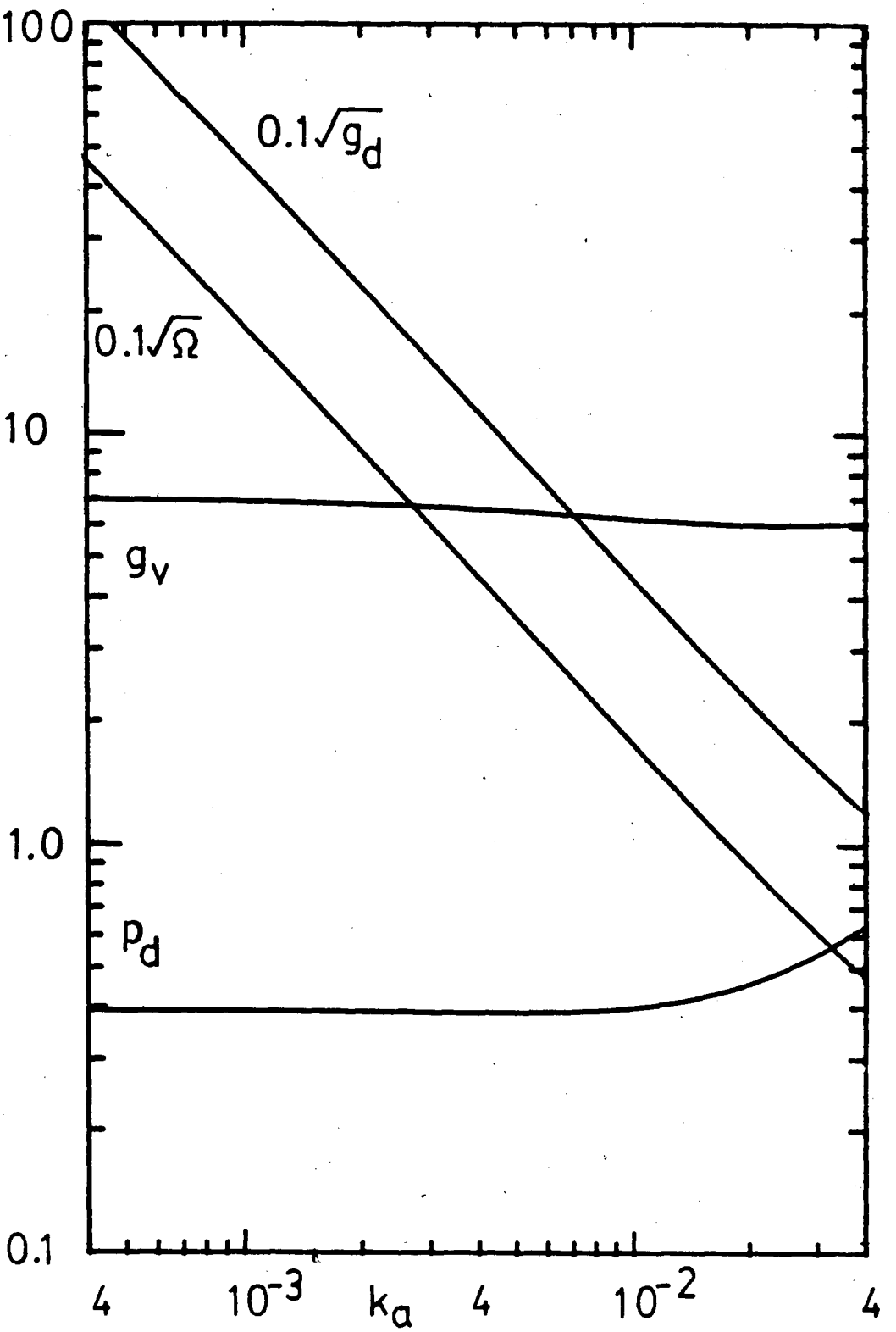

Figure 15. Minimum Dissipation Solution, $T/T_{st}=10$ Laminar Flow, Seating Valve.

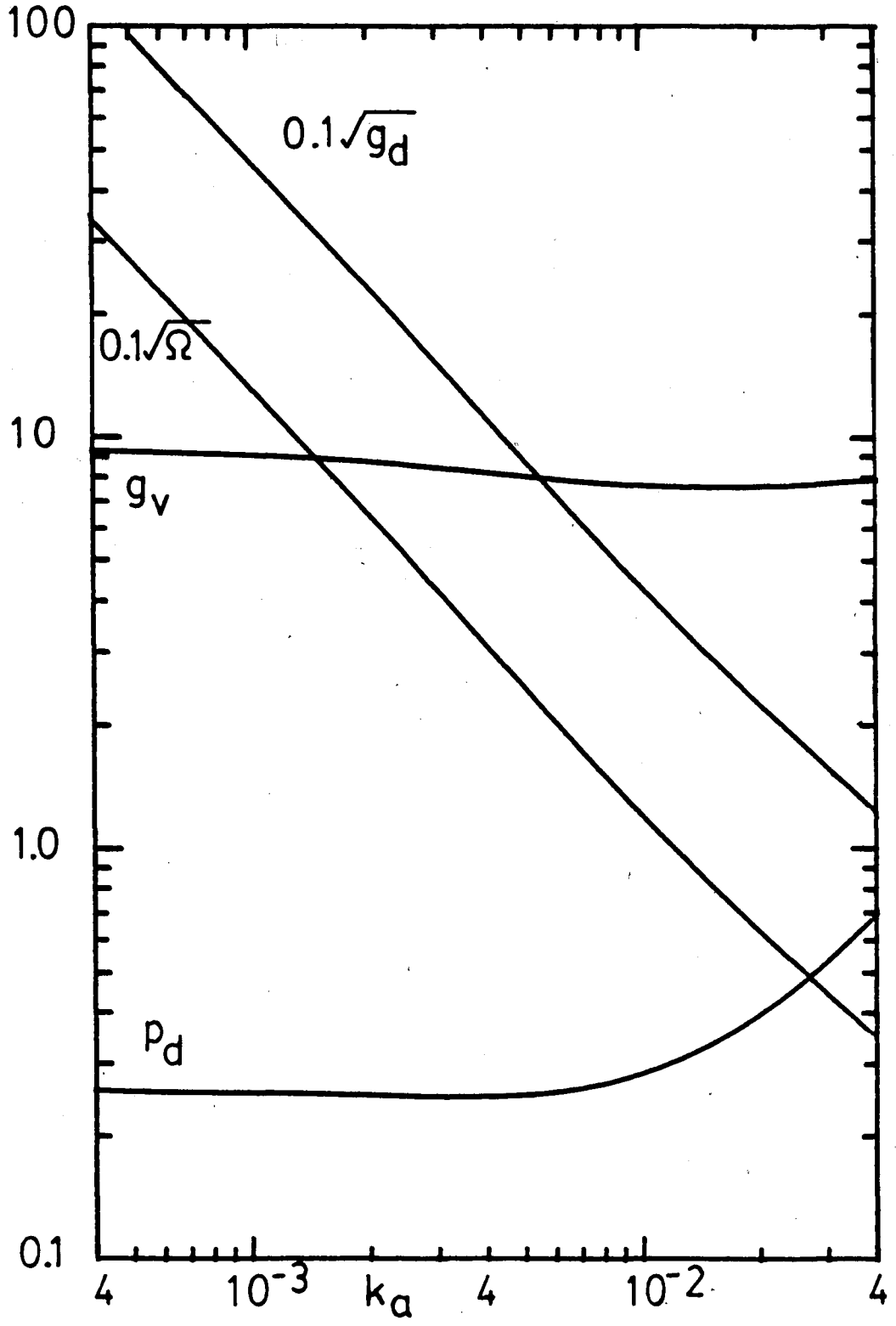

Figure 16. Minimum Dissipation Solution, $T/T_{st}=20$
Laminar Flow, Seating Valve.

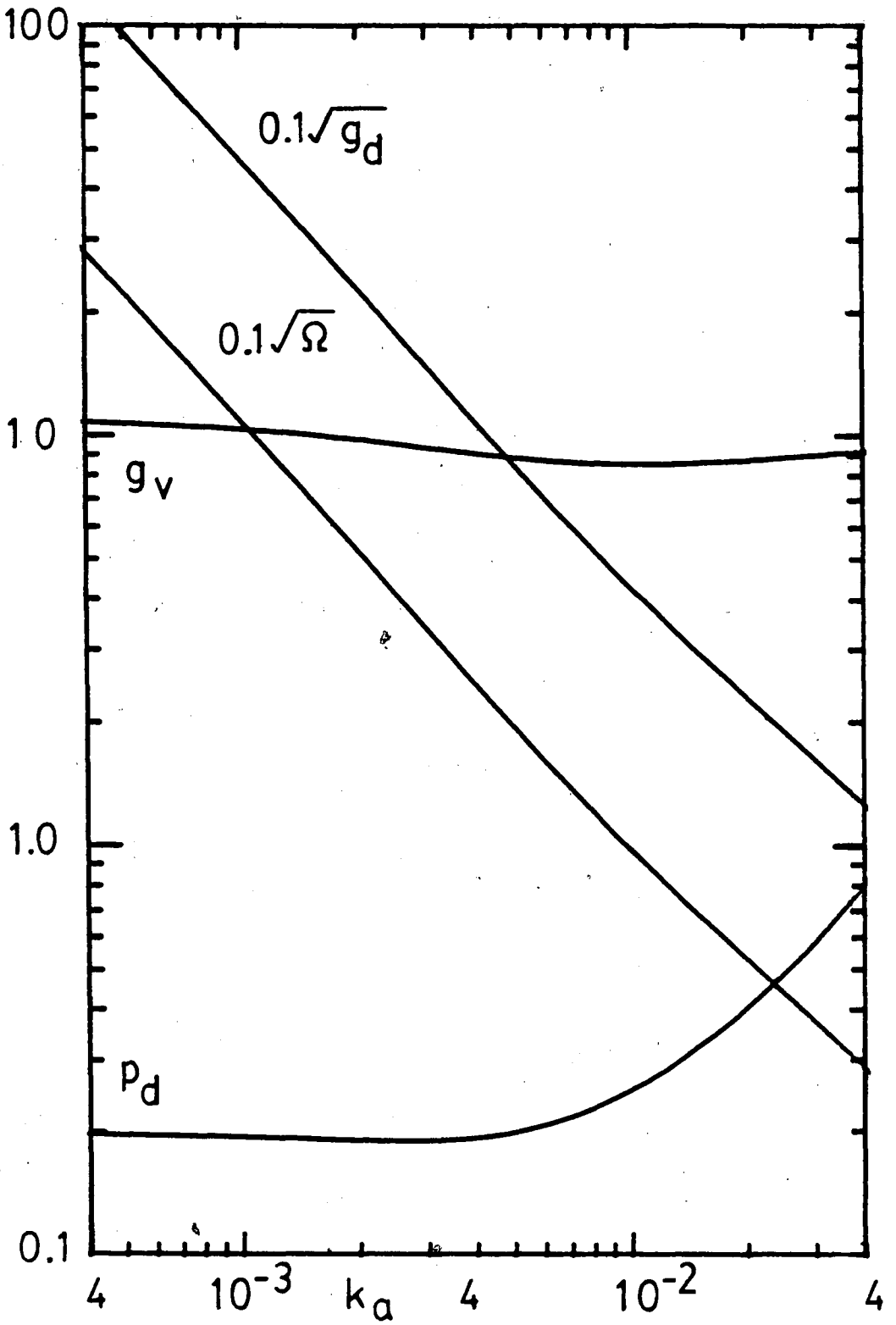

Figure 17. Minimum Dissipation Solution, $T/T_{st}=30$
Laminar Flow, Seating Valve.

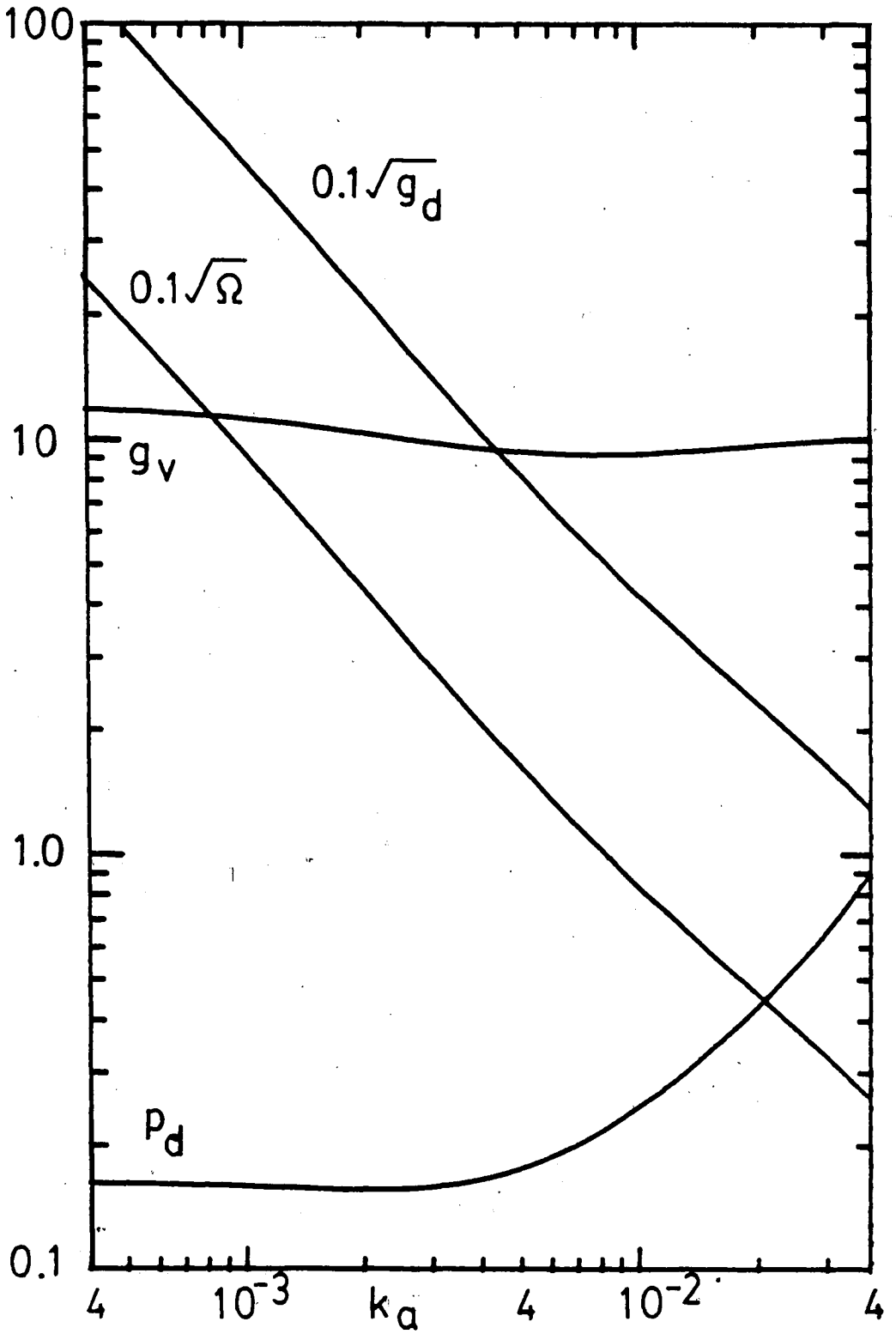

Figure 18. Minimum Dissipation Solution, $T/T_{st}=40$
Laminar Flow, Seating Valve.

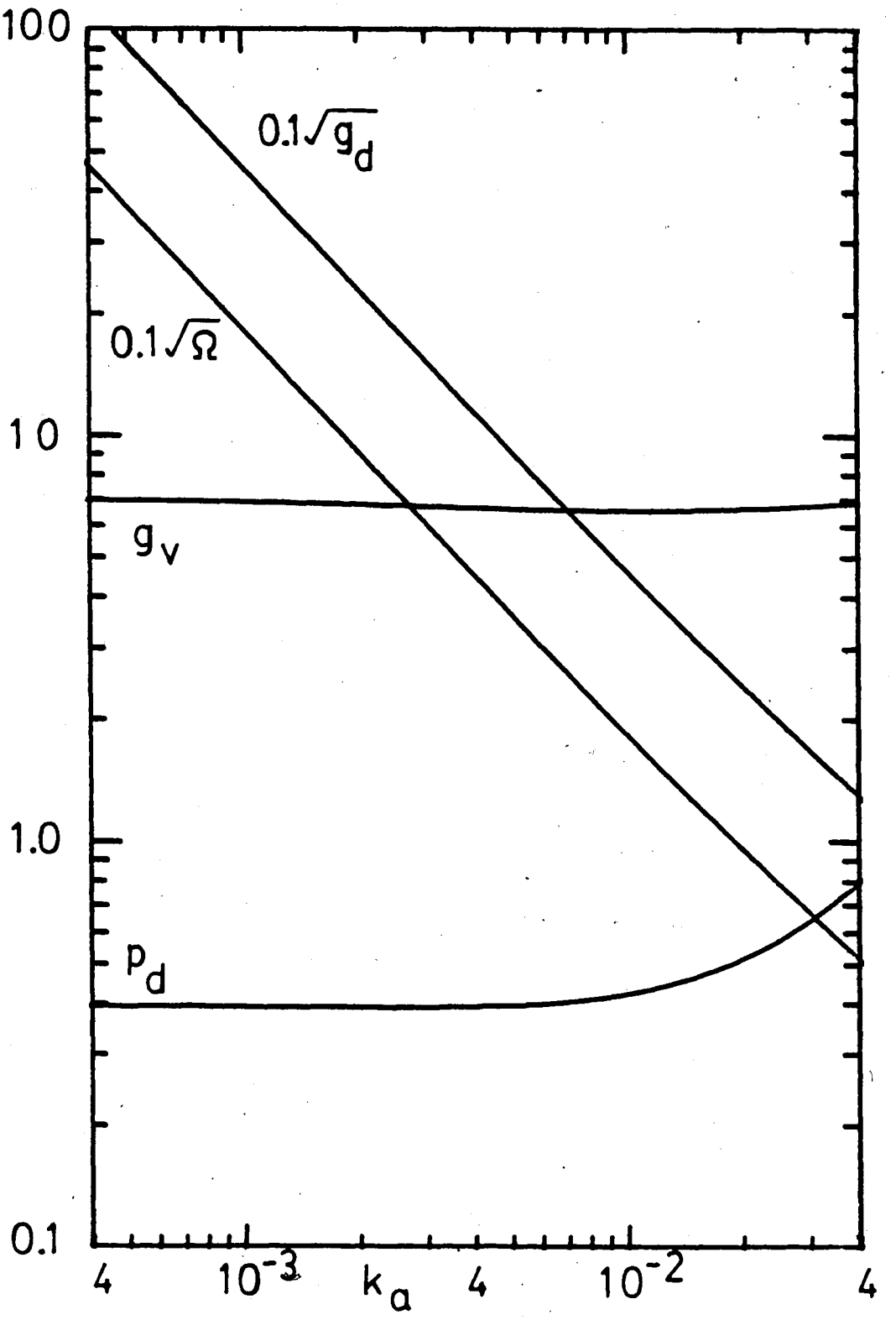

Figure 19. Minimum Dissipation Solution, $T/T_{st}=10$ $g_\mu=1.3*10^{-4}$, Seating Valve.

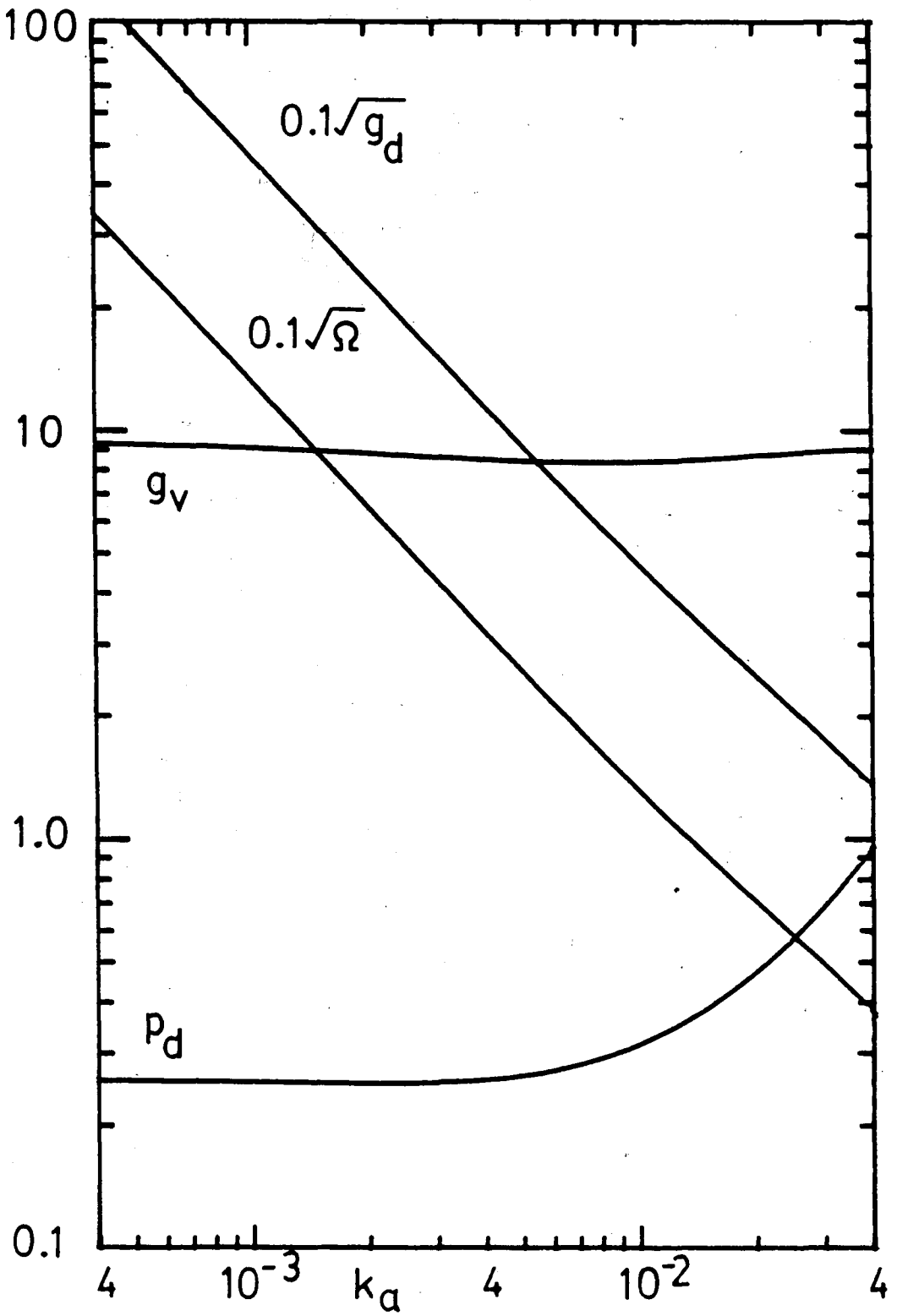

Figure 20. Minimum Dissipation Solution, $T/T_{st}=20$ $g_\mu=1.3*10^{-4}$, Seating Valve.

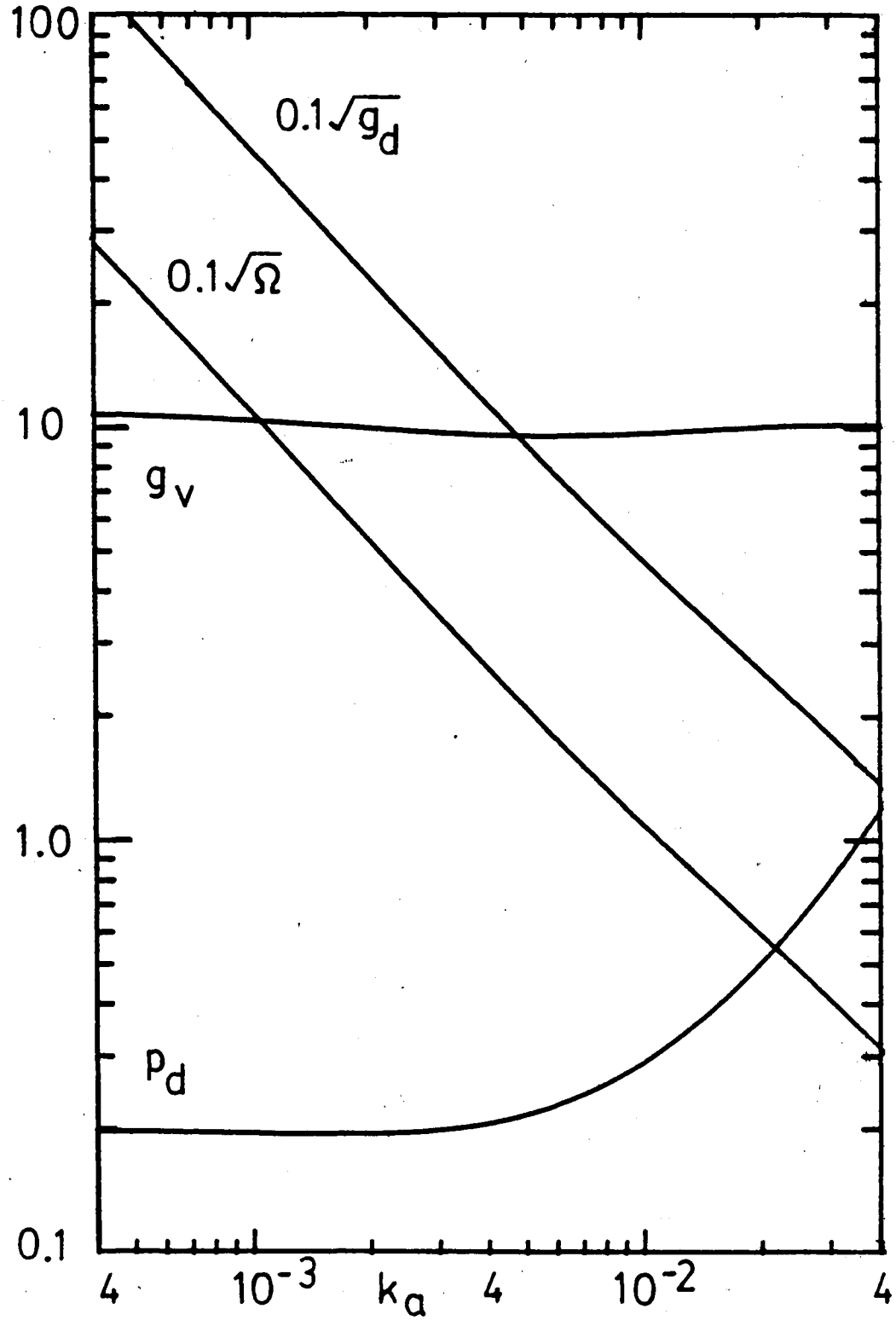

Figure 21. Minimum Dissipation Solution, $T/T_{st}=30$ $g_\mu=1.3*10^{-4}$, Seating Valve.

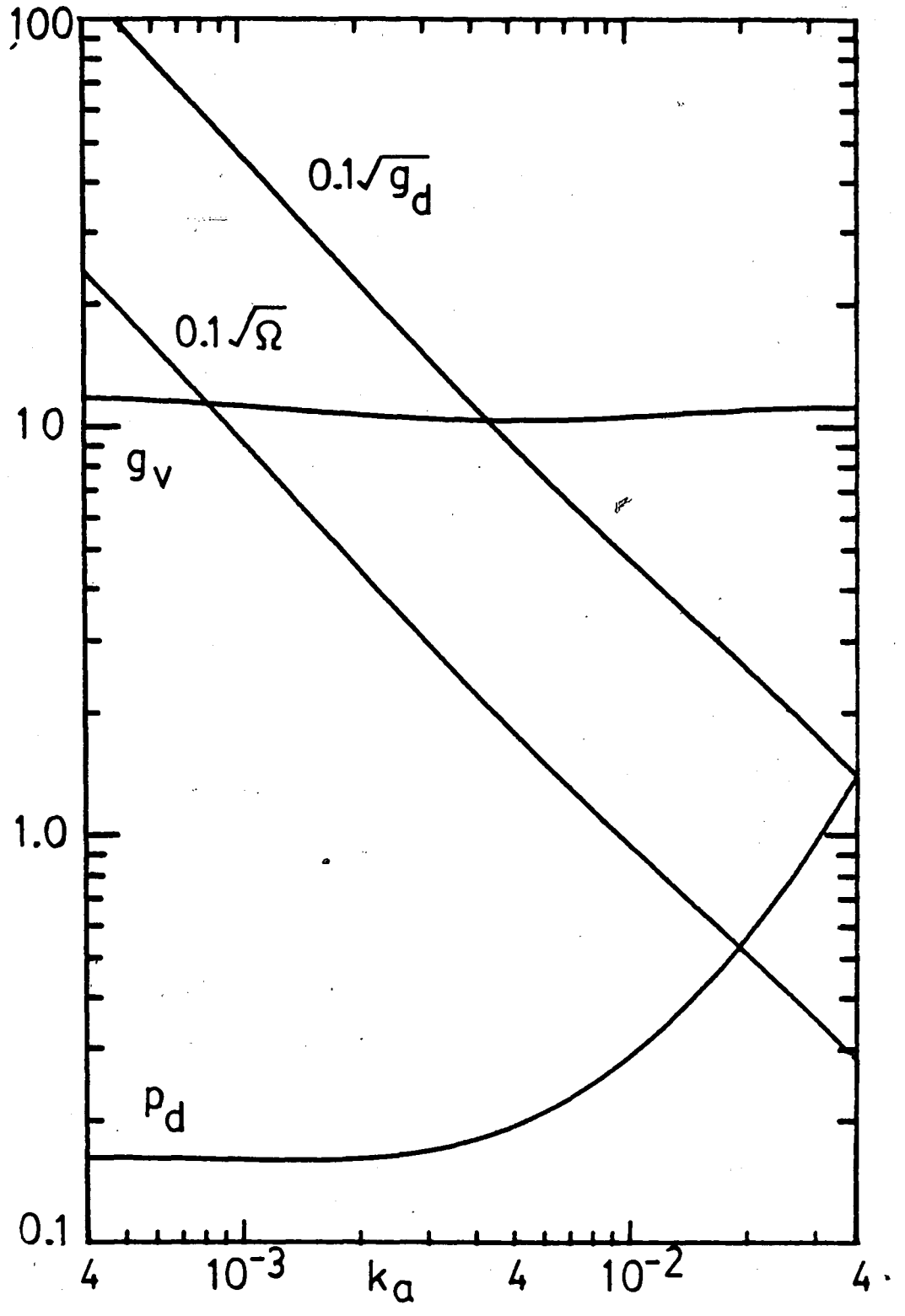

Figure 22. Minimum Dissipation Solution, $T/T_{st}=40$ $g_\mu 1.3*10^{-4}$, Seating Valve.

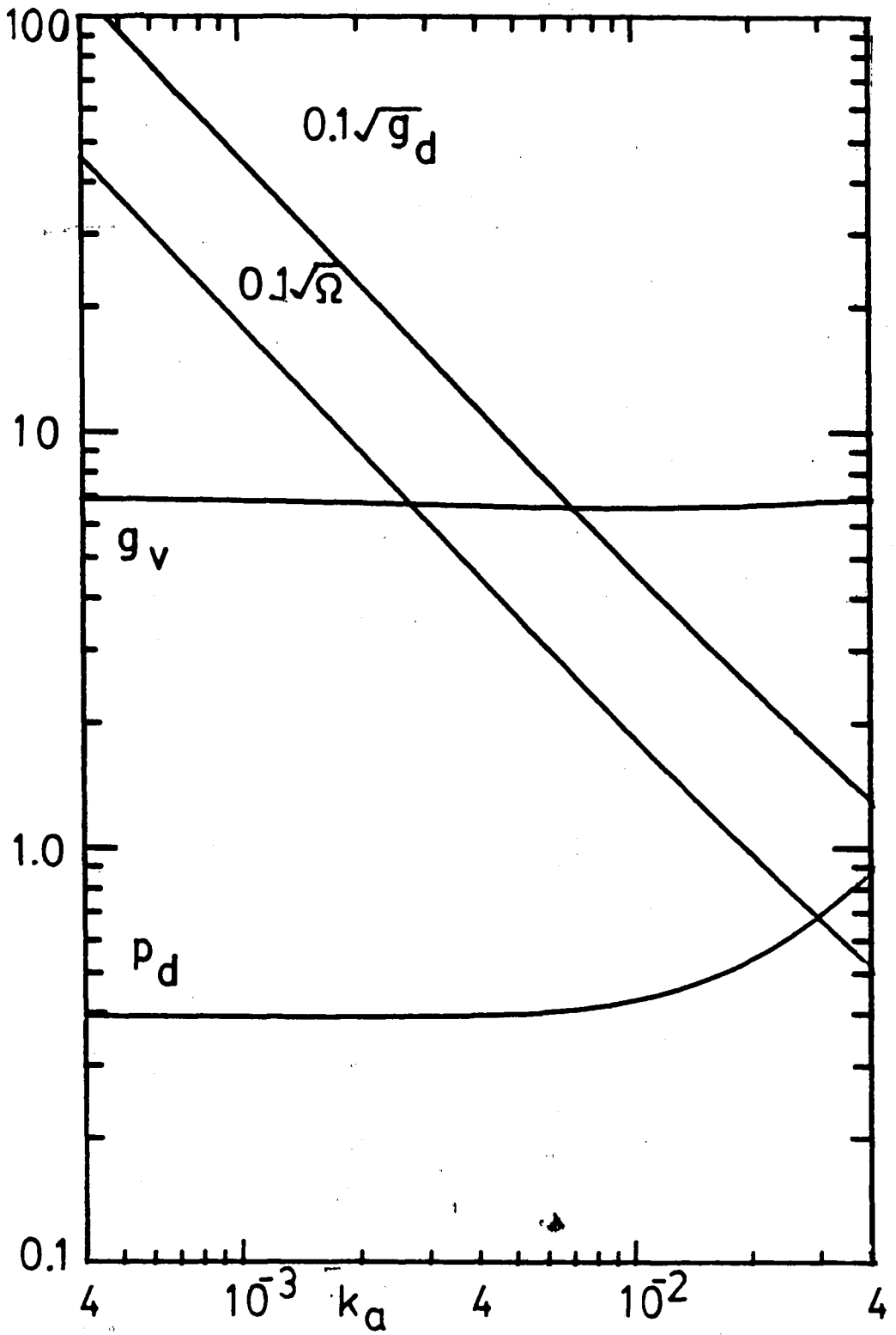

Figure 23. Minimum Dissipation Solution, $T/T_{st}=10$ $g_\mu=10^{-4}$, Seating Valve.

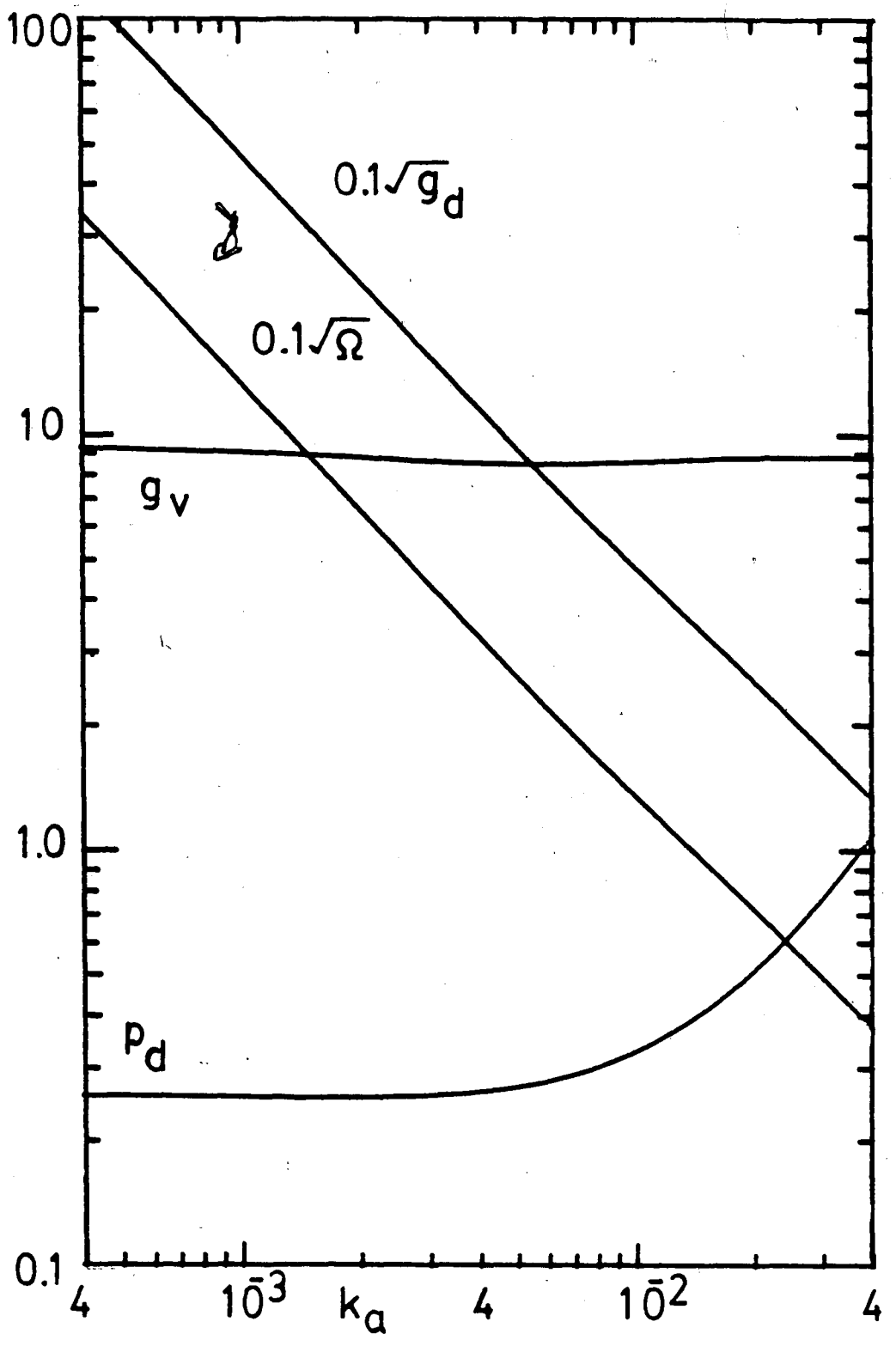

Figure 24. Minimum Dissipation Solution, $T/T_{st}=20$ $g_\mu=10^{-4}$, Seating Valve.

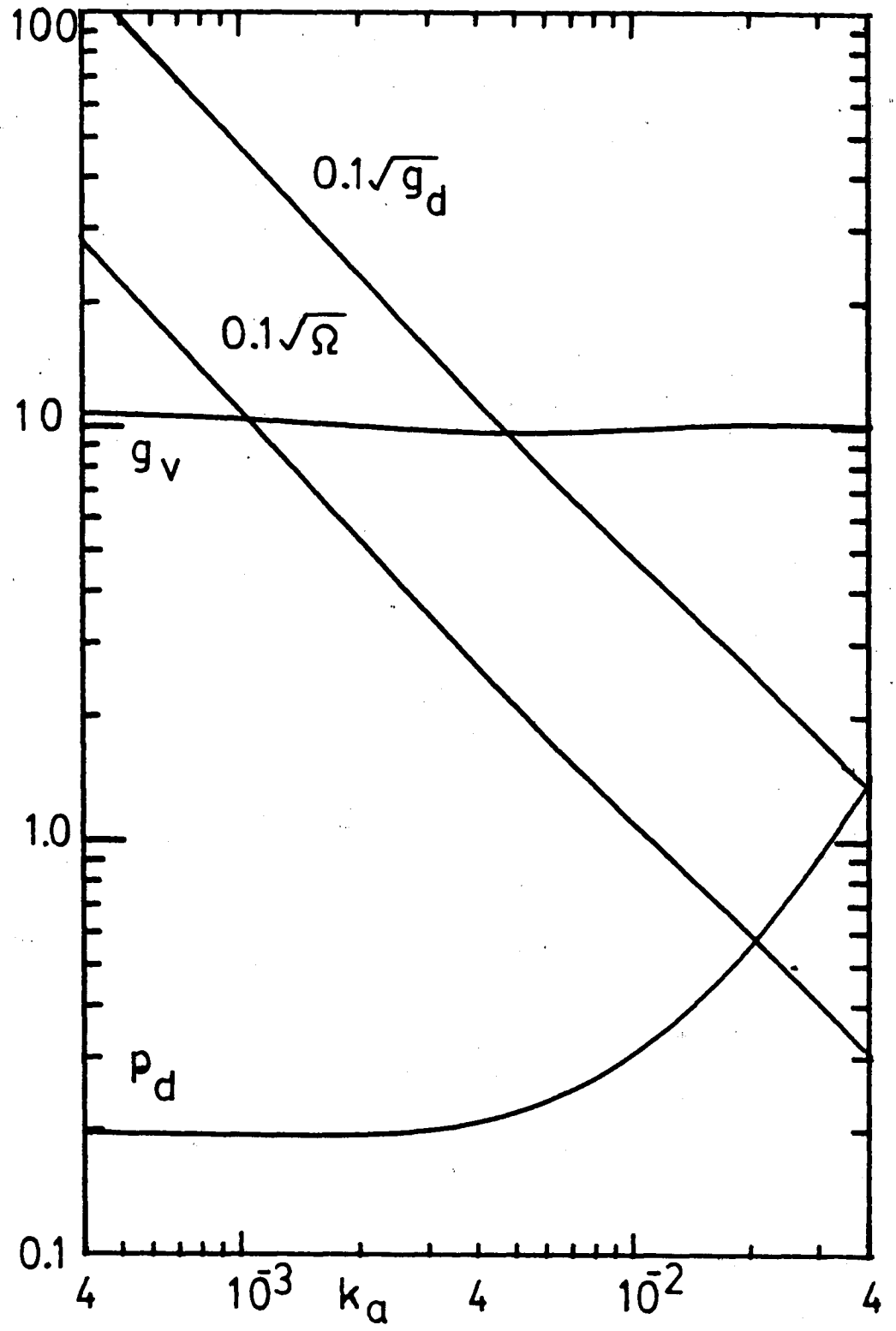

Figure 25. Minimum Dissipation Solution, $T/T_{st}=30$ $g_\mu=10^{-4}$, Seating Valve.

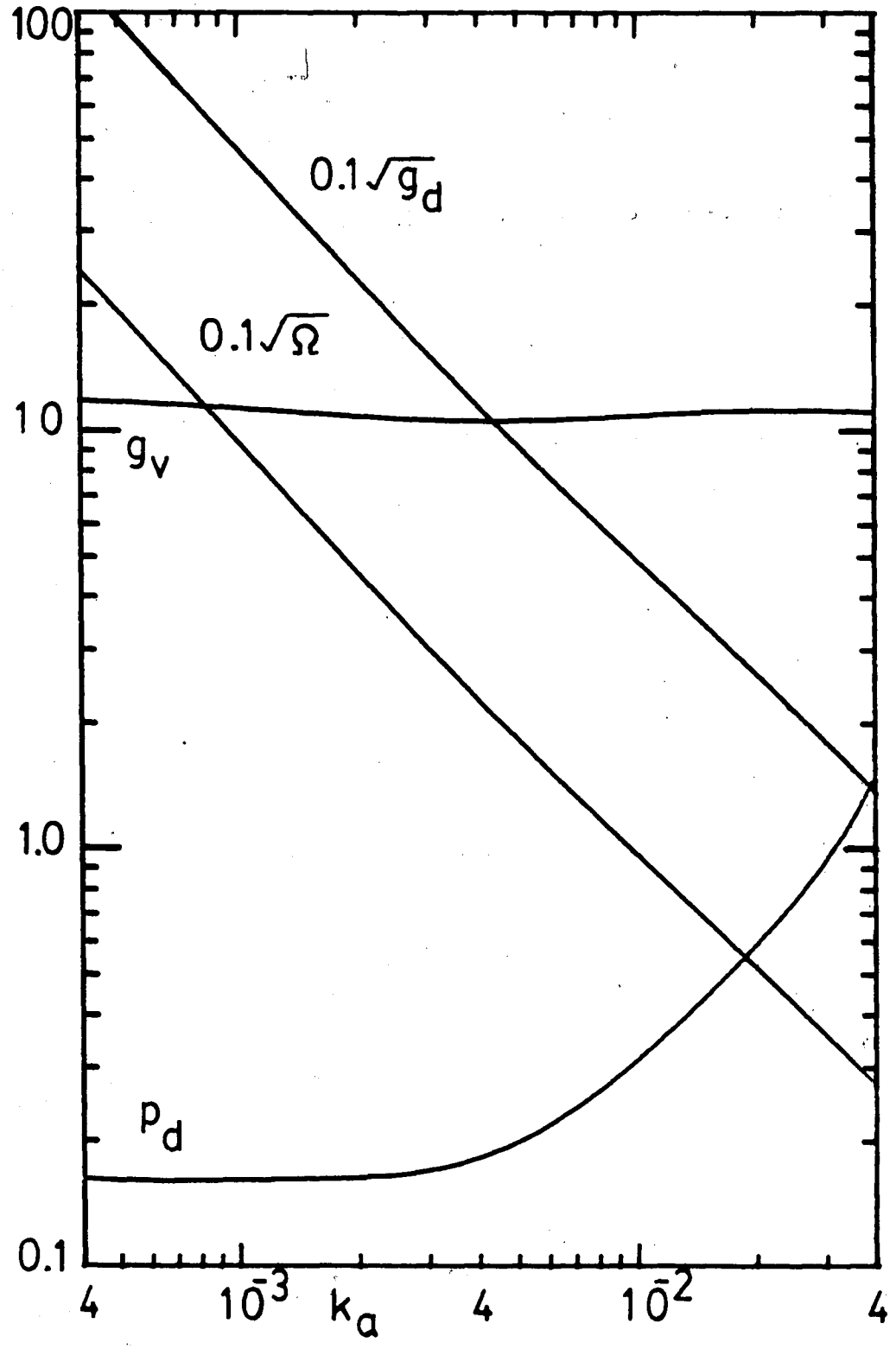

Figure 26. Minimum Dissipation Solution, $T/T_{st}=40$ $g_\mu=10^{-4}$, Seating Valve.

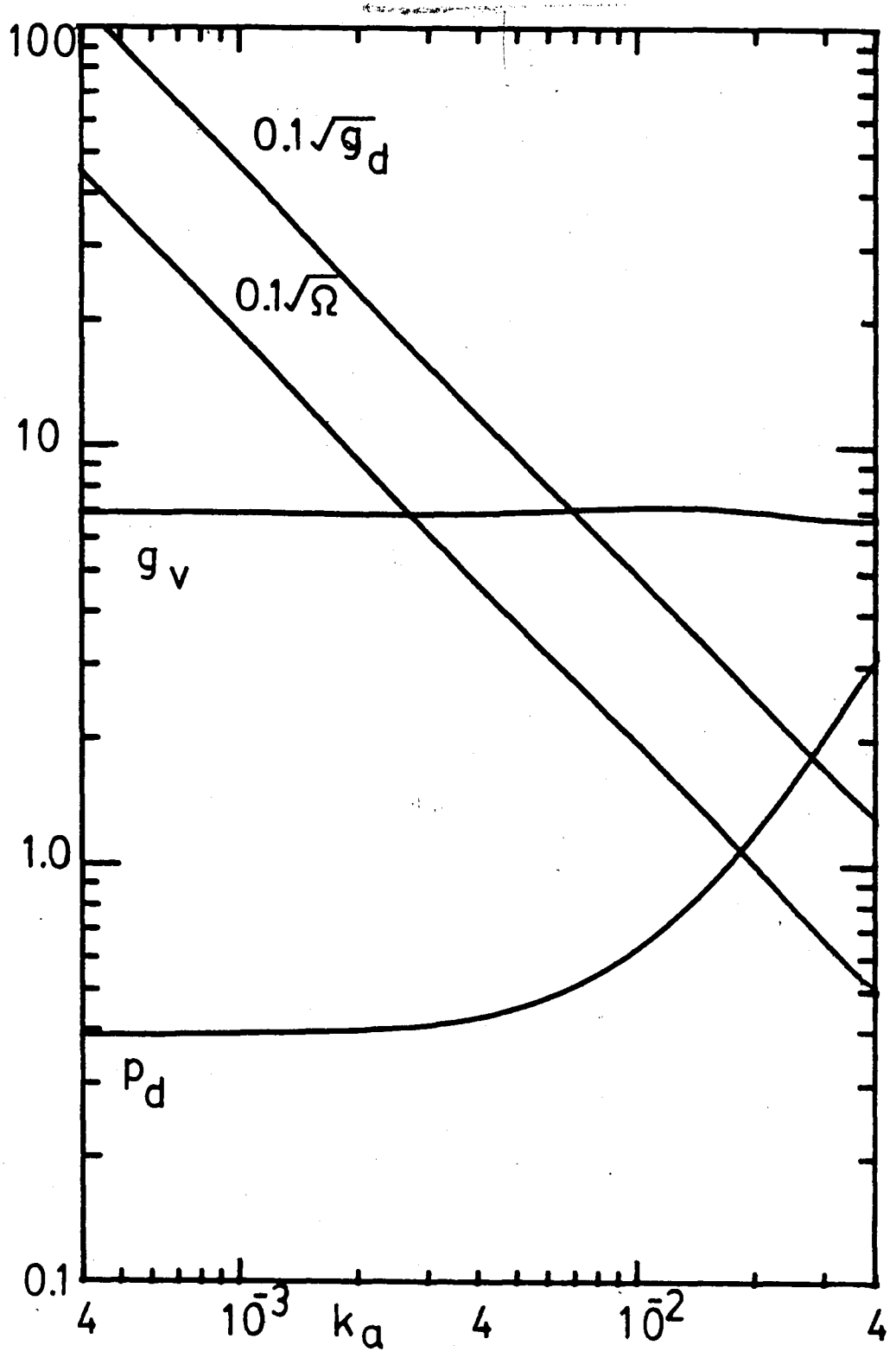

Figure 27. Minimum Dissipation Solution, $T/T_{st}=10$ $g_\mu=10^{-5}$, Seating Valve.

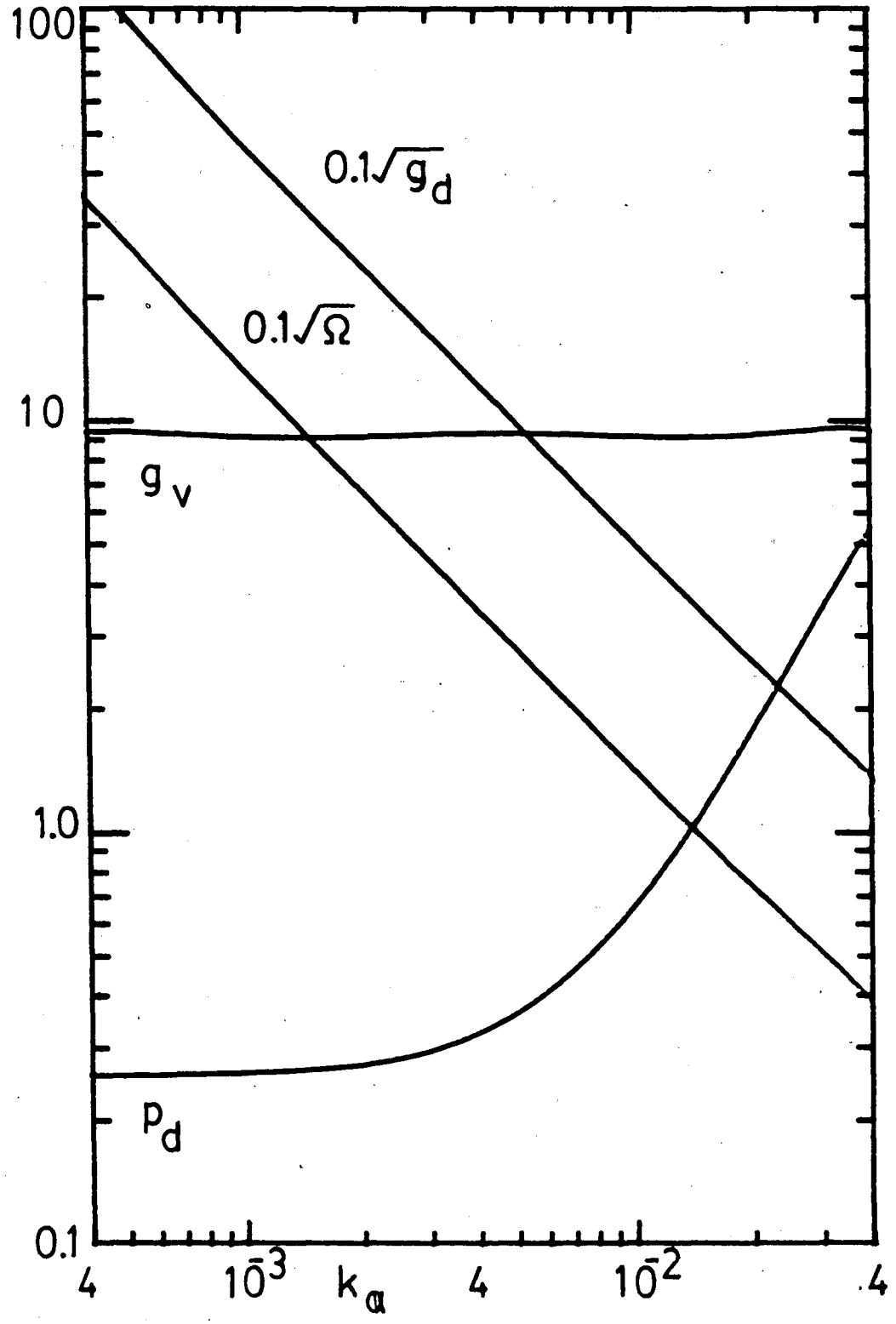

Figure 28. Minimum Dissipation Solution, $T/T_{st}=20$ $g_\mu=10^{-5}$, Seating Valve.

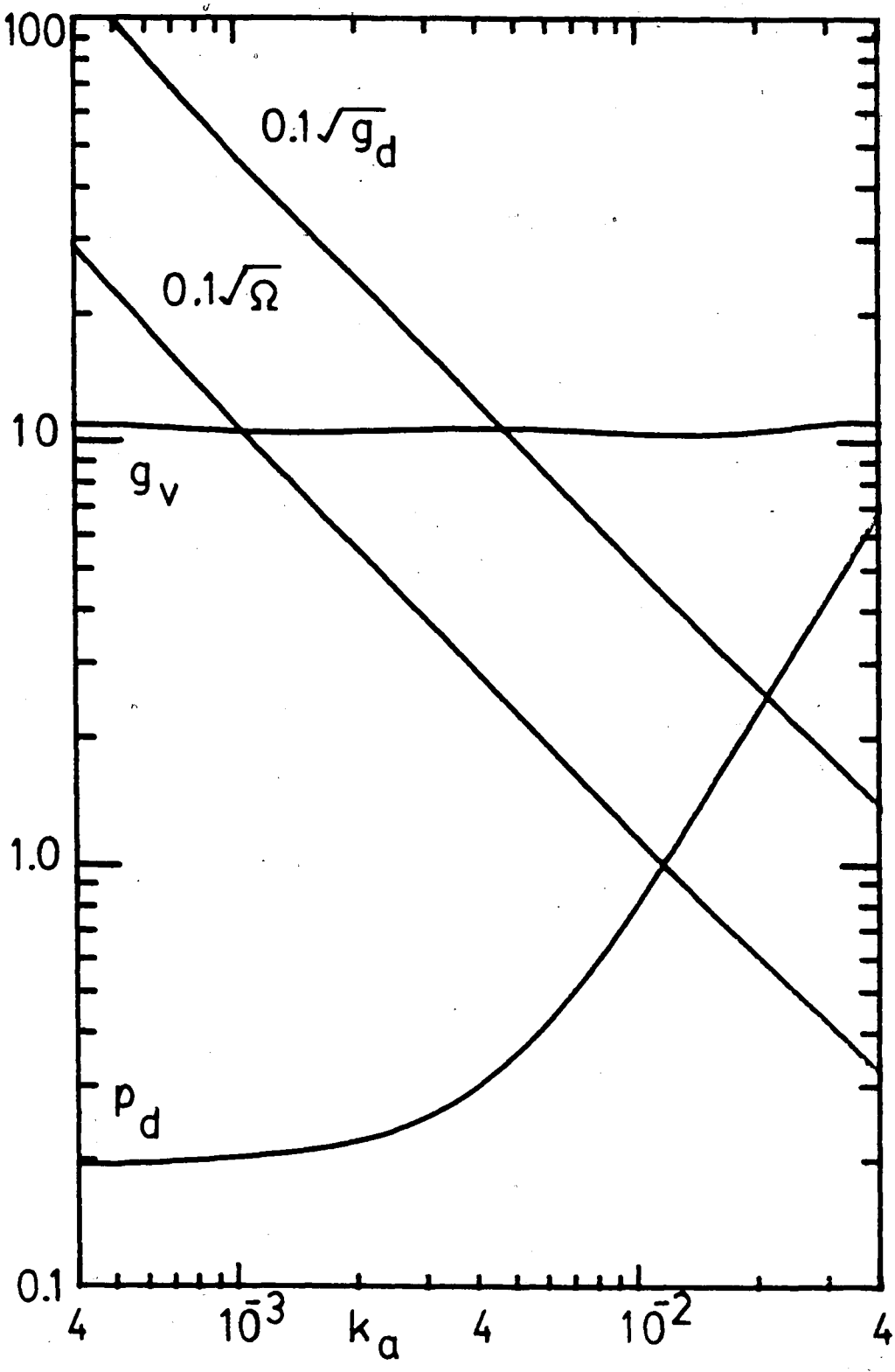

Figure 29. Minimum Dissipation Solution, $T/T_{st}=30$ $g_\mu=10^{-5}$, Seating Valve.

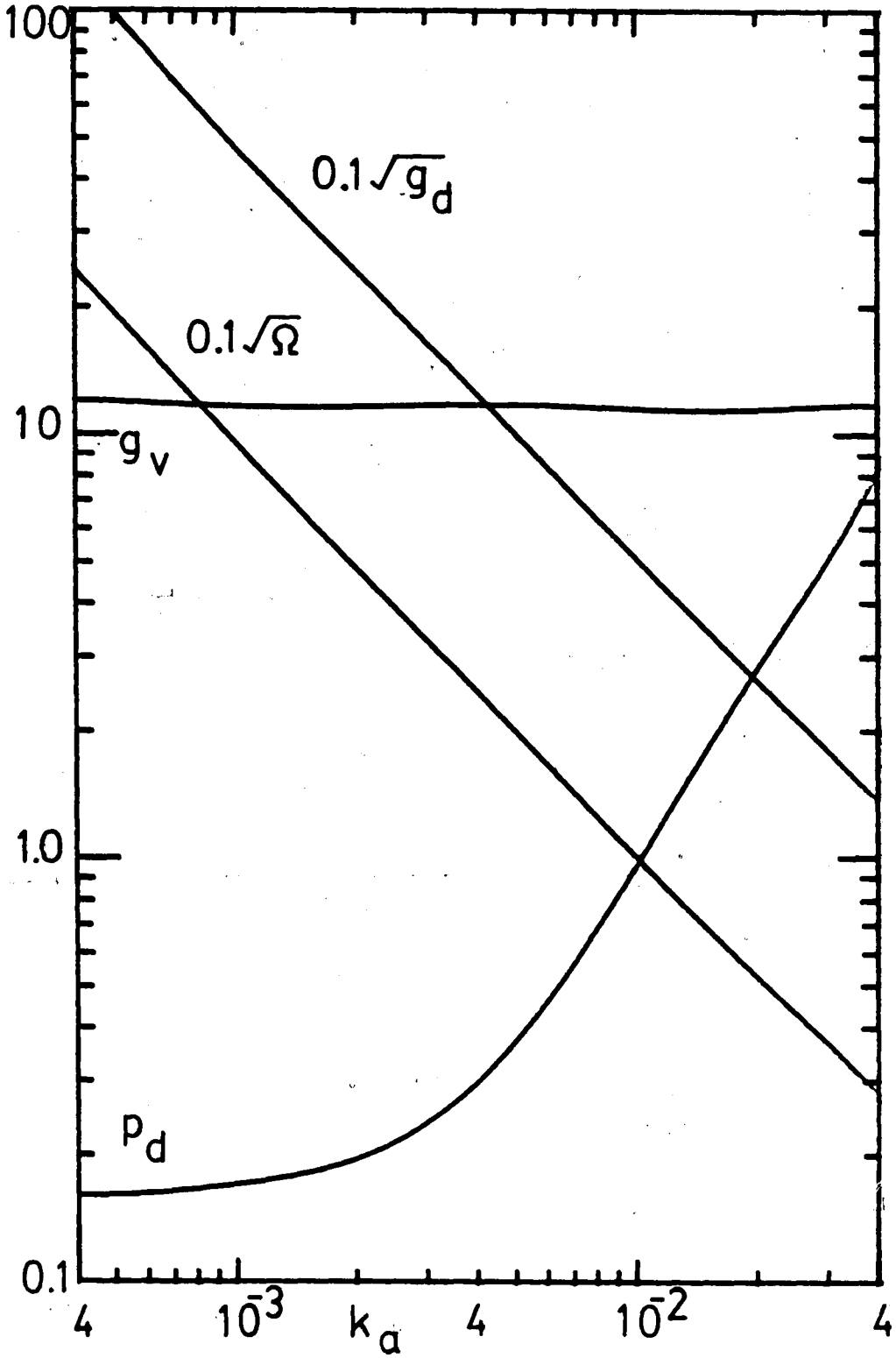

Figure 30. Minimum Dissipation Solution, $T/T_{st}=40$ $g_\mu=10^{-3}$, Seating Valve.

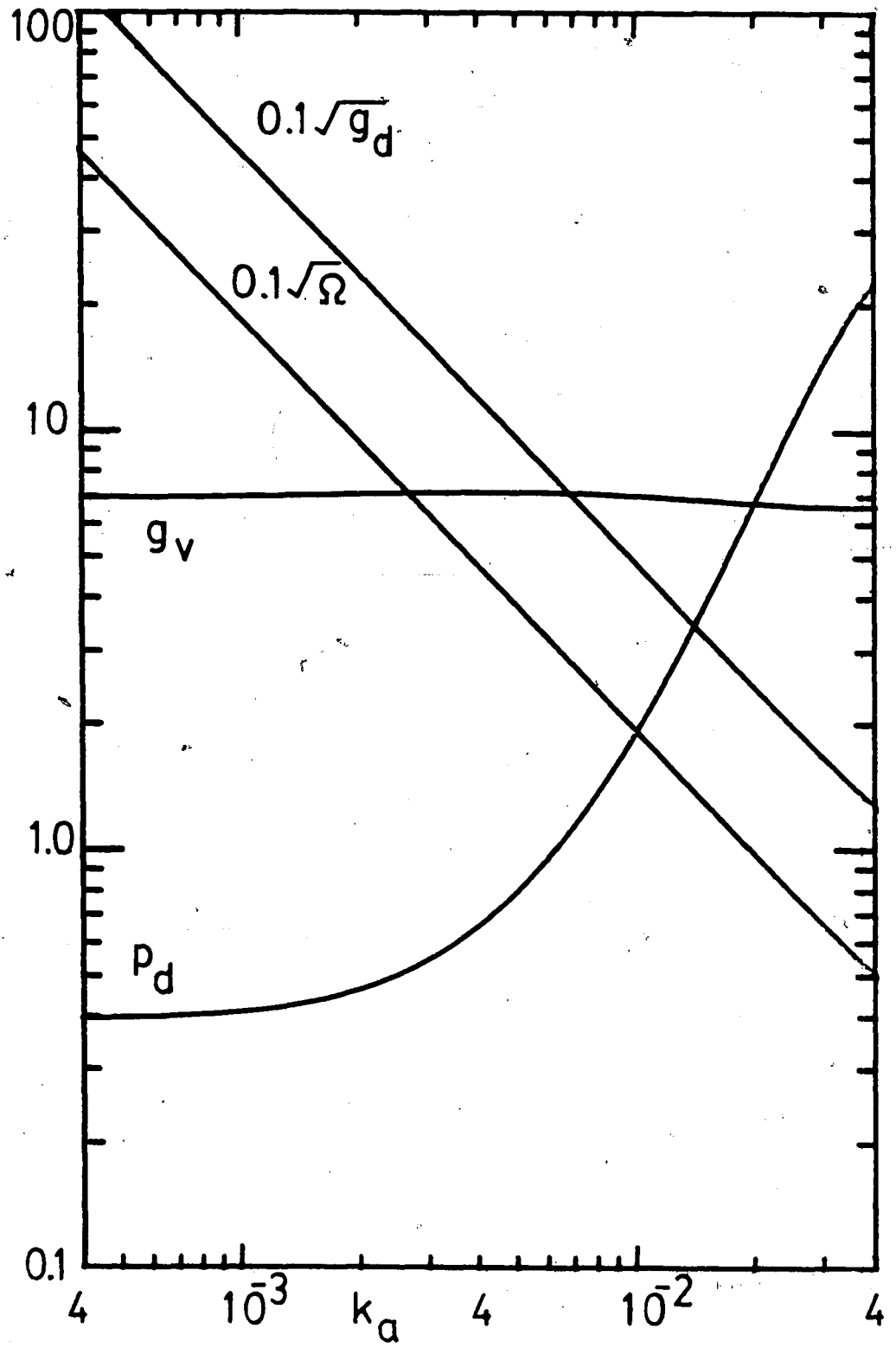

Figure 31. Minimum Dissipation Solution, $T/T_{gt}=10$ $g_\mu=10^{-6}$, Seating Valve.

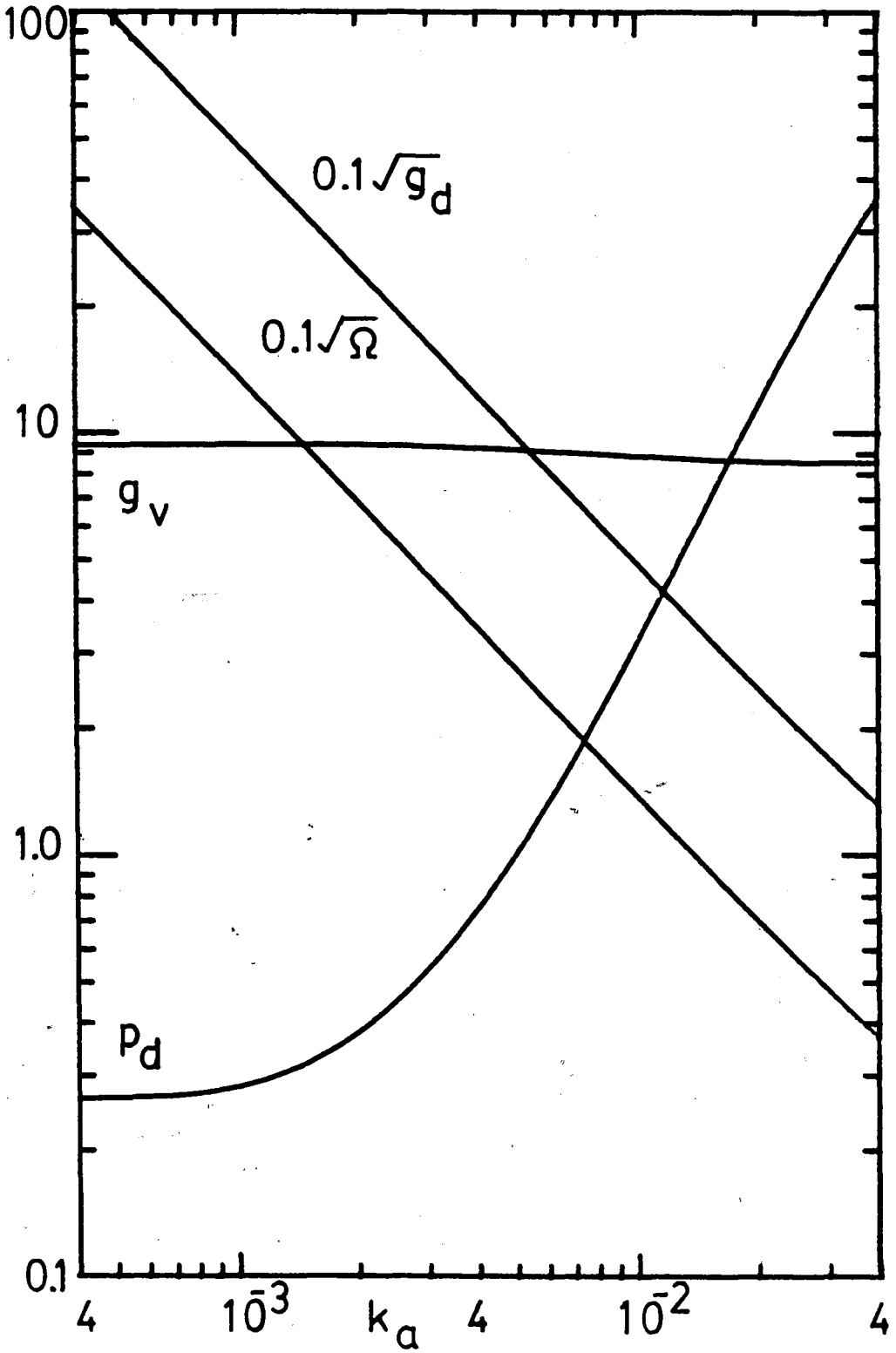

Figure 32. Minimum Dissipation Solution, $T/T_{st}=20$ $g_\mu=10^{-6}$, Seating Valve.

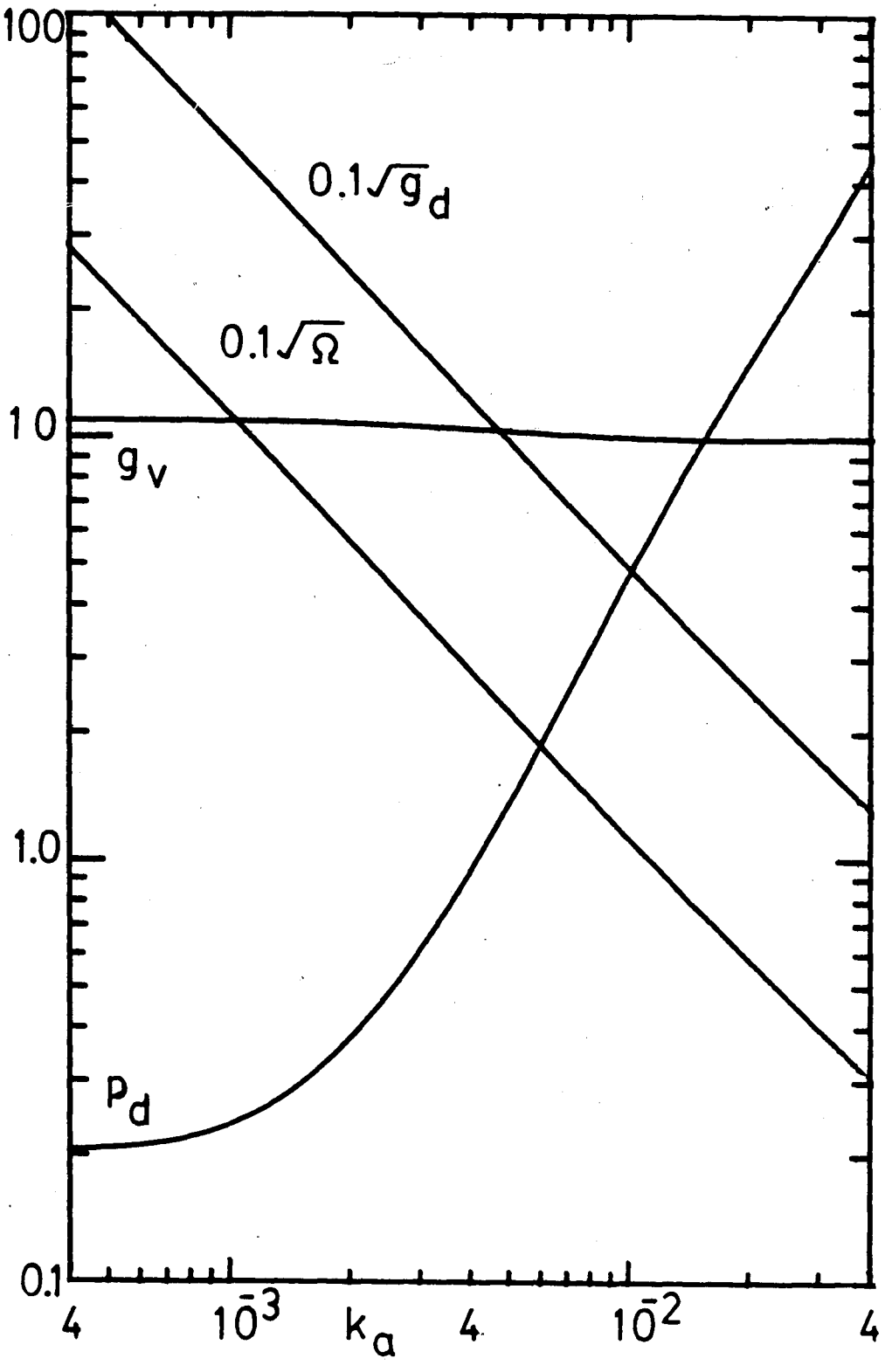

Figure 33. Minimum Dissipation Solution, $T/T_{st}=30$ $g_\mu=10^{-6}$, Seating Valve.

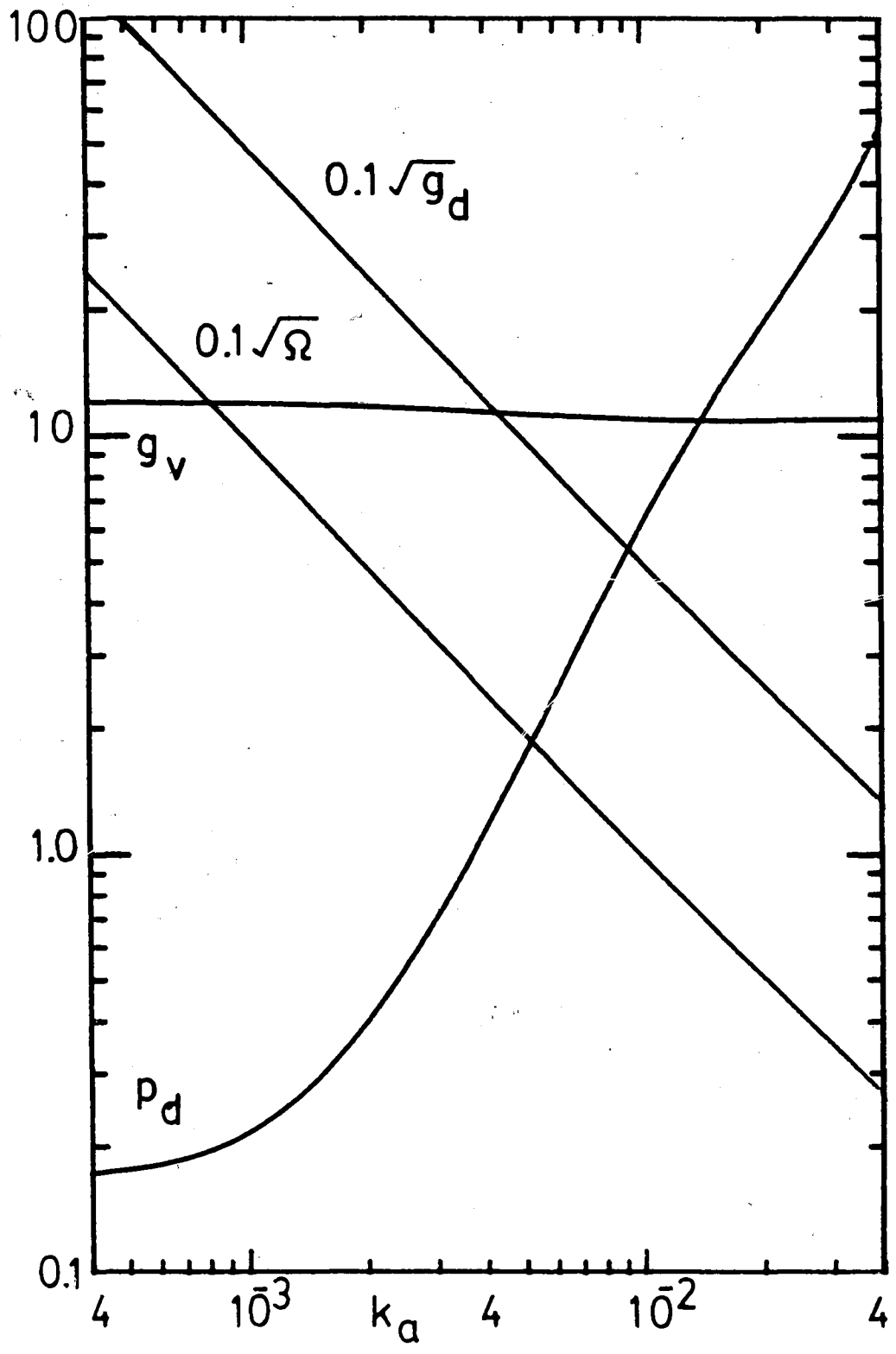

Figure 34. Minimum Dissipation Solution, $T/T_{st}=40$ $g_\mu=10^{-6}$, Seating Valve.

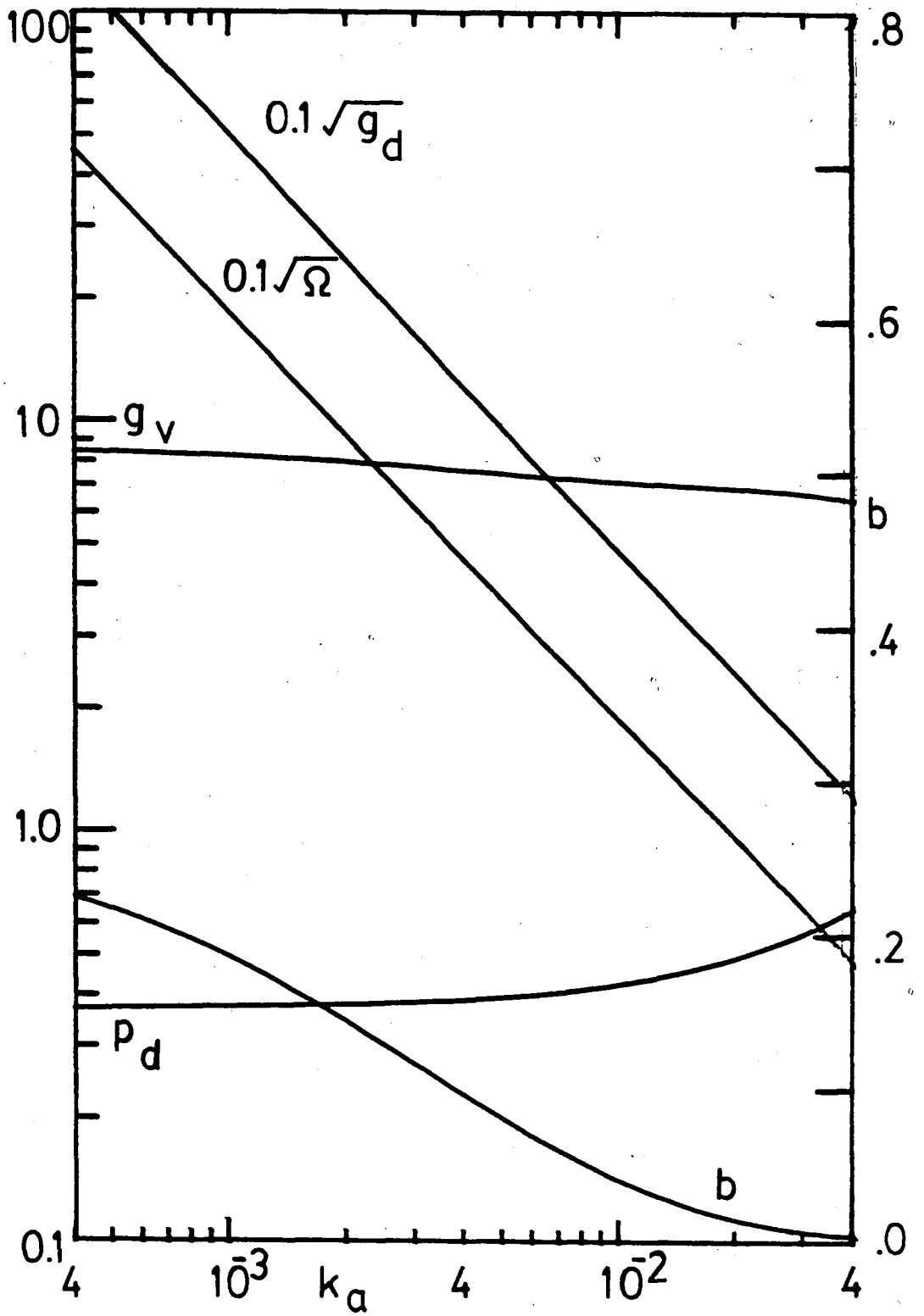

Figure 35. Minimum Dissipation Solution, $T/T_{st}=10$ Laminar Flow, Sliding Valve.

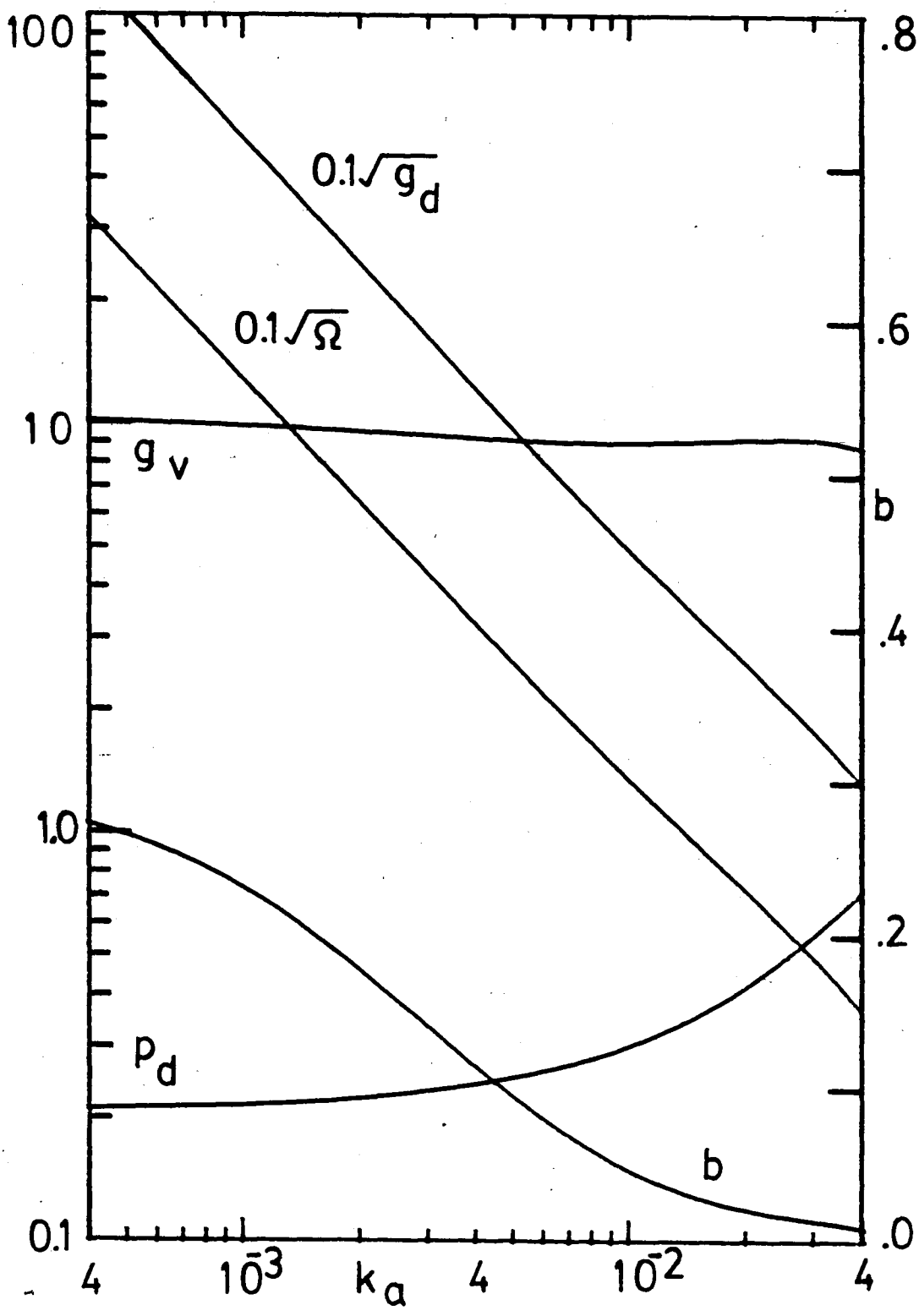

Figure 36. Minimum Dissipation Solution, $T/T_{st}=20$
Laminar Flow, Sliding Valve.

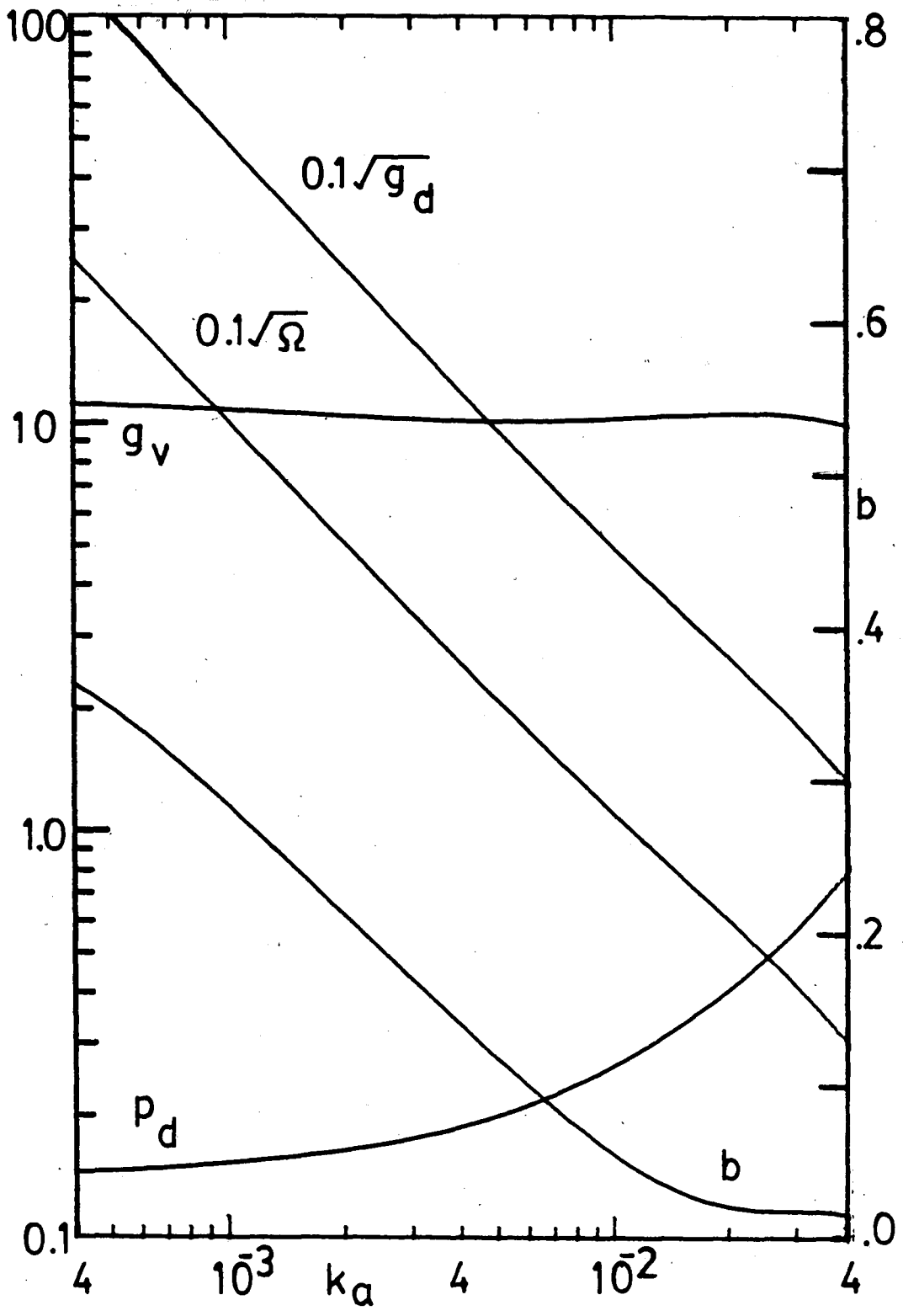

Figure 37. Minimum Dissipation Solution, $T/T_{st}=30$
Laminar Flow, Sliding Valve.

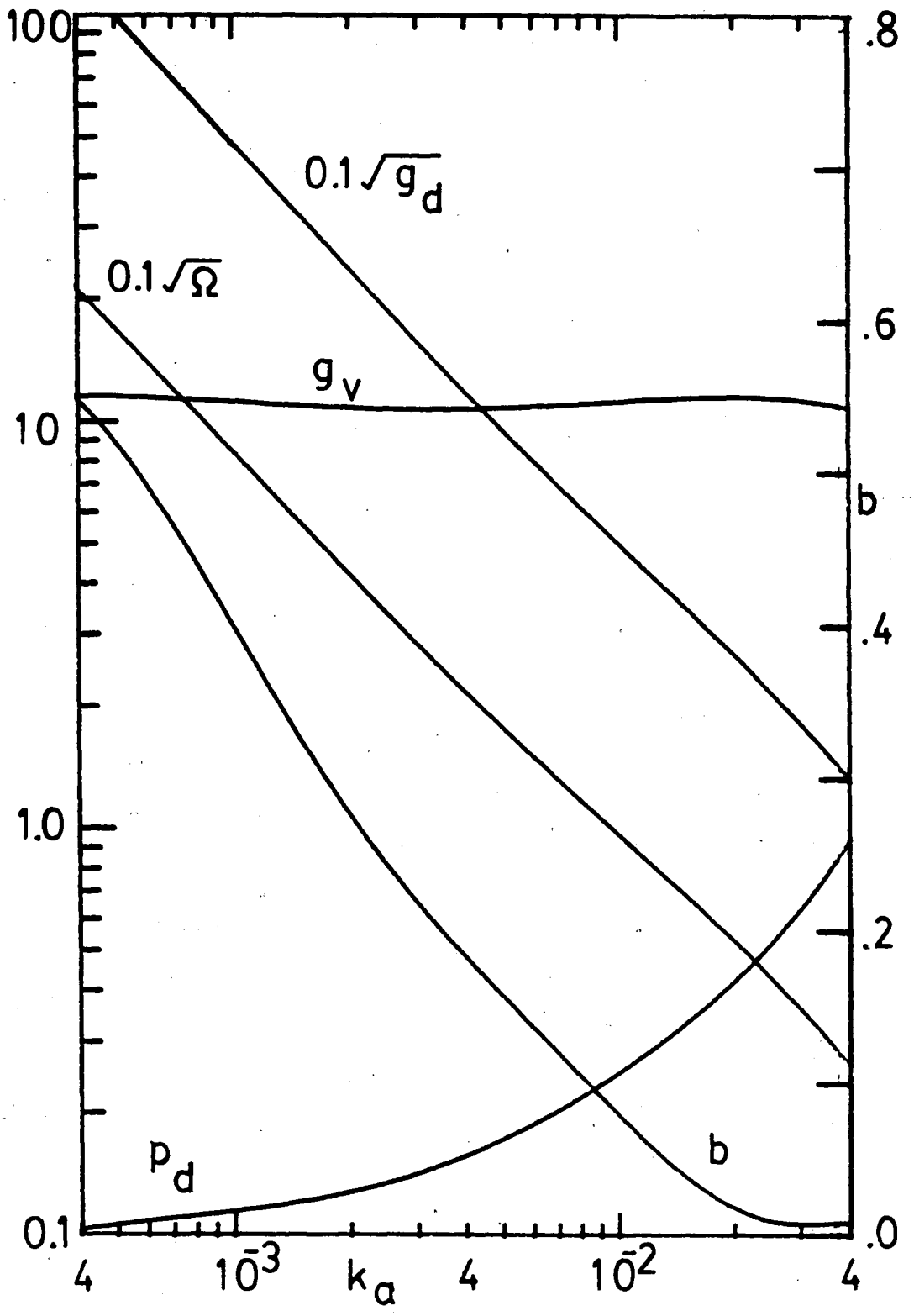

Figure 38. Minimum Dissipation Solution, $T/T_{st}=40$
Laminar Flow, Sliding Valve.

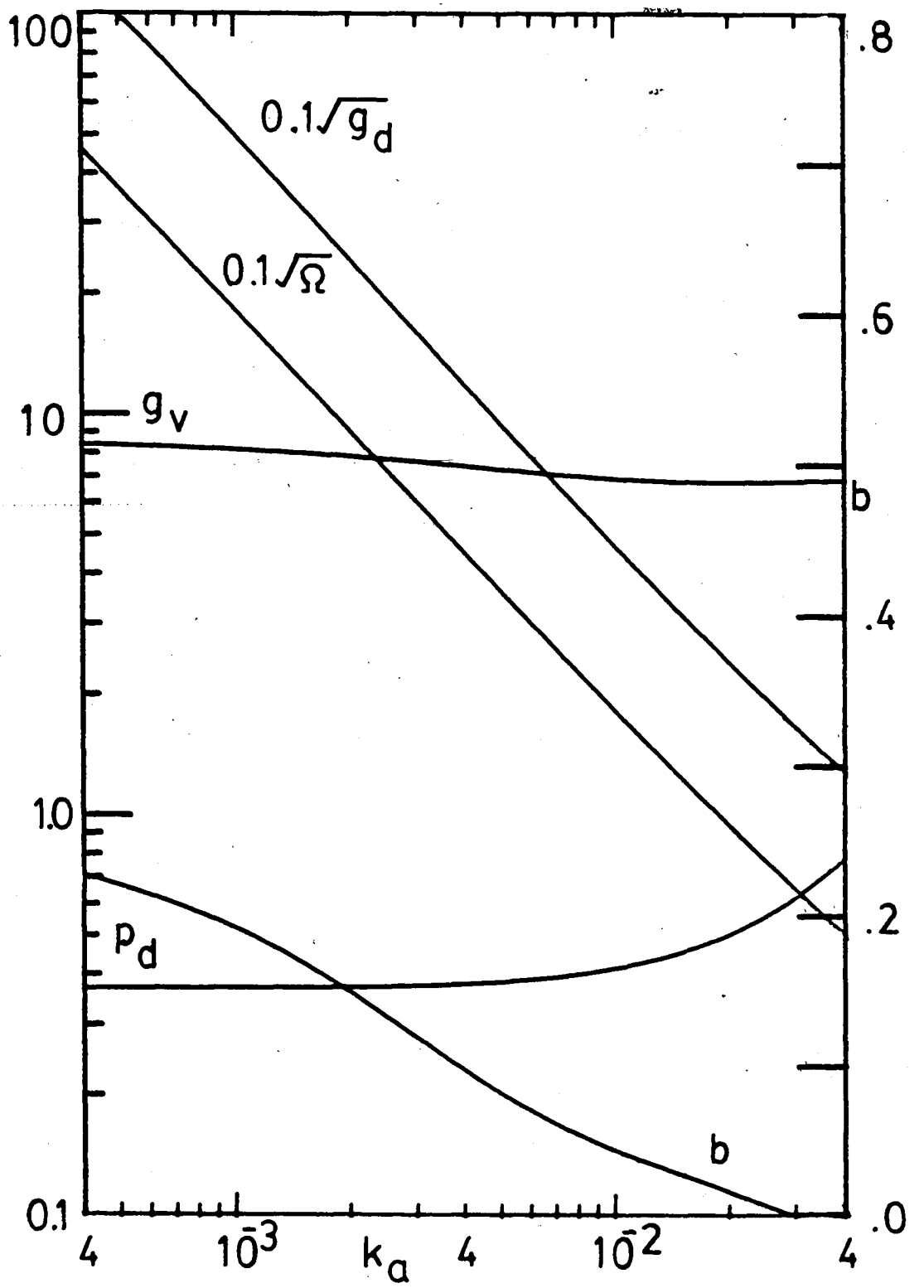

Figure 39. Minimum Dissipation Solution, $T/T_{st}=10$ $g_\mu=1.3*10^{-4}$, Sliding Valve.

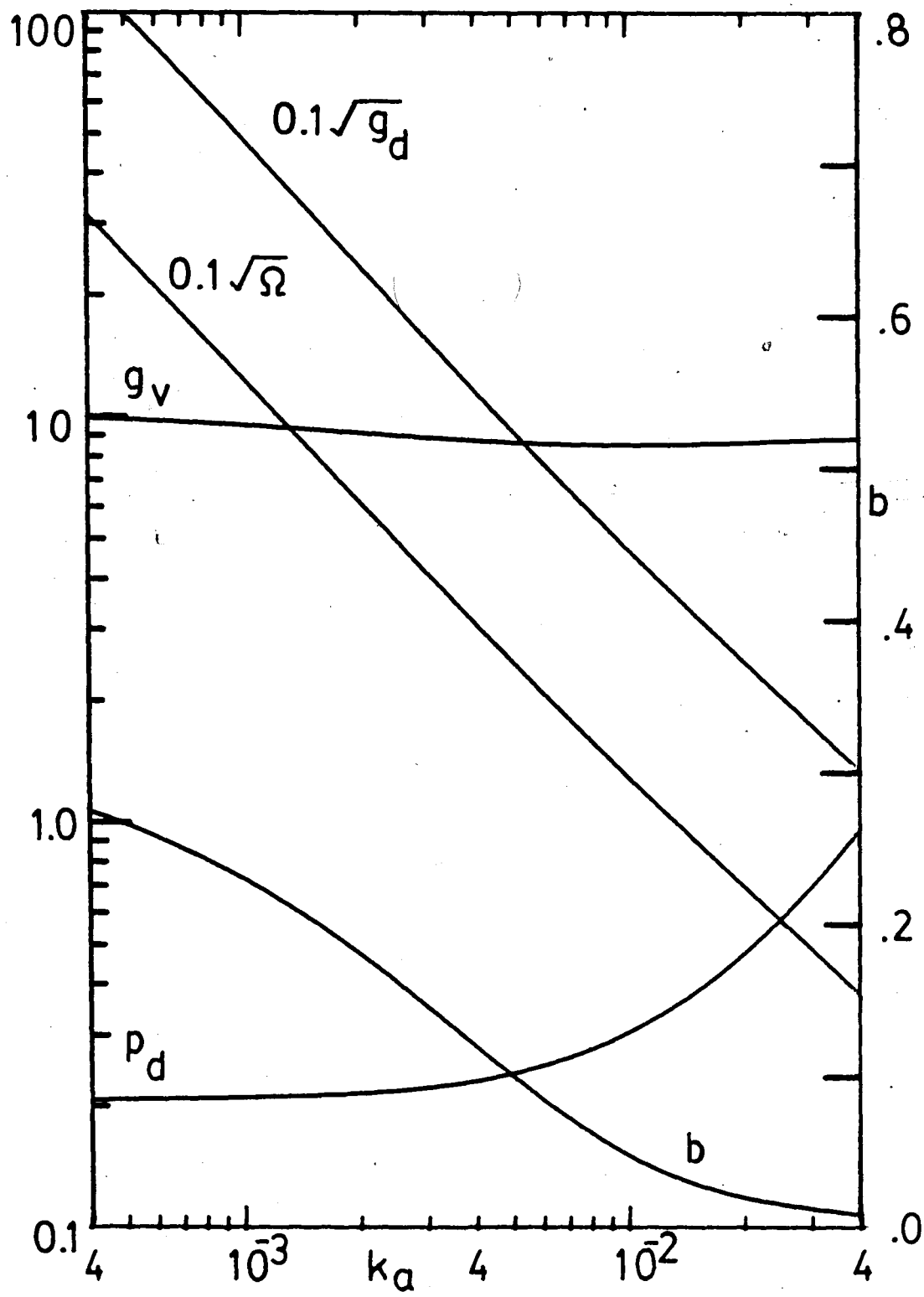

Figure 40. Minimum Dissipation Solution, $T/T_{st}=20$ $g_\mu=1.3*10^{-4}$, Sliding Valve.

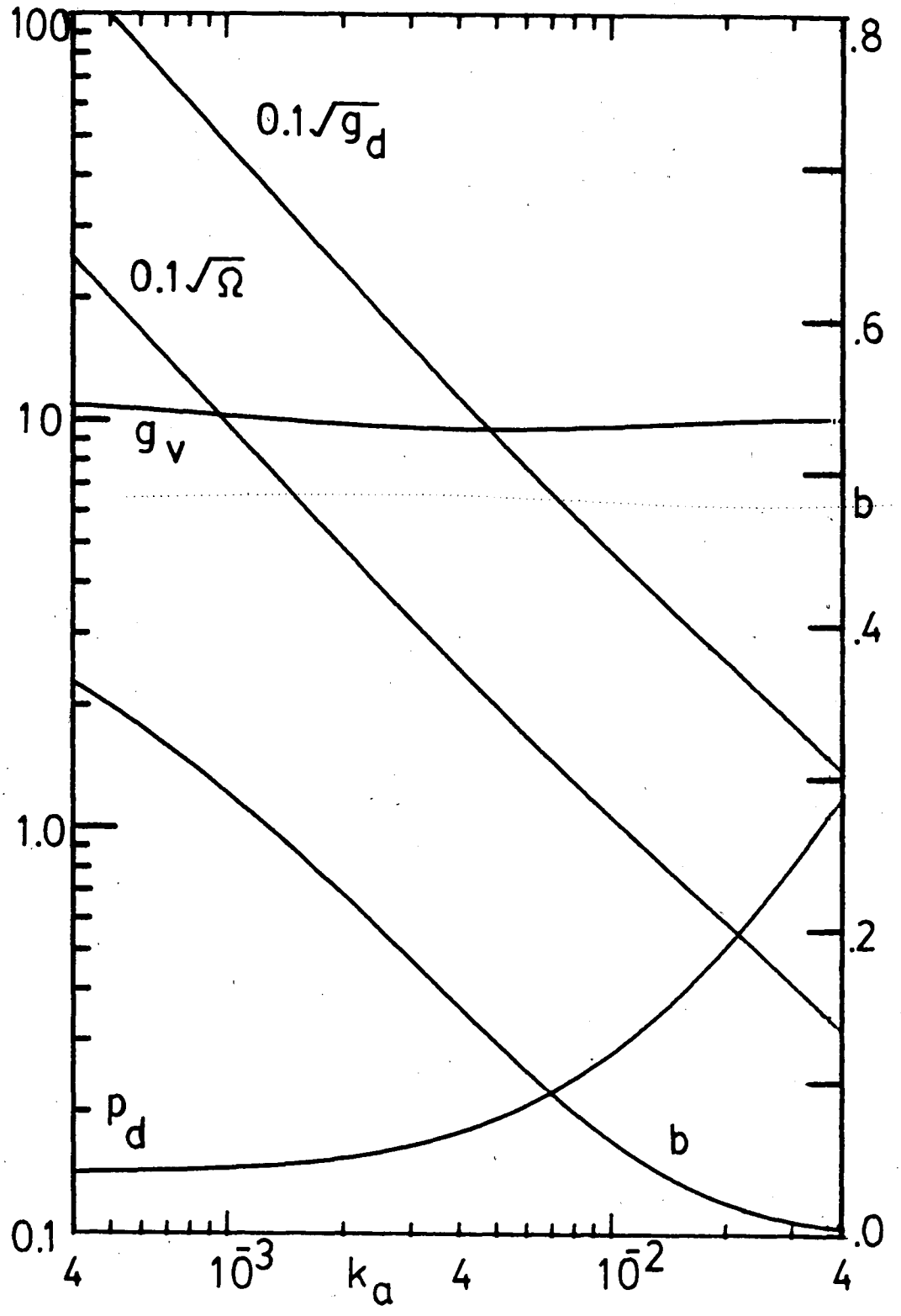

Figure 41. Minimum Dissipation Solution, $T/T_{st}=30$ $\varepsilon_\mu=1.3*10^{-4}$, Sliding Valve.

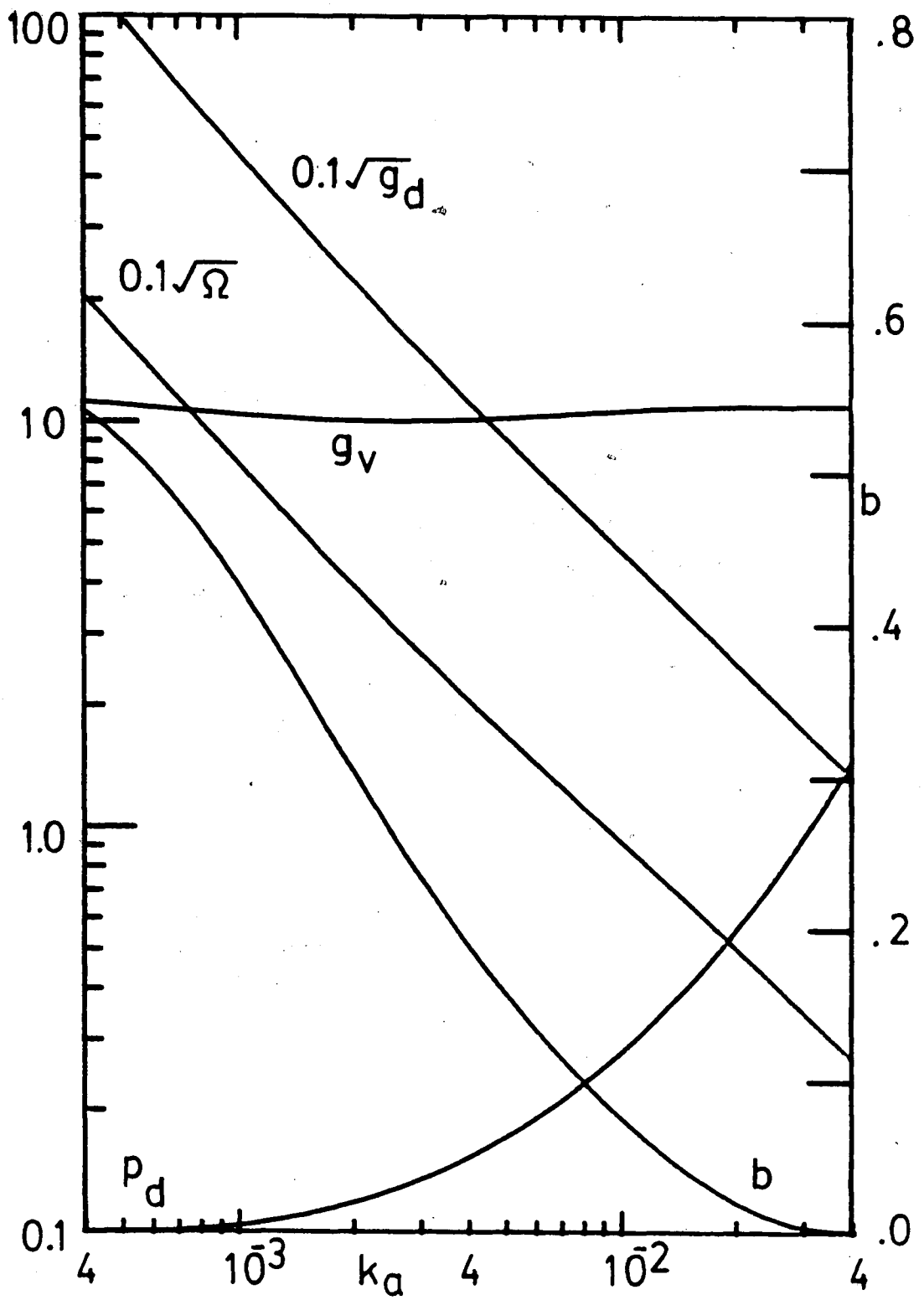

Figure 42. Minimum Dissipation Solution, $T/T_{st}=40$ $g_\mu=1.3*10^{-4}$, Sliding Valve.

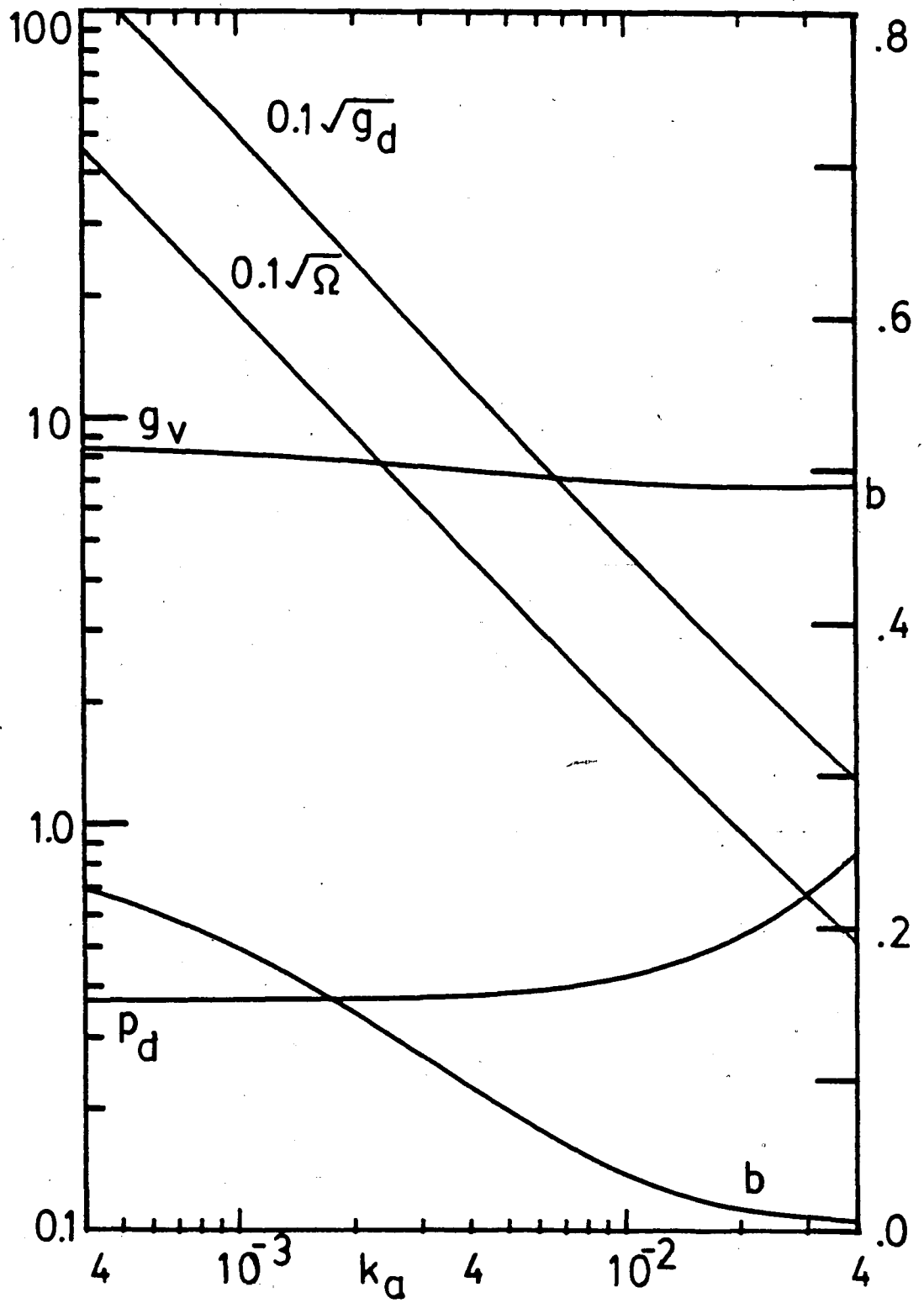

Figure 43. Minimum Dissipation Solution, $T/T_{st}=10$ $g_\mu=10^{-4}$, Sliding Valve.

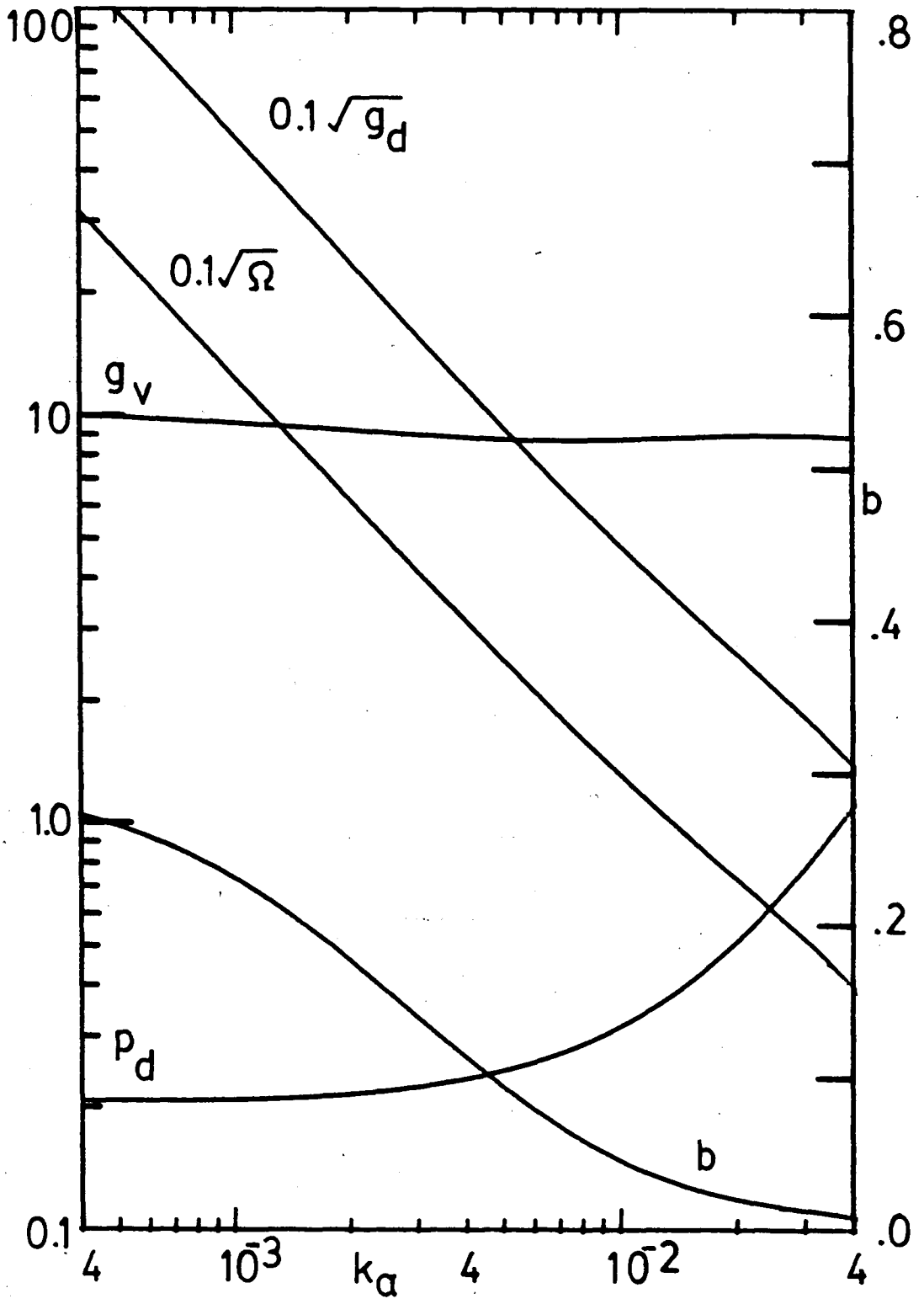

Figure 44. Minimum Dissipation Solution, $T/T_{st}=20$ $g_\mu=10^{-4}$, Sliding Valve.

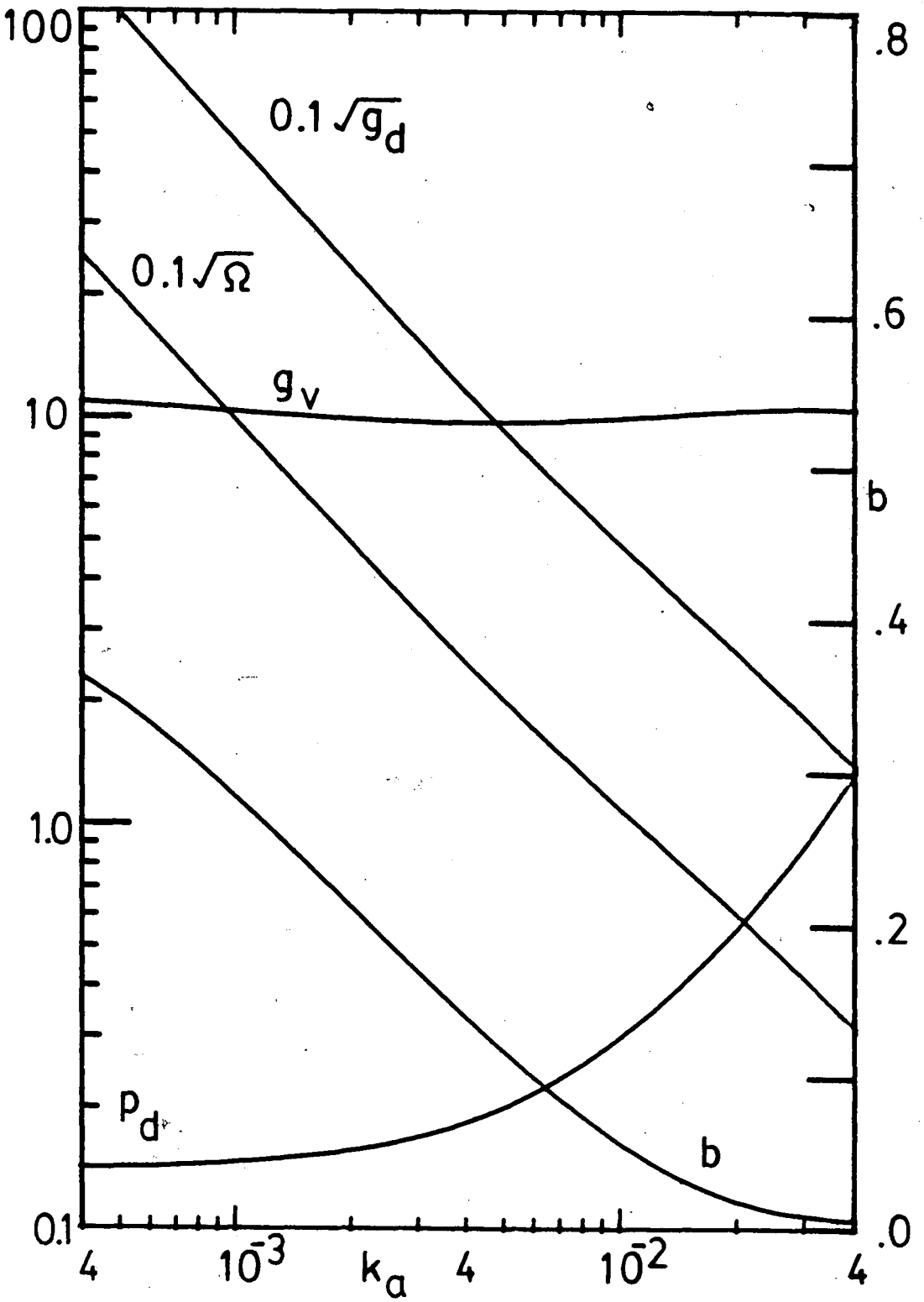

Figure 45. Minimum Dissipation Solution, $T/T_{st}=30$ $g_\mu=10^{-4}$, Sliding Valve.

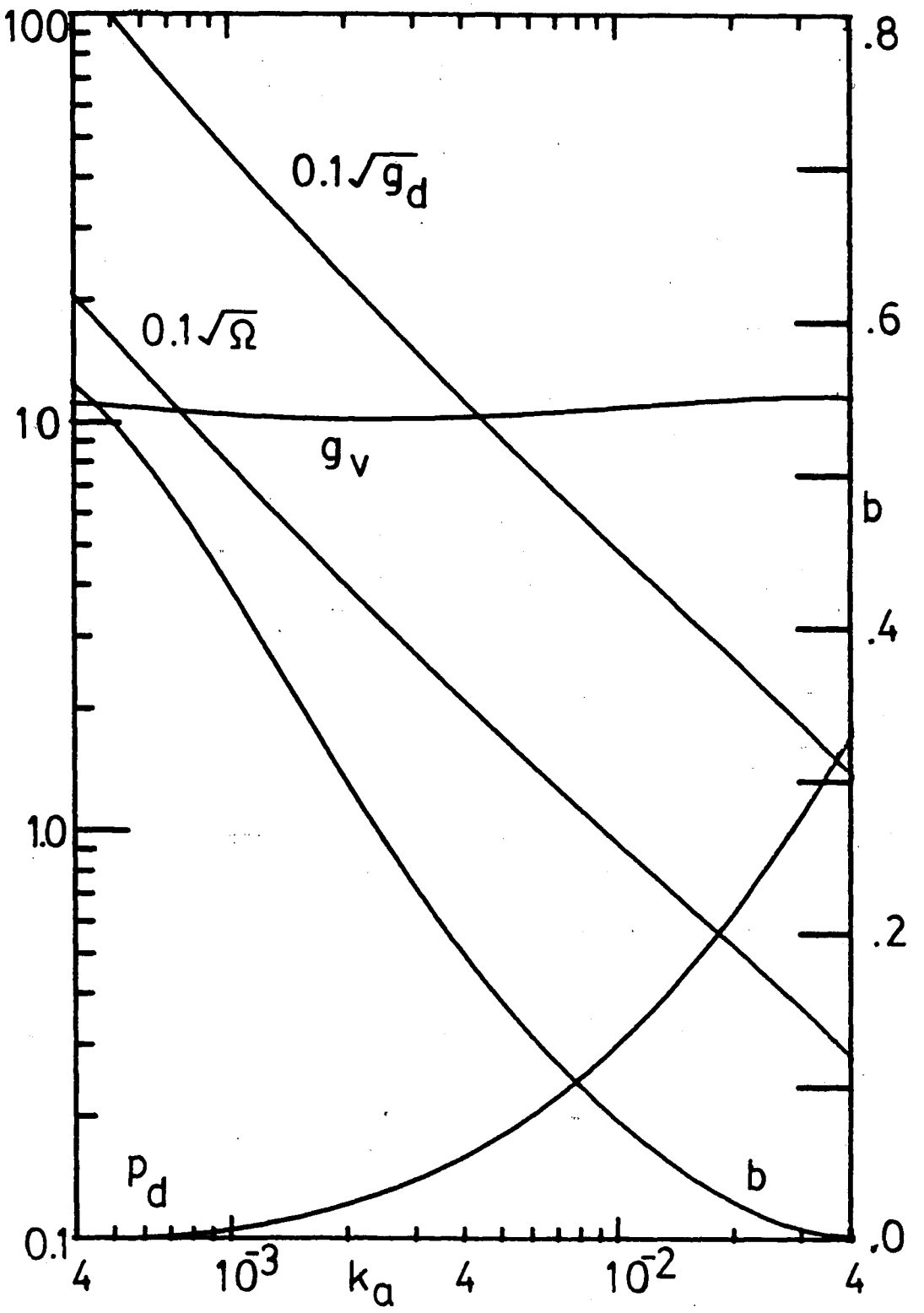

Figure 46. Minimum Dissipation Solution, $T/T_{st}=40$ $g_\mu=10^{-4}$, Sliding Valve.

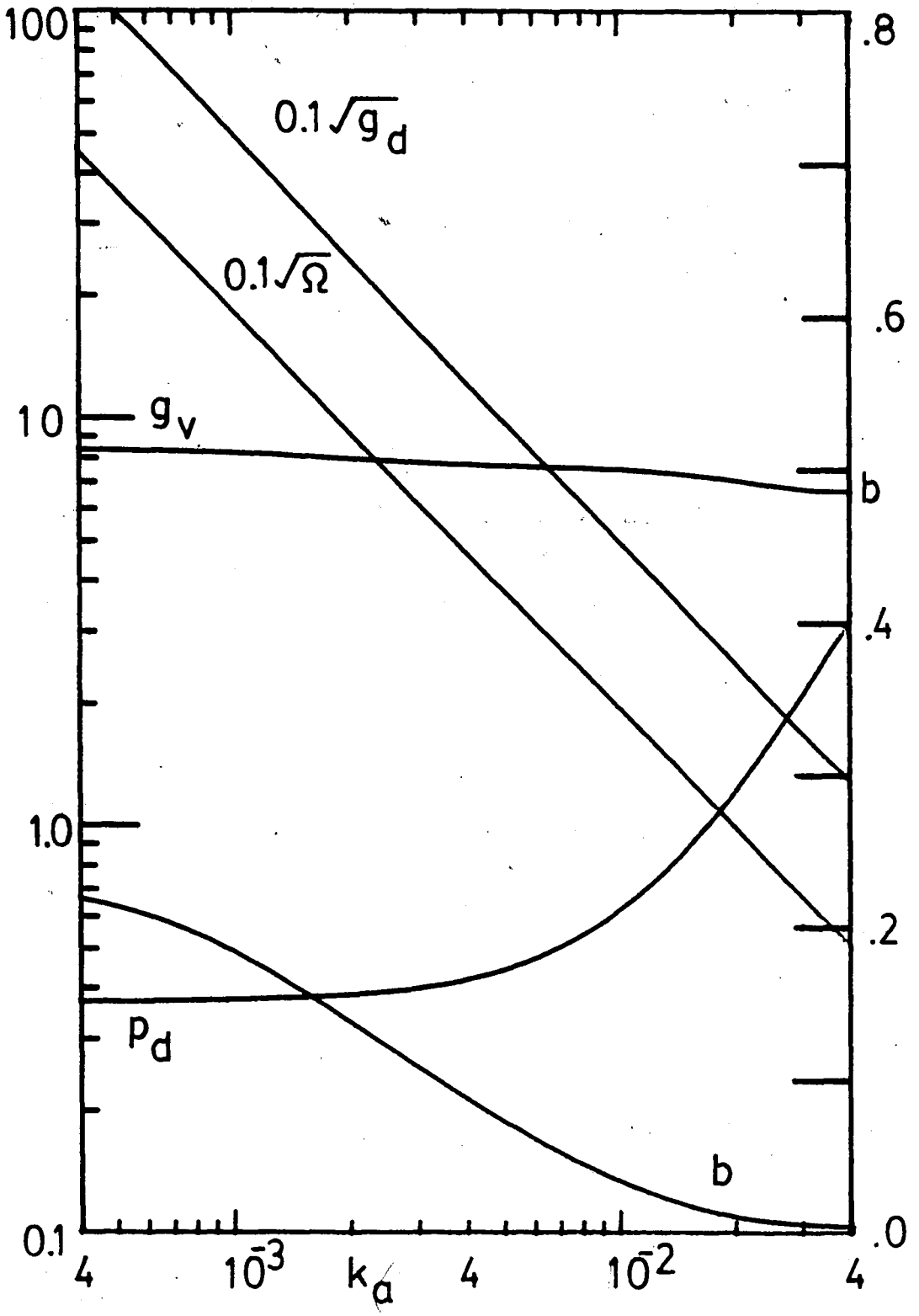

Figure 47. Minimum Dissipation Solution, $T/T_{st}=10$ $g_\mu=10^{-3}$, Sliding Valve.

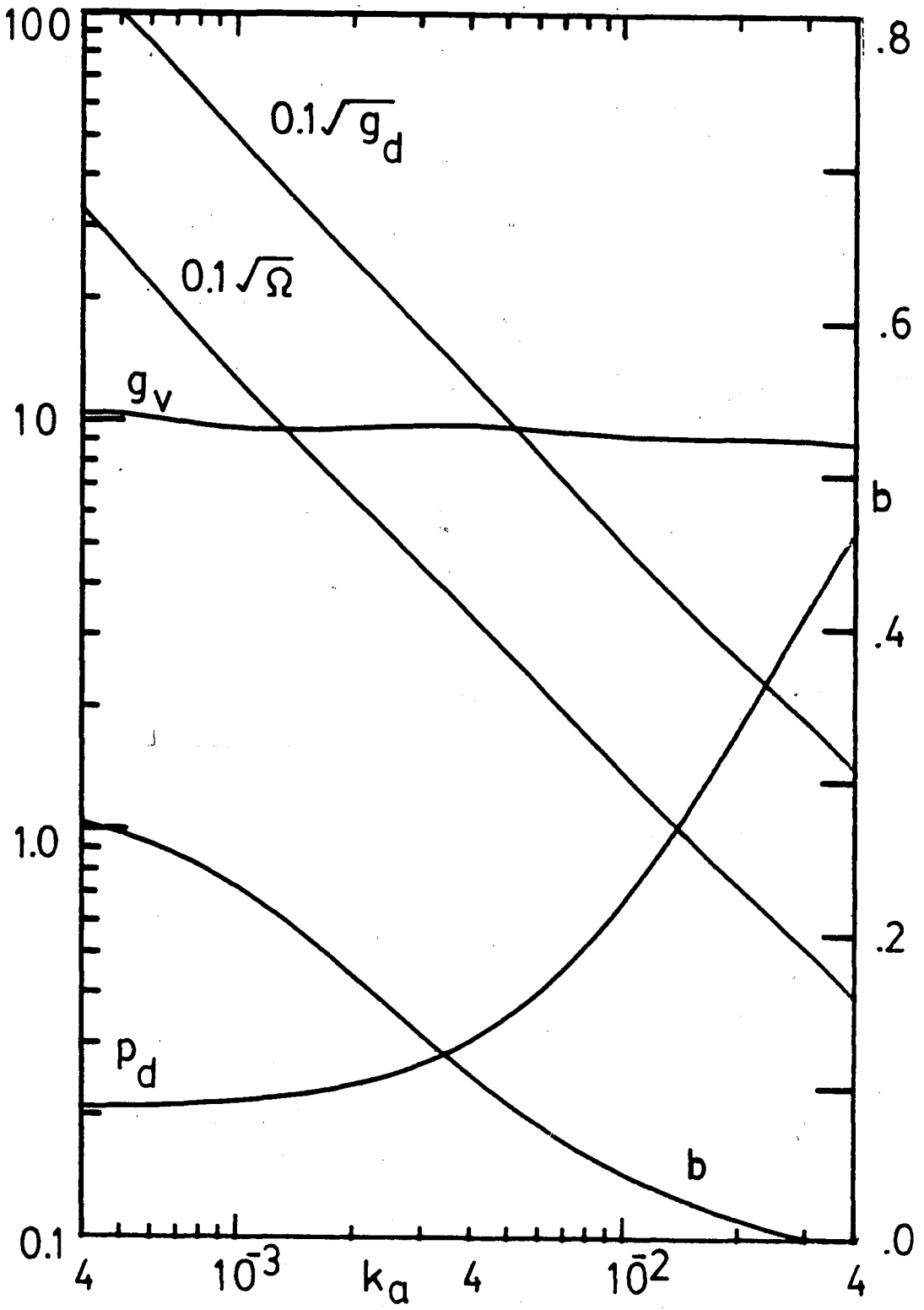

Figure 48. Minimum Dissipation Solution, $T/T_{st}=20$ $\epsilon_\mu=10^{-5}$, Sliding Valve.

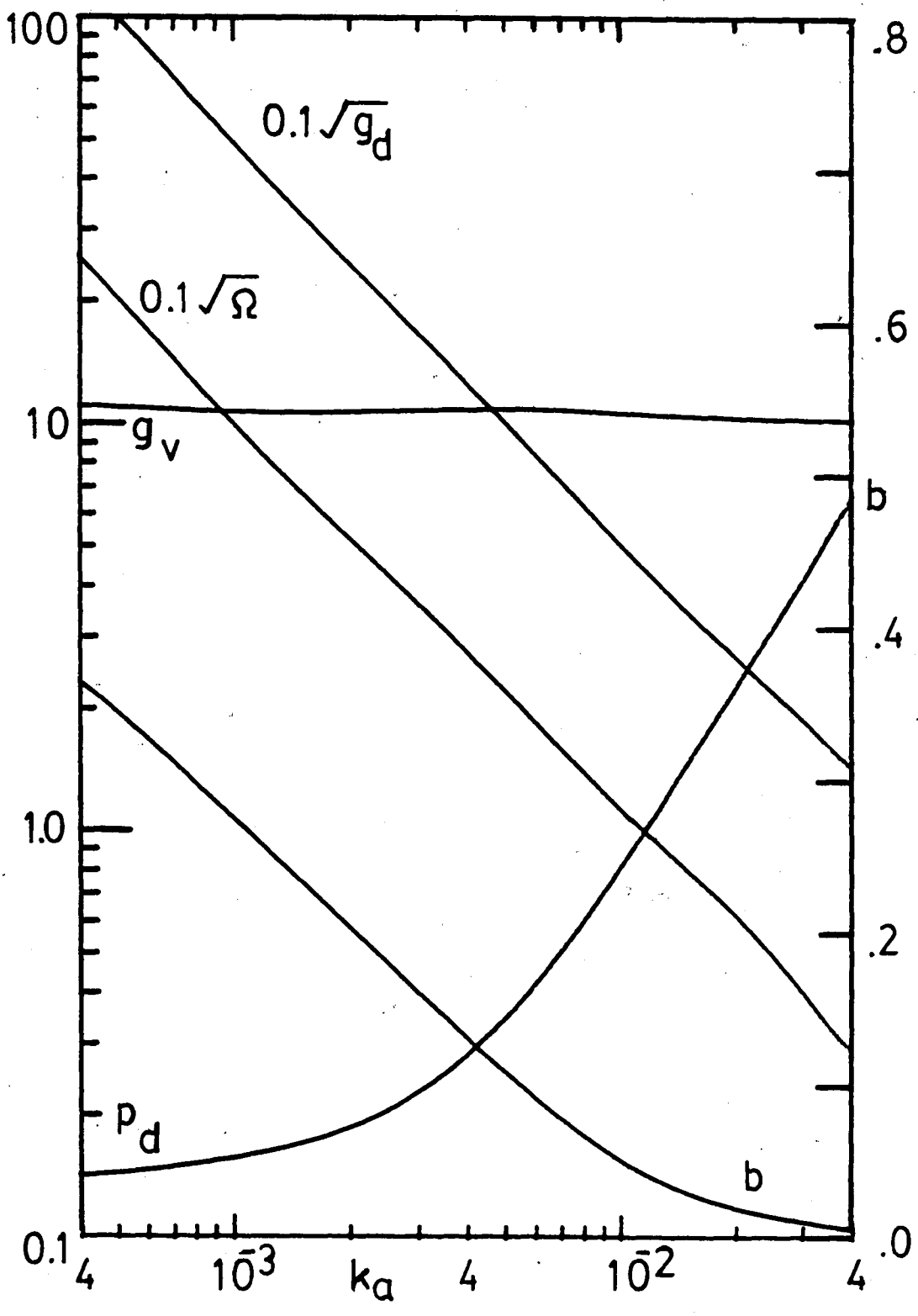

Figure 49. Minimum Dissipation Solution, $T/T_{st}=30$ $g_\mu=10^{-5}$, Sliding Valve.

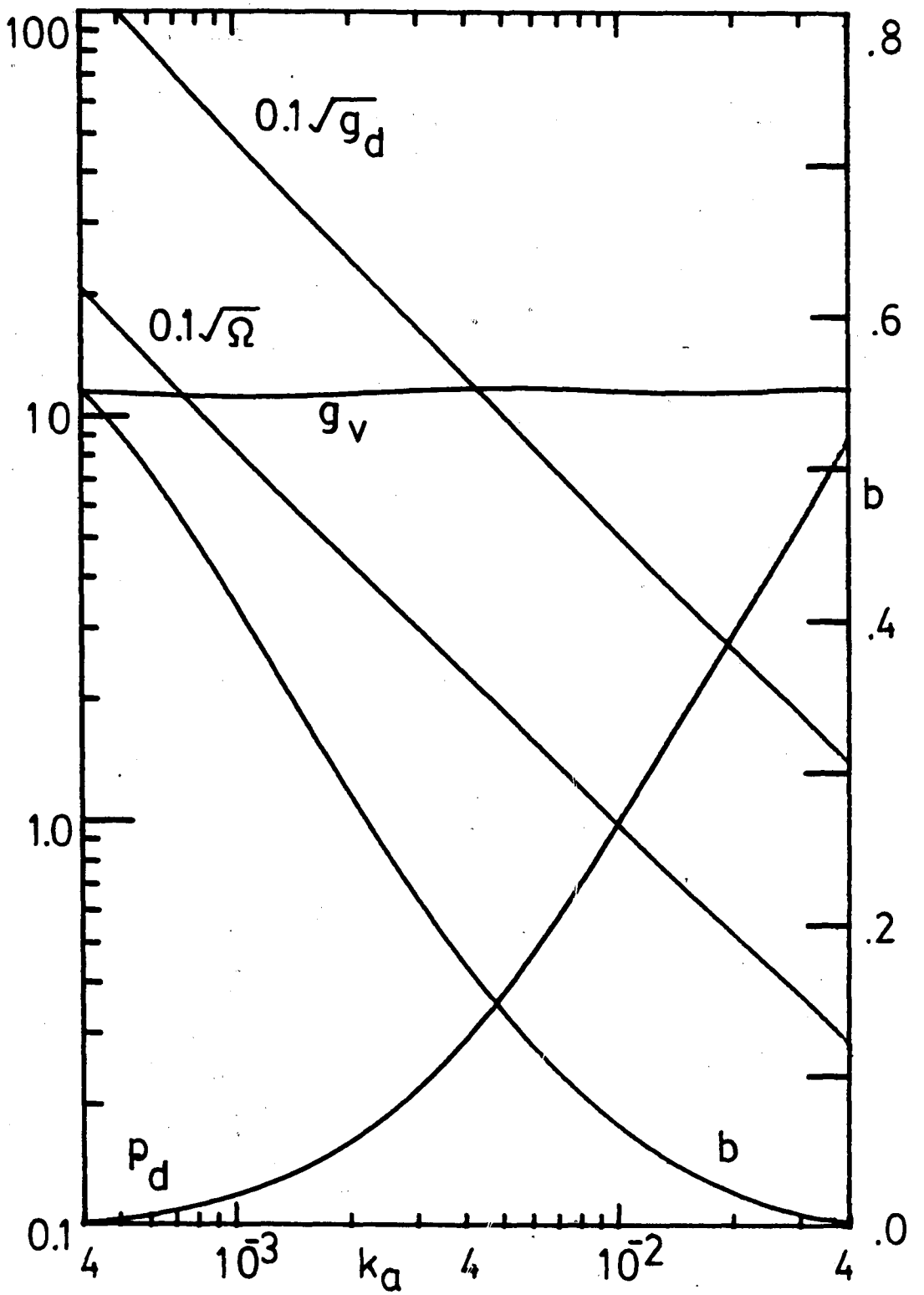

Figure 50. Minimum Dissipation Solution, $T/T_{st}=40$ $g_\mu=10^{-5}$, Sliding Valve.

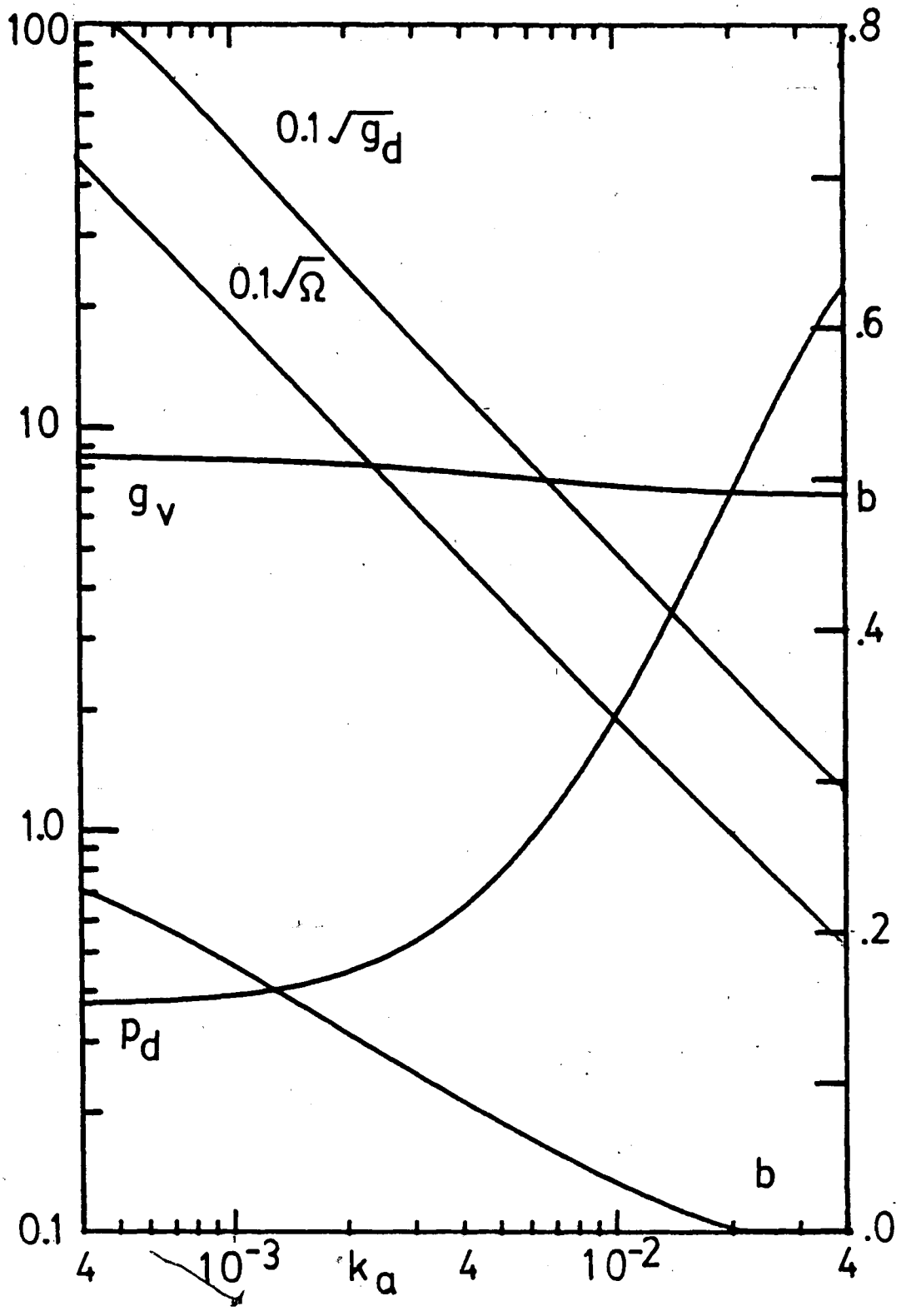

Figure 51. Minimum Dissipation Solution, $T/T_{st}=10$ $g_\mu=10^{-6}$, Sliding Valve.

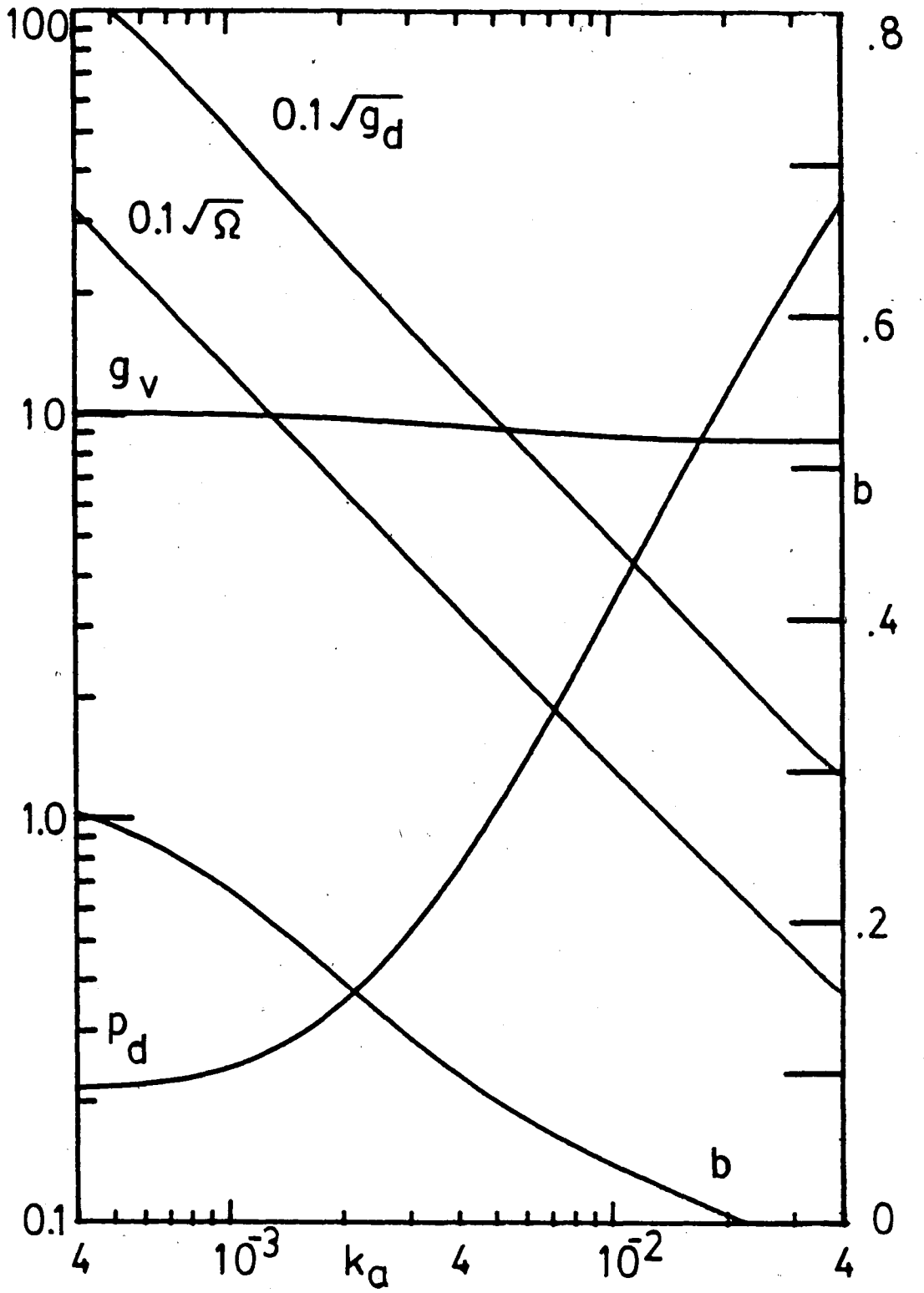

Figure 52. Minimum Dissipation Solution, $T/T_{st}=20$ $g_\mu=10^{-6}$, Sliding Valve.

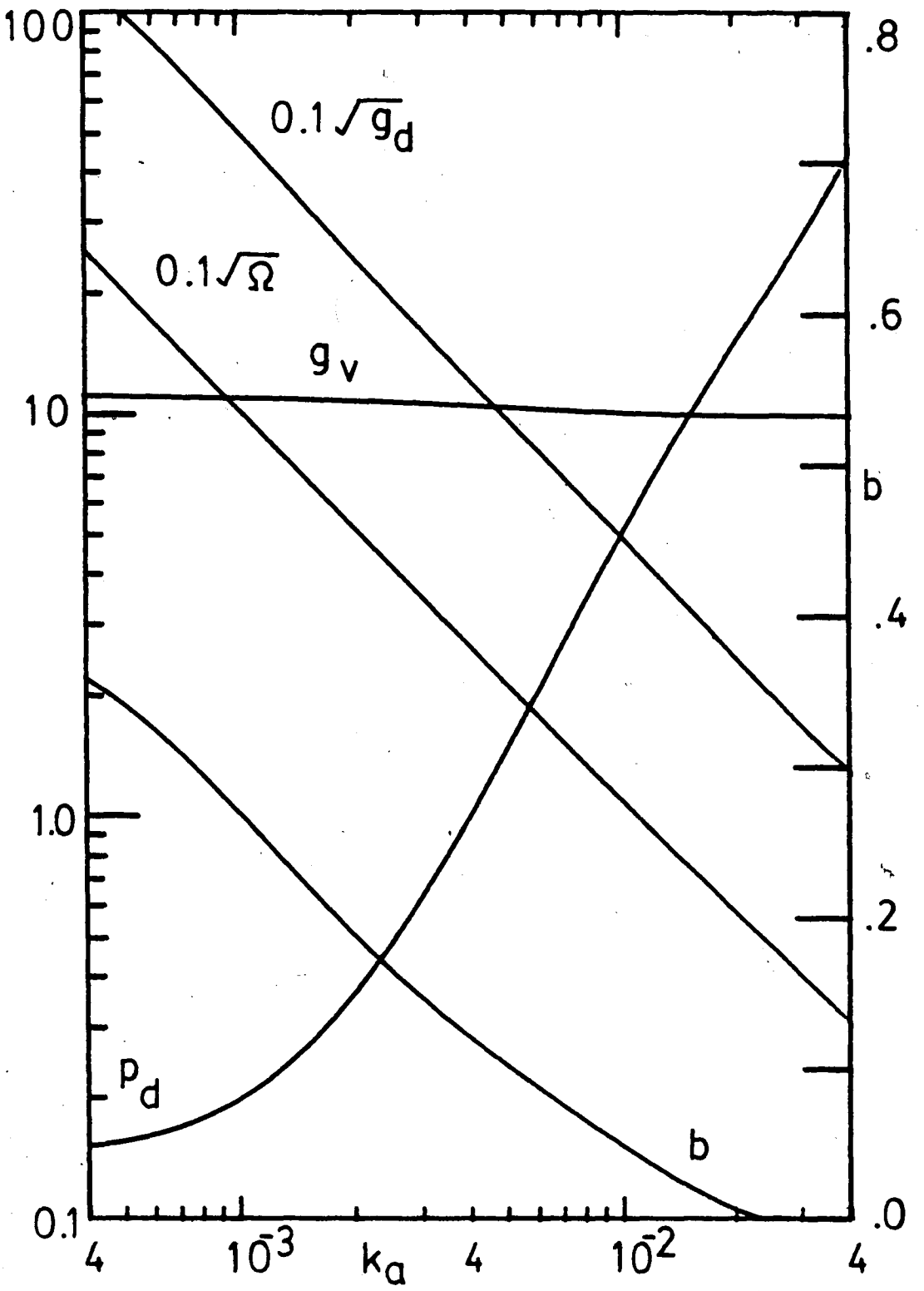

Figure 53. Minimum Dissipation Solution, $T/T_{st}=30$ $g_\mu=10^{-6}$, Sliding Valve.

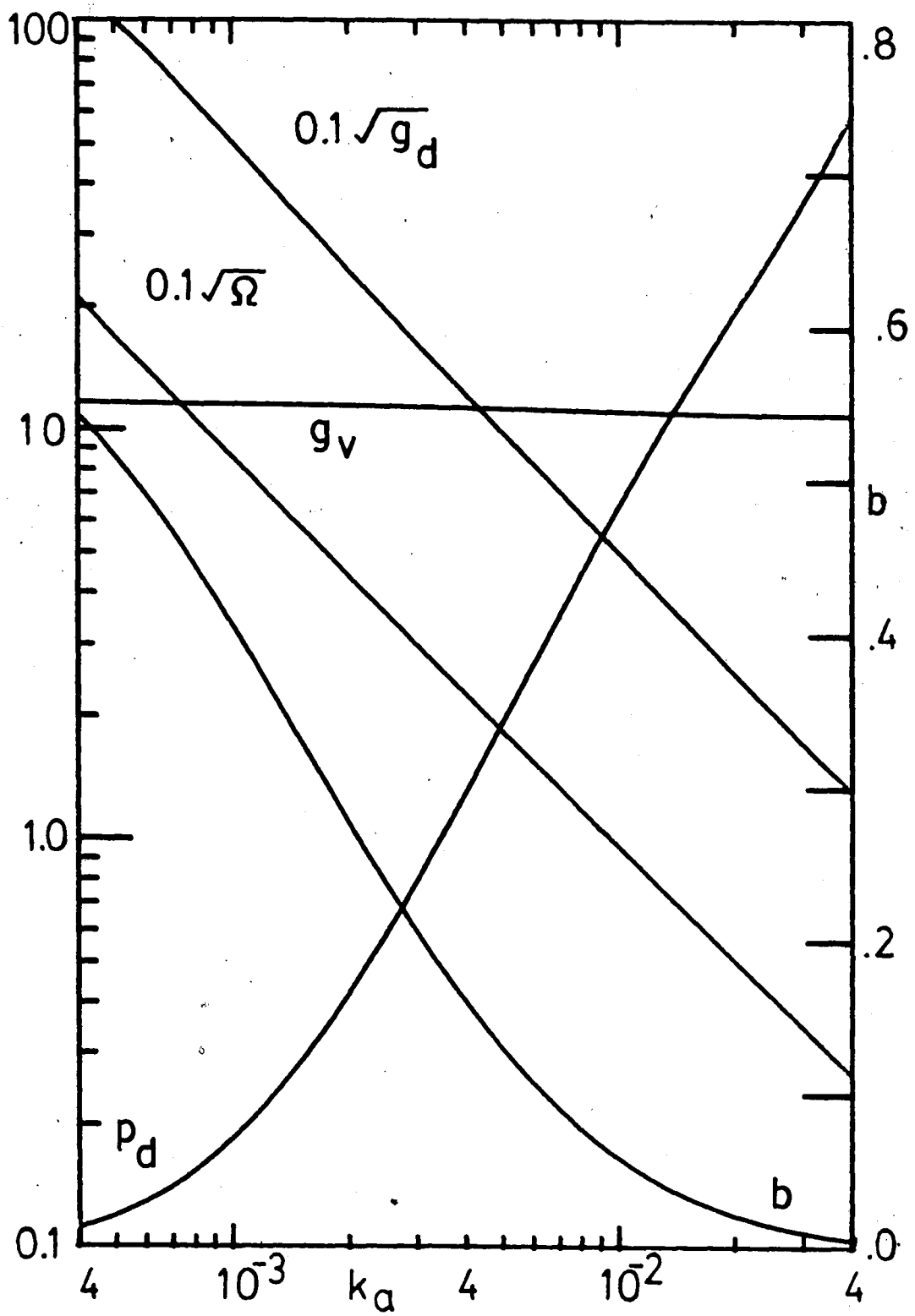

Figure 54. Minimum Dissipation Solution, $T/T_{st}=40$ $g_\mu=10^{-6}$, Sliding Valve.

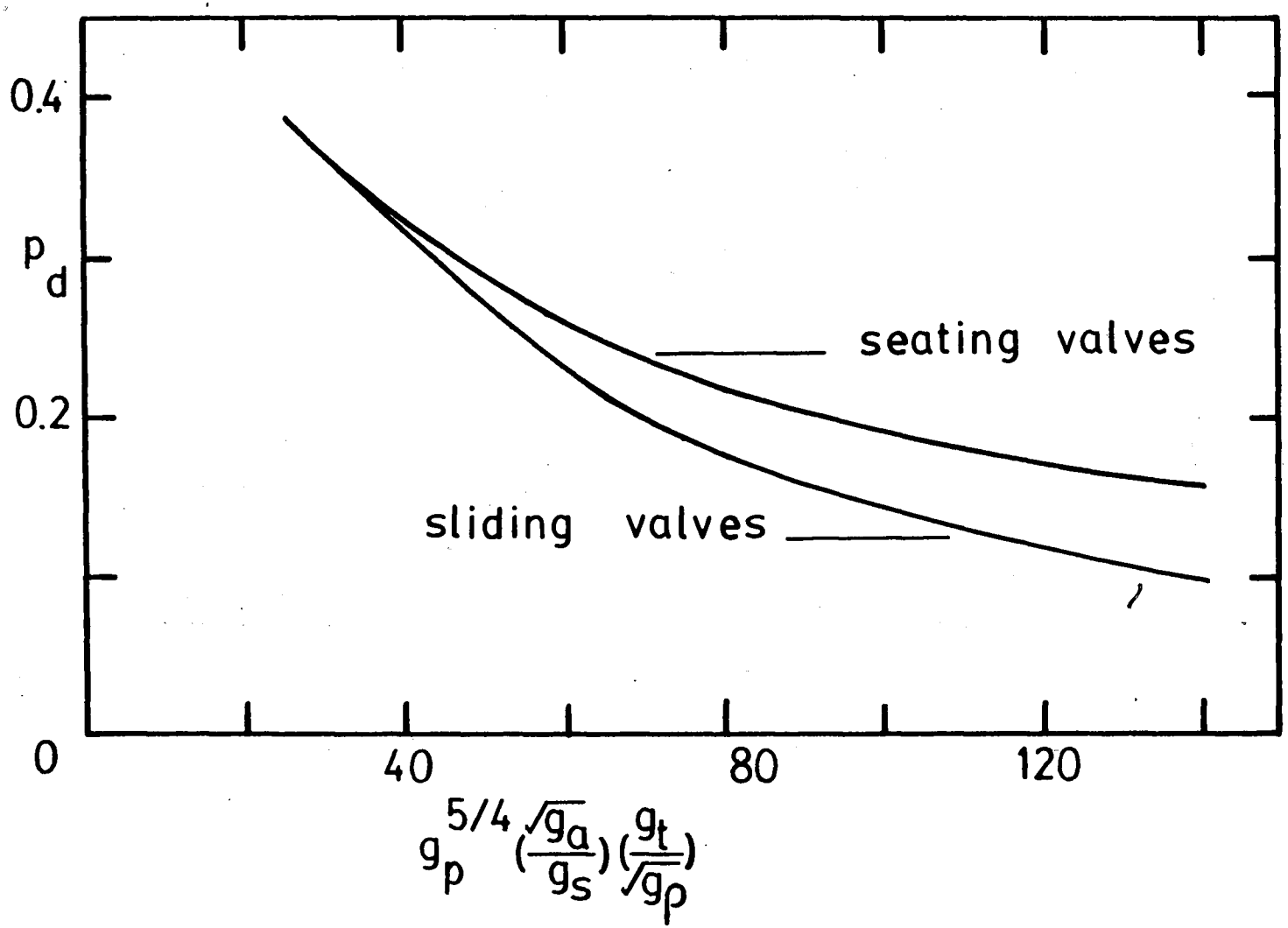

Figure 55. Global Minimum Dissipation as a Function of Normalized Period.

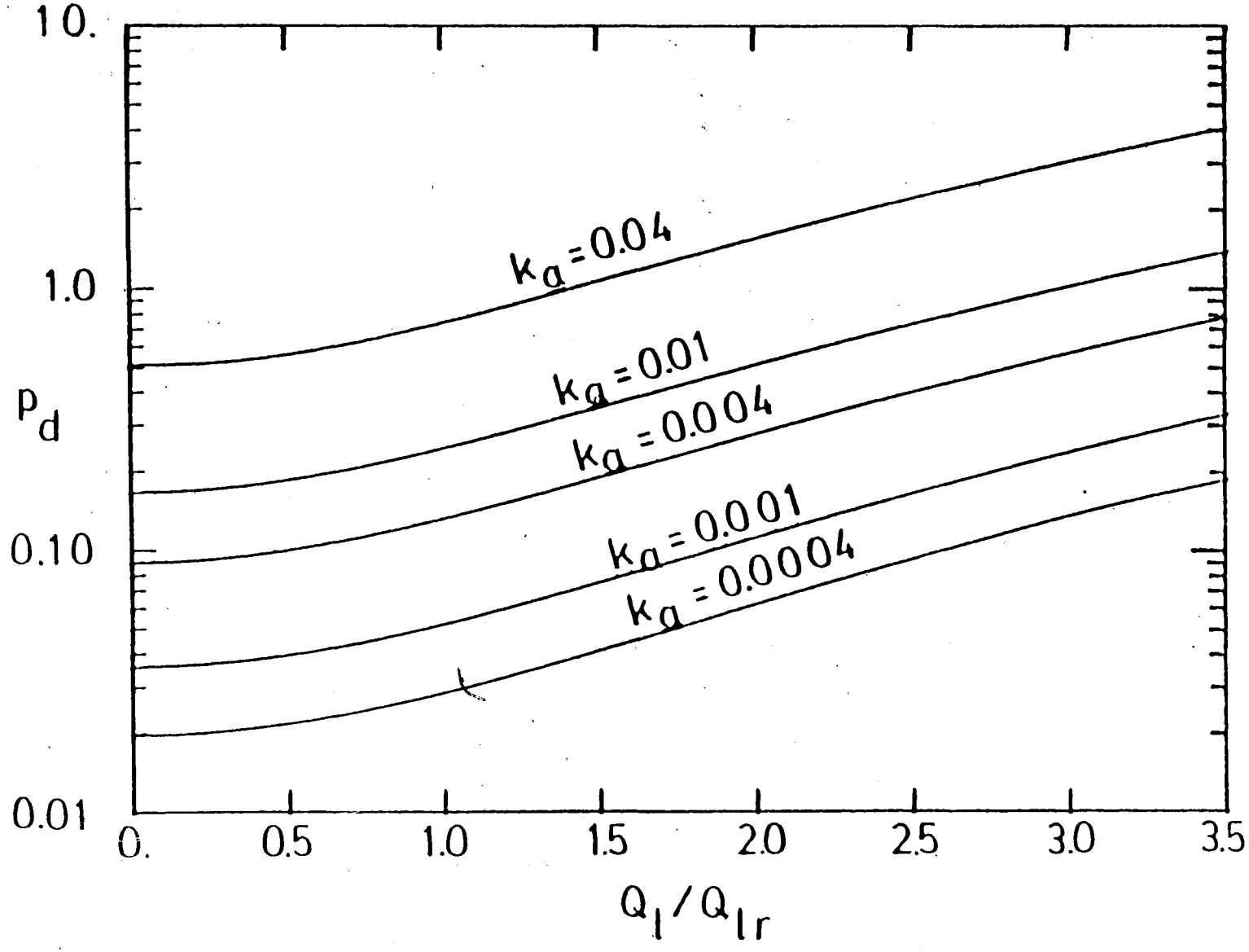

Figure 5[illegible]. Energy Dissipation Corresponding to Non-Optimal Flow, Seating Valve. (No Constraint, Laminar Flow)

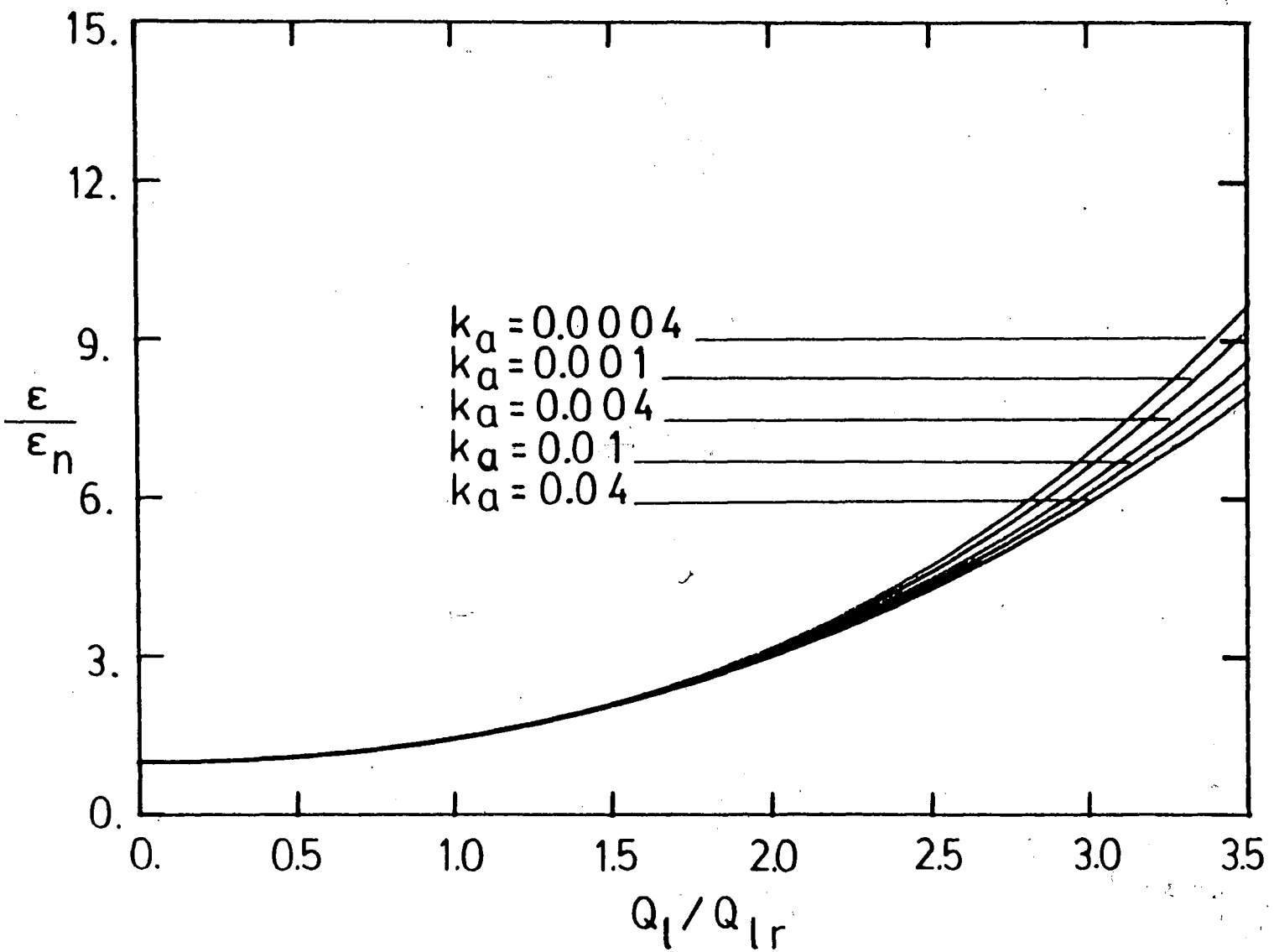

Figure 57. Non-Optimal Dissipation Compared to its Value at the Null State (used with Figure 56).

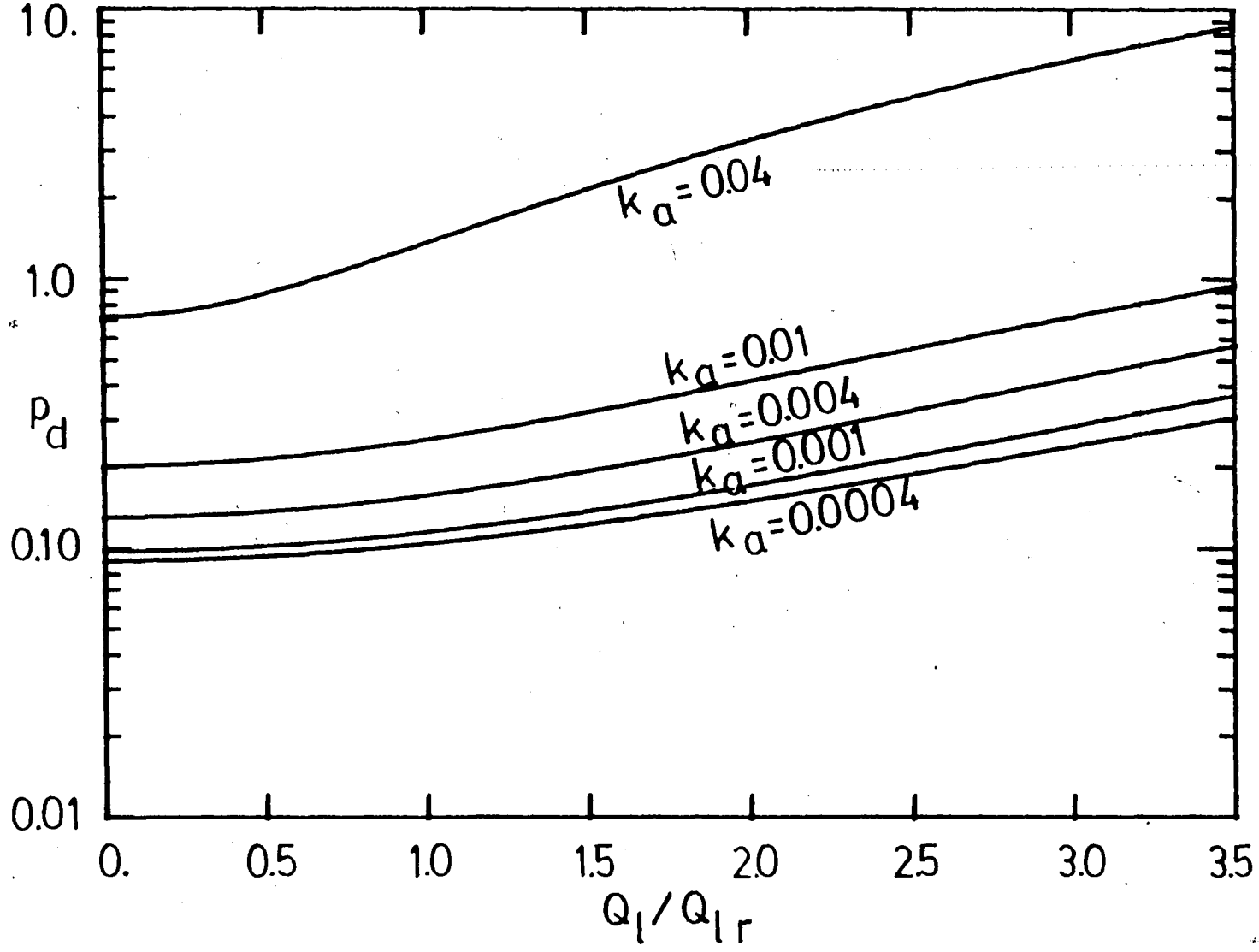

Figure 58. Energy Dissipation Corresponding to Non-Optimal Flow, Sliding Valve (T/T_{st}=40, Laminar Flow).

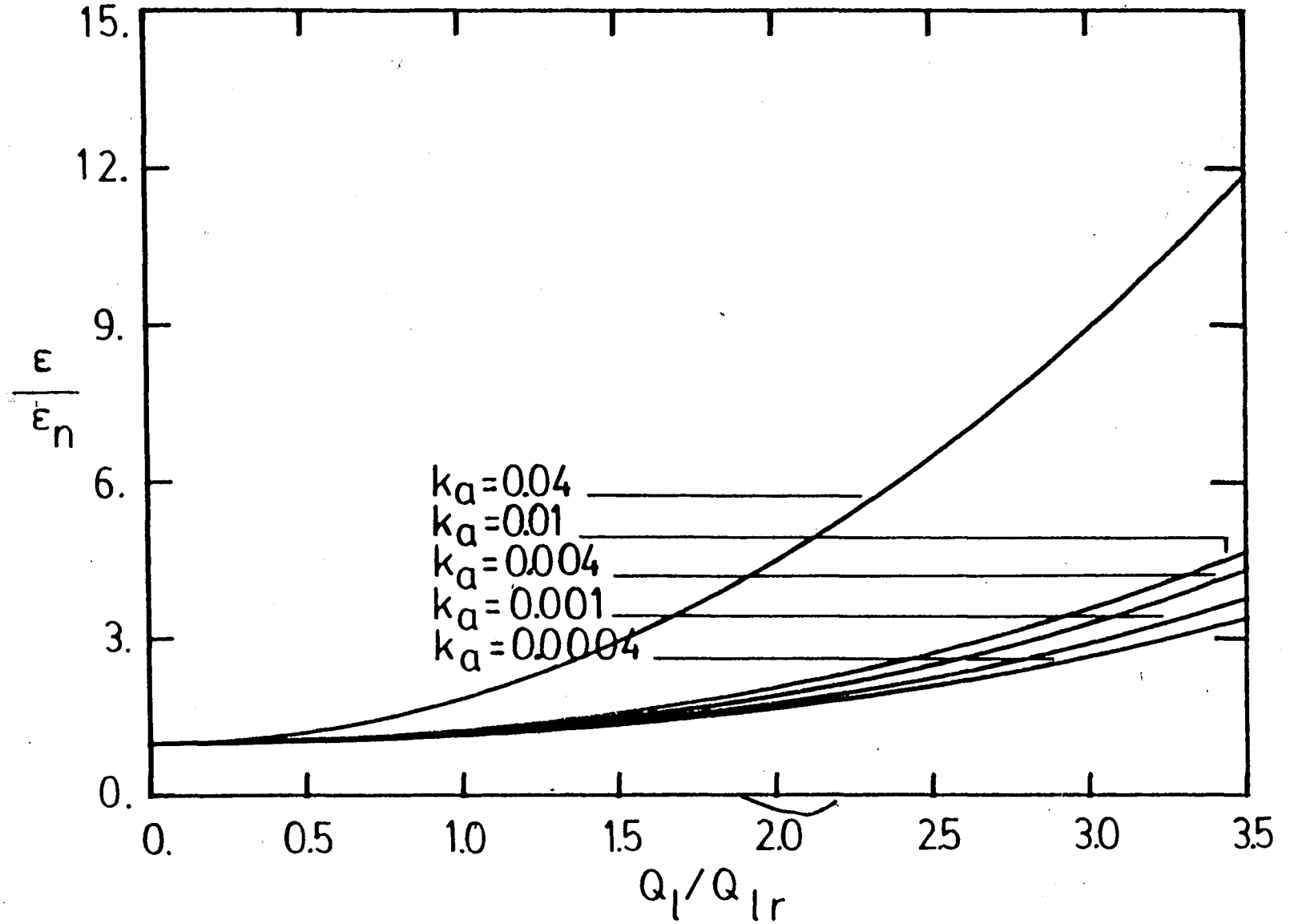

Figure 59. Non-Optimal Dissipation Compared to Its Value at the Null State (used with Figure 58).

BIBLIOGRAPHY

1. S.A. Murtaugh, "An Introduction to the Time-Modulated Acceleration Switching Electronydraulic Servomechanism", Journal of Basic Engineering, Trans. ASME, Series D, V.81, June 1959, pp. 263-271.
2. F.T. Brown, "Hydraulic Switching Servosystems: Part I, Aperiodic Switching".
3. F.T. Brown, "The Use of Fluid Inertia for D/A Conversion in Hydraulic PLM Circuits with Seating Valves, Part I: Concepts".
4. S.C. Tsai and P.R. Ukrainetz, "Response Characteristics of a Pulse-Width Modulated Electrohydraulic Servo", Journal of Basic Engineering, Trans. ASME, Series D, V. 92, June 1970, pp. 204-214.
5. A. Mansfeld, "Fast Switching Ball Valve as Digital Control Elements for an Electro-Hydraulic Servo Actuator", 6th Int. Fluid Power Symposium, BHRA Fluid Engineering, April 1981, pp. 335-348.
6. F.T. Brown, "Hydraulic Switching Servosystems: Part II, Periodic Switching".
7. F.T. Brown, "The Transient Response of Fluid Lines",

Journal of Basic Engineering, Trans. ASME, Series D, V. 84, n3, December 1962, pp. 547-.

8. N.B. Nichols, "The Linear Properties of Pneumatic Transmission Lines", ISA Transactions, V. 1, n1, January 1962.

9. F.T. Brown, D.L. Margolis and R.P. Shah, "Small Amplitude Frequency Behavior of Fluid Lines with Turbulent Flow", Journal of Basic Engineering, Trans. ASME Series D, V. 91, n4, December 1969, pp. 678-693.

10. F.T. Brown, "Wave Propagation in Tubes with Turbulent Flow", Proceedings ASME Symposium on Fluid Transmission Line Dynamics, November 1981, pp. 1-32.

11. F.T. Brown and A.S. Koseoglu, "The Use of Fluid Inertia for D/A Conversion in Hydraulic PLM Circuits with Seating Valves, Part II, Results".

APPENDIX A: ENERGY LOSS IN THE VALVE (ZERO LOAD)

After the equations of motion (equations (13) and (14)) are summed to eliminate p, substituting equation (23) gives

$$[\frac{Q_s}{Q_t}] \equiv M = \frac{m_1^2 \mathrm{sgn}(Q_s-Q_t) - \sqrt{m_1^4 - m_3 m_1^2 [\mathrm{sgn}(Q_s-Q_t) - \frac{m_2^2}{c_v^2}(1+2b)^2]}}{m_3} \tag{97}$$

where

$$m_1 \equiv (\gamma^2 - \frac{b}{1+2b}) \tag{98}$$

$$m_2 \equiv (\gamma^2 - \frac{1+b}{1+2b}) \tag{99}$$

$$m_3 \equiv m_2^2 \mathrm{sgn} Q_s + m_1^2 \mathrm{sgn}(Q_s-Q_t) \tag{100}$$

Note that the sign change for Q_s occurs when $\gamma = \gamma_{cr}$ where

$$\gamma_{cr} \equiv \sqrt{\frac{1+b-c_v}{1+2b}} \tag{101}$$

The energy dissipations ε_{s1}, ε_{s2}, ε_{s3} during a single

switch, then, are computed using equations (16), (17) and (18) respectively.

Equation (16) gives

$$\frac{d\varepsilon_{s1}}{dt} = \frac{Q_t^3}{a_o^2(1+2b)^2 m_2^2} \qquad (102)$$

Substituting equation (23) and, then, integrating equation (102), one gets

$$\frac{\varepsilon_{s1}}{PQ_d T_{st}} = c_v^2 \int_o^{\gamma_1} \frac{d\gamma}{(1+2b)^2 m_2^2} \qquad (103)$$

and use of equation (22) gives

$$E_{s1} = \frac{1}{(1+2b)^2} \int_o^{\gamma_1} \frac{d\gamma}{m_2^2} \qquad (104)$$

Repeating the same with equation (18) gives

$$E_{s3} = \frac{1}{(1+2b)^2} \int_{\gamma_2}^{1} \frac{d\gamma}{m_1^2} \qquad (105)$$

which gives

$$E_{s1} + E_{s3} = g(b)$$

giving equation (24a) in the text.

The dissipation when both ports are open is more

complicated, however. Equation (17) gives

$$\frac{d\epsilon_{s2}}{dt} = \frac{Q_t^3}{a_o^2(1+2b)^2}\left[\frac{(absM)^3}{m_1^2} + \frac{[abs(M-1)]^3}{m_2^2}\right] \qquad (106)$$

and similarly, the result is obtained as

$$\frac{\epsilon_{s2}}{PQ_dT_{st}} = \frac{c_v^2}{(1+2b)^2}\int_{\gamma_1}^{\gamma_2}\left[\frac{(absM)^3}{m_1^2} + \frac{[abs(M-1)]^3}{m_2^2}\right]d\gamma \qquad (107)$$

or

$$E_{s2} = \frac{1}{(1+2b)^2}\int_{\gamma_1}^{\gamma_2}\left[\frac{(absM)^3}{m_1^2} + \frac{[abs(M-1)]^3}{m_2^2}\right]d\gamma \cdot \qquad (108)$$

Note that M includes the valve parameter, c_v. The above equation is given in the text as equations (21a) and (21b).

These equations have been derived while the valve was turning on and similar derivations have been applied while the valve was turning off. The results show that E_s remains the same if no cavitation is assumed. Therefore

$$E_s = 2[g(b) + E(c_v,b)]$$

which is equation (25a) in the text.

It has been seen that in the principal range of interest ($0 \leq e_v < 0.9$; $0 \leq b \leq 2$), the classical separation of variable technique can be applied to give equations (26a) and (26b).

The approximations are, then, given in terms of simple functions and the coefficients of equations (27), (28), (29) are given below:

$a_1 = 0.343$

$a_2 = 1.08$

$a_3 = 0.8$

$f_0 = 1.0$

$f_1 = -2.11$

$f_2 = 10.42$

$f_3 = -41.03$

$f_4 = 101.84$

$f_5 = -159.14$

$f_6 = 159.16$

$f_7 = -101.64$

$f_8 = 40.07$

$f_9 = -8.83$

$f_{10} = 0.85$

$g_0 = 0.0$

$g_1 = 5.32$

$$g_2 = -34.22$$

$$g_3 = 128.12$$

$$g_4 = -297.62$$

$$g_5 = 441.86$$

$$g_6 = -425.55$$

$$g_7 = 264.26$$

$$g_8 = -101.99$$

$$g_9 = 22.23$$

$$g_{10} = -2.09$$

The respective errors in these approximations are quite negligible in the range where the previously mentioned separation applies.

Derivation of the energy dissipation when the valve is not switching is given in Appendix B for the most general case ($Q_\ell \neq 0$), and the result for zero load flow is given in equation (30a).

APPENDIX B: ENERGY LOSS IN THE VALVE (NON-ZERO LOAD)

Introducing the load flow via equation (33) and changing the definition of c_v through equation (36) enables one to write the governing equations in the most general way. The new definitions

$$c_{v1} \equiv \frac{Q_{t1}}{a_o\sqrt{P}} \tag{109}$$

and

$$c_{v2} \equiv \frac{Q_{t2}}{a_o\sqrt{P}} \tag{110}$$

give

$$\frac{Q_s}{Q_{t1}} \equiv M_1 \tag{111}$$

and

$$\frac{Q_s}{Q_{t2}} \equiv M_2 \tag{112}$$

respectively.

Notice that

$$\begin{aligned} M_1 &= M_1(c_{v1}, b) \\ M_2 &= M_2(c_{v2}, b) \end{aligned} \tag{113}$$

Then ε_{s1} and ε_{s3} (for turning on) are given as

$$\varepsilon_{s1} = \frac{Pc_{v2}^2 |Qt_2| T_{st}}{(1+2b)^2} \int_o^{\gamma_1} \frac{d\gamma}{m_2^2} \qquad (114)$$

$$\varepsilon_{s3} = \frac{Pc_{v2}^2 |Qt_2| T_{st}}{(1+2b)^2} \int_{\gamma_2}^{1} \frac{d\gamma}{m_1^2} \qquad (115)$$

giving

$$\frac{\varepsilon_{s1}+\varepsilon_{s3}}{PQ_d T_{st}} = c_{v2}^2 \left|\frac{Qt_2}{Q_d}\right| g(b) \quad . \qquad (116)$$

Similarly, for turning off, we get

$$\frac{\varepsilon_{s1}+\varepsilon_{s3}}{PQ_d T_{st}} = c_{v1}^2 \left(\frac{Qt_1}{Q_d}\right) g(b) \quad . \qquad (117)$$

Finally, ε_{s2} (for turning on) is derived using

$$\frac{d\varepsilon_{s2}}{dt} = \frac{Qt_2^3}{a_o^2 (1+2b)^2} \left[\frac{(absM_2)^3}{m_1^2} + \frac{[abs(M_2-1)]^3}{m_2^2}\right] \qquad (118)$$

and becomes

$$\frac{\varepsilon_{s2}}{PQ_d T_{st}} = \frac{Qt_2}{Q_d} c_{v2}^2 E(c_{v2},b) \quad . \qquad (119)$$

Similarly, ε_{s2} for turning off becomes

$$\frac{\varepsilon_{s2}}{PQ_d T_{st}} = \frac{Q_{t1}}{Q_d} c_{v1}^2 E(c_{v1}, b) \quad . \tag{120}$$

The energy dissipation in the valve during switching for a complete cycle, ε_s, is then obtained by summing the above results to give equations (41a) and (41b).

Using equations (33), (36), (109) and (110), the above equations can be simplified via definitions

$$c_{v1} = c_v(c_q+1) \tag{121}$$

$$c_{v2} = c_v(c_q-1) \quad . \tag{122}$$

One can also define

$$E(c_{v1}) = \frac{1}{2c_v^2(c_q+1)^2}\left[\frac{a_1}{c_v(c_q+1)} + a_2 c_v(c_q+1) + a_3 c_v^3(c_q+1)^3\right] \tag{123}$$

$$E(c_{v2}) = \frac{1}{2c_v^2(c_q-1)^2}\left[\frac{a_1}{c_v(c_q-1)} + a_2 c_v(c_q-1) + a_3 c_v^3(c_q-1)^3\right] \tag{124}$$

by making use of the approximations given in equation (27).

Then, equations (116) and (117) add to become

$$\frac{\varepsilon_{s1}+\varepsilon_{s3}}{PQ_dT_{st}} = [c_v^2(c_q+1)^3+c_v^2(c_q-1)^2|c_q-1|]g(b) \qquad (125)$$

or

$$\frac{\varepsilon_{s1}+\varepsilon_{s3}}{PQ_dT_{st}} = \begin{cases} 2c_v^2(1+3c_q^2)g(b) & c_q \leq 1 \\ 2c_qc_v^2(3+c_q^2)g(b) & c_q \geq 1 \end{cases} \qquad (126)$$

Equations (119) and (120), however, give

$$\frac{\varepsilon_{s2}}{PQ_dT_{st}} = \frac{a_1}{c_v} + a_2c_v(1+c_q^2)+a_3c_v^3[(1+c_q^2)^2+4c_q^2] \qquad (127)$$

Finally, the energy dissipation when the valve is not switching, ε_{ns}, is derived assuming that the flow varies linearly as shown in Figure 4. This assumption gives

$$Q_s(t) = \begin{cases} Q_{t2} + \frac{2Q_d}{\alpha}\left(\frac{t}{T}\right) & 0 \leq t \leq \alpha T \\ Q_{t2} + \frac{2Q_d}{(\alpha-1)}\left[\frac{t}{T}-1\right] & \alpha T \leq t \leq T \end{cases} \qquad (128)$$

Therefore,

$$\frac{d\varepsilon_{ns}}{dt} = \frac{Q_s^3}{a_o^2(1+b)^2} \tag{129}$$

is integrated in the following ranges:

$$\begin{aligned} \frac{T_{st}}{2} \leq t \leq \alpha T - \frac{T_{st}}{2} \\ \alpha T + \frac{T_{st}}{2} \leq t \leq T - \frac{T_{st}}{2} \end{aligned} \tag{130}$$

One should be careful, however, about the integration when $c_q \leq 1$. The final results, unfortunately, are quite complex and some approximation is necessary. The results after the approximation (using $\alpha = 1/2$) are given in equations (42a) and (42b). Using equations (33), (36), (38) and

$$Q_{t1}^4 + Q_{t2}^4 = 2[(Q_\ell^2 + Q_d^2) + 4Q_\ell^2 Q_d^2] \tag{131}$$

$$|Q_{t1}|^3 + |Q_{t2}|^3 = \begin{cases} 2Q_d(3Q_\ell^2 + Q_d^2) & c_q \leq 1 \\ 2Q_\ell(Q_\ell^2 + 3Q_d^2) & c_q \geq 1 \end{cases} \tag{132}$$

along with equations (126) and (127) gives the total dissipation in the valve, which is given in equations (43a) and (43b), and the related equations (44) through (47).

APPENDIX C: NOMENCLATURE

symbol	meaning	equation of definition or first use
a	valve orifice area	1
a_0	total valve orifice area for seating valves	1
a_s	upper orifice area	2
a_t	lower orifice area	2
a_1, a_2, a_3		27
b	ratio of length of additional opening to maximum stroke	2
C	compliance of fluid volume	82
c_d	orifice flow coefficient	11
c_q, c_{qd}	ratio mean:perturbation flows	33,58
c_s, c_{sd}	nondimensionalized switching time	37,59
c_t, c_{td}	nondimensionalized tube resistance	49,60
c_v, c_{vd}	nondimensionalized valve flow	23,57
c_{v1}, c_{v2}	c_v for respective switches	109,110
c_1		63
d	tube diameter	50

E_s	nondimensionalized ε_s	19
E_{s1}, E_{s2}, E_{s3}	nondimensionalized energies, $\varepsilon_{s1}, \varepsilon_{s2}, \varepsilon_{s3}$	19
f	friction factor	63
$\tilde{f}$	perturbation friction factor	67
$f_0, \ldots, f_{10}$		28
g	loss factor, turbulent flow	62
g_a	valve orifice area normalized to valve size	84
g_d	normalized tube area	77
g	normalized valve size	87
g_p	normalized supply pressure	88
g_s	normalized switching time	85
g_t	normalized period	89
g_v	valve orifice area normalized to flow	76
g_μ	normalized viscosity	78
g_ρ	normalized density of solid	91
$g_0, \ldots, g_{10}$		29
I	tube inertance	34
I_d	dynamic inertance of tube	56
I_s, I_t	valve port inertances	9,10

K_a	independent dimensionless quantity	73
ℓ	length of tube	6
ℓ_0	characteristic valve length	84
M, M_1, M_2		97,111,112
m		43
m_1, m_2, m_3		98,99,100
N	ratio wavelength:tube length	6
N_m	minimum acceptable value of N	7
n		3
P	supply pressure	9
p	pressure at valve-tube junction	9
P_d	normalized power dissipation	71
Q_d	amplitude flow perturbations	25
Q_ℓ	mean load flow	33
$Q_{\ell r}$	referance load flow	96
Q_s	supply flow	9
Q_t	volume flow through tube	10
Q_{t1}, Q_{t2}	Q_t for respective switches	40
R	resistance of tube	48
Re	tube flow Reynolds number	70
R_J	dynamic resistance of tube	55
r	surge loss coefficient	67

r_I	ratio dynamic:steady tube inertance	56
r_R	ratio dynamic:steady tube resistance	55
r_1, r_2, r_3		43
T	period of cycle	6
T_s	switching time for seating valves	39
T_{st}	switching time for sliding valves	3
t	running time	3
t_1, t_2		3
V	load chamber volume	82
v_p	phase velocity of waves	6
α	proportion of time valve on	34
β	fluid bulk modulus	82
γ_{cr}		101
$\gamma, \gamma_1, \gamma_2$		24
ε_{ns}	energy dissipated while valve is not switching	30
ε_s	energy dissipated in valve switch	15
$\varepsilon_{s1}, \varepsilon_{s2}, \varepsilon_{s3}$		16,17,18

ε_{st}	steady flow loss in tube	48
ε_{su}	surge loss in tube	53
ε_{t}	energy dissipated in tube	61
ε_{V_a}	total valve energy dissipation	31
μ	fluid viscosity	50
ν	kinematic viscosity	77
ρ	fluid density	11
ρ_s	density of solid	85
τ	inertive time constant	33
ψ	minimum dissipation function	95
Ω	dimensionless frequency	54
ω	actual frequency	54
ω_n	natural frequency	81

VITA

Ata S. Köseoğlu was born on 17th January 1960 in Istanbul, Turkey and is the second son of Mrs. İffet Köseoğlu and Mr. İlnan Köseoğlu. He received his diplom from Işık Lisesi as the best student in May 1976 and graduated from Boğaziçi University in June 1982 with B.S in Mechanical Engineering as a nigh honor student. The author pursued graduate studies in Mechanical Engineering at Lehigh University from August 1982 to May 1984. During this time the author performed research for this thesis and wrote a paper (as a co-author) with Prof. Brown on "The Use of Fluid Inertia for D/A Conversion in Hydraulic PLM circuits with Seating Valves".